MOLECULAR GENETICS OF FLUOROQUINOLONE RESISTANCE AND THE STRUCTURES OF KEY PYRIMIDINE BIOSYNTHESIS PATHWAY ENZYMES FROM *MYCOBACTERIUM TUBERCULOSIS*

GHODE PRAMILA BABAN

(M.Sc., University of Pune)

A THESIS SUBMITTED

FOR THE DEGREE OF DOCTOR OF PHILOSOPHY

DEPARTMENT OF BIOLOGICAL SCIENCES

NATIONAL UNIVERSITY OF SINGAPORE

2015

DECLARATION

I hereby declare that this thesis is my original work and it has been written by me in its entirety. I have duly acknowledged all the sources of information which have been used in the thesis.

This thesis has also not been submitted for any degree in any university previously.

Ghode Pramila Baban

August 2015

ACKNOWLEDGEMENTS

I wish to express my deepest gratitude to my supervisor at NITD, Dr. Pablo Bifani for his guidance in my PhD project and helping me develop my background in molecular genetics (Chapter 3).

I would like to express my deepest gratitude to my supervisor at NUS, Prof. J. Sivaraman for his immense support, constant encouragement and guidance in structural biology that has made this thesis work (Chapters 4 and 5).

I would like to acknowledge Novartis Institute for Tropical Diseases, Singapore, for sponsoring my PhD program at NUS.

I would like to express my gratitude to Prof. Paul Herrling for not only giving me an opportunity to work at NITD but also for constant support and encouragement throughout my PhD tenure.

I wish to express my gratitude to Prof. Srikant Datar for guiding me during the initiation of my research journey.

I wish to thank, Patricia, for your emotional support, Meera, for transforming me with all your encouraging thoughts, be it science or life. I wish to thank my cheerful colleagues at NITD- Bee Huat, Boon Heng, Adeline, Vivian and Jessie, for their advice and help in the lab. A huge thanks to my friends at NITD- Pamela, Michelle, Vanessa, Hazel, Jessica, Vimala, Priya and Ponnu for all the fun-filled times and dinner outings.

I wish to extend my thanks to my NUS colleagues, Jobi, Priyanka, Deepti, Digant and specially Sarath for the discussions and helping me in the work at NUS. A huge thanks to my friends at NUS- Pavithra, Pradeep, Bidhan and Tanusya for their care and for being there always.

Finally, I express my deepest gratitude to my parents for their love, encouragement and blessings throughout.

I thank God for the strength throughout. I dedicate this thesis to my late grandfather and my brother.

TABLE OF CONTENTS

SUMMARY

Tuberculosis (TB) is an infectious disease caused by *Mycobacterium tuberculosis* (*Mtb*). In 2013, 9 million new active-TB cases were estimated globally and 1.4 million TB-related deaths were recorded (CDC). Although the current drugs are effective against TB they are challenged by the emergence and spread of drug resistant TB at an alarming rate (Zumla & Grange, 2001). Approximately 1 in 13 *Mtb* clinical isolates currently shows a form of drug resistance (CDC, 2009). The rise in multidrug resistant (MDR) and extensively drug-resistant (XDR) cases results mainly due to poor or non-compliance of patients (owing to the long treatment duration and side effects) and the characteristic ability of *Mtb* to go into non-replicating or dormant state (Gengenbacher & Kaufmann, 2012). The situation is further exacerbated by the increase in co-infection with human immunodeficiency virus (HIV) which compromises the TB therapy. Together these factors present a major challenge to TB control and underscore the need for the identification of novel anti-TB entities (O'Brien & Nunn, 2001, Fogel, 2015) that can shorten the TB treatment duration (Ma *et al.*, 2010). However, inappropriate use of drugs and drug regimens is unavoidable resulting in the inevitable emergence of resistance. To avoid this issue optimal formulation of dosing strategy and development of efficient diagnostic tools for detecting resistance in the existing and newly introduced drugs is imperative to the control of emergence of resistance. Concomitant to the design and development of novel drugs, exploring novel drug targets in *Mtb* is required immediately (Ramaswamy & Musser, 1998). Thus, this thesis delves into applying molecular genetics

approach firstly to understand the fluoroquinolone (FQ) resistance and secondly, to explore drug targets in *Mtb*.

To understand the basis of selection of FQ resistant mutants, 669 FQ resistant *Mtb* mutants were analyzed for their allelic diversity. Newer generation FQs, gatifloxacin and moxifloxacin, were the most potent and exhibited lowest mutation frequency. Enrichment of DNA gyrase variants depended on the type and concentration of FQ used. At higher FQ concentrations, only high-level resistant mutants occurred and importantly, mutant prevention concentration could be reached with all FQs. However, low level resistant mutants showed increased inhibitory concentrations emphasizing their importance in clinical setup. All the six FQs exhibited cross resistance and called for consideration of re-designing the FQ formulation in TB regimen.

Concomitantly, we identified two probable *Mtb* target enzymes namely, *Mtb* uracil phosphoribosyltransferases (UPRTases) and pyrimidine operon regulatory protein (PyrR) from the essential pyrimidine biosynthesis pathway, with the activity UPRTase. Here we report the structures of *Mt*UPRT and PyrR-5-fluorouracil complex (PyrR-5FU) for the first time. 5FU is uracil (an UPRTase substrate) analogue, has anti-tuberculous activity and mutations in these two enzymes on 5FU exposure implicate their interactions with 5FU. Both 5-phosphoribosyl 1-pyrophosphate (PRPP, another UPRTase substrate) and uridine monophosphate (UMP) binding sites are conserved in the above enzymes. Spontaneous mutational sites of mutants selected on 5FU mapped to either conserved or substrate binding residues. Structural insights in these two proteins

and the protein-5FU complex would aid in the screening of their inhibitors and thus assist in TB drug design and development.

LIST OF FIGURES

LIST OF TABLES

LIST OF ABBREVIATIONS

7H9c	Middlebrook 7H9 media supplemented with 10% ADS, 0.05% Tween80 and 0.2% glycerol
5FU	5-fluorouracil
ADS	Albumin-Dextrose-Saline
BCG	Bacille Calmette-Guerin
BSA	Bovine Serum Albumin
CDC	Center for Disease Control and prevention
CFU	Colony Forming Units
CIP	Ciprofloxacin
DLS	Dynamic light scattering
DMSO	DiMethylSulfOxide
dNTP	deoxyriboNucleotideTriPhosphate
DOTS	Directly Observed treatment Short-course
DSBs	Double-strand breaks
DST	Drug susceptibility testing
EMB/ E	Ethambutol
FQs	Fluoroquinolones
GFX	Gatifloxacin
GyrA	DNA gyrase subunit A
gyrA	DNA gyrase subunit A encoding gene
GyrB	DNA gyrase subunit B
gyrB	DNA gyrase subunit B encoding gene
HIV	Human immunodeficiency virus

IGRA	Interferon gamma release assay
INH/ H	Isoniazid
KAN	Kanamycin
LB	Luria -Bertani
LTBI	Latent Tuberculosis Infection
LVX	Levofloxacin
MDRTB	MultiDrug- Resistant tuberculosis
MIC	Minimum Inhibitory Concentration
MPC	Mutant Prevention Concentration
Mtb	*Mycobacterium tuberculosis*
MTBC	*Mycobacterium tuberculosis* complex
*Mt*UPRT	*Mtb* Uracil phosphoribosylytransferase
MXF	Moxifloxacin
NAATs	Nucleic acid amplification tests
$O.D._{600}$	Optical Density or absorbance of a sample measured at a wavelength of 600 nm
OFX	Ofloxacin
PAS	Para-aminosalycilic acid
PCR	Polymerase Chain Reaction
PPi	Pyrophosphate
PRPP	5-Phosphoribosyl 1-pyrophosphate
PyrR	Pyrimidine operon regulatory protein
pyrR	PyrR encoding gene
PZA/ Z	Pyrazinamide
QBP	Quinolone binding pocket

QFT	QuantiFeron Test
QRDR	Quinolone resistance determining region
QRDR-A	QRDR of DNA gyrase subunit A (GyrA)
QRDR-B	QRDR of DNA gyrase subunit B (GyrB)
RIF/ R	Rifampicin
SDS-PAGE	Sodium Dodecyl Sulphate polyacrylamide gel electrophoresis
SFX	Sparfloxacin
SNP	Single Nucleotide Polymorphism
STR	Streptomycin
TB	Tubercle Bacillus (Tuberculosis)
TDR	Totally Drug-Resistant
TST	Tuberculin Skin Test
upp	*Mtb* gene encoding uracil phosphoribosylytransferase
UMP	Uridine monophosphate
UPRTase	Uracil phosphoribosylytransferase
WHO	World Health Organization
WT	Wild Type
XDR	eXtensively Drug-Resistant

PUBLICATIONS

Pramila Ghode, Chacko Jobichen, Sarath Ramachandran, Pablo Bifani and J. Sivaraman (2015) Structural basis of mapping the spontaneous mutations with 5-flurouracil in uracil phosphoribosyltransferase from *Mycobacterium tuberculosis*. *Biochem Biophys Res Commun*. 467(3):577-82.

Pramila Ghode, Sarath Ramachandran, Pablo Bifani and J. Sivaraman (2016) Structure and mapping of spontaneous mutational sites of PyrR from *Mycobacterium tuberculosis*. *Biochem Biophys Res Commun*. 471(4):409-15.

Hana L. Haver, Adeline Chua, **Pramila Ghode**, Suresh B. Lakshminarayana, Amit Singhal, Barun Mathema, René Wintjens, Pablo Bifani (2015) Mutations in Genes for the F_{420} Biosynthetic Pathway and a Nitroreductase Enzyme Are the Primary Resistance Determinants in Spontaneous *In Vitro*-Selected PA-824-Resistant Mutants of *Mycobacterium tuberculosis*. *Antimicrob Agents Chemother*.59(9):5316-23.

MANUSCRIPTS SUBMITTED

Vanessa Mathys, Amit Singhal, **Pramila Ghode**, Mehdi Kiass, Amanda Bifani, SeowHwee Ng, Adeline Chua, Natalia Kurepina, Karine Soetaert, Whitney Barnes, Kevin Pethe, Barry N. Kreiswirth, John Walker, Alain Baulard, Barun Mathema, Philippe Lefevre, Rene Wintjens and Pablo Bifani. Mutations in the uracil phosphoribosyltransferase (Upp) and the bifunctional pyrimidine operon regulatory protein (PyrR) confer resistance to the anti-cancer drug 5-fluorouracil in *Mycobacterium tuberculosis*

MANUSCRIPTS IN PROGRESS

Pramila Ghode, Adeline Chua, Suresh Lakshminarayana, Karl Drlica and Pablo Bifani. Selection of resistant *Mycobacterium tuberculosis* mutants with commercially available fluoroquinolones.

POSTER PRESENTATIONS

18th BIOLOCIAL SCIENCES GRADUATE CONGRESS

University of Malaya, Kuala Lumpur, Malaysia, 6 January – 10 January 2014

Mathys V., Singhal A., **Ghode P.**, Kiass M., Bifani A., Ng SH., Chua A., Kurepina N., Soetaert K., Barnes W., Pethe K., Kreiswirth B., Walker J., Baulard A., Mathema B., Lefevre P., Wintjens R. and Bifani P.

Mutations in the uracil phosphoribosyltransferase (Upp) and the bifunctional pyrimidine operon regulatory protein (PyrR) confer resistance to the anti-cancer drug 5-fluorouracil in *Mycobacterium tuberculosis*

EMBO CONFERENCE- Tuberculosis 2012: Biology, pathogenesis, intervention strategies

Institut Pasteur, Paris, France, 11 September – 15 September 2012

Pramila Ghode, Adeline Chua and Pablo Bifani

Determination and comparison of mutation frequency and type of fluoroquinolone resistance in *Mycobacterium tuberculosis*

NOVARTIS INSTITUTE FOR TROPICAL DISEASES TUBERCULOSIS SYMPOSIUM

Yaoundé, Cameroon, 11 October – 15 October 2010

Pramila Ghode, Youjin Teo, Xiu Hua Lim, Bee Huat Tan and Pablo Bifani

The Frequency of Mutation associated with Rifamycin Resistance in *Mycobacterium bovis* BCG and *M. tuberculosis*

1

Introduction: Tuberculosis

The global burden of tuberculosis

Tuberculosis (TB) is an infectious disease caused by *Mycobacterium tuberculosis* (*Mtb*) (Barnes, 2000). TB primarily affects the lungs (pulmonary) but can also affect other organs (extra-pulmonary). In 2013, TB claimed 1.5 million lives along with estimated 9 million new active cases (WHO, 2014). About one third of the world population harbors this pathogen as latent TB infection (LTBI), 5-10% of which has a probability to progress into an active TB infection. Consequently, efforts are being made worldwide to control the spread of this infection. As a result, recent years have witnessed slow decline in the number of active TB cases (37 million lives were saved between 2000 and 2013 through effective diagnosis and treatment) (WHO, 2014). The current 1st line anti-TB treatment is a combination therapy comprising of isoniazid (INH), rifampicin (RIF), pyrazinamide (PZA) and ethambutol (EMB) (Beena & Rawat, 2012). The emergence and spread of multidrug resistance TB (MDR TB, defined as isolates resistant to at least INH and RIF) and extensively drug resistance TB (XDR TB, MDR isolates additionally resistant to fluoroquinolone (FQ) and at least one injectable- aminoglycoside or capreomycin) at an alarming rate is rendering the existing drugs inefficient (Zumla & Grange, 2001). Approximately 1 in 13 *Mtb* clinical isolates currently shows a form of drug resistance (Figure 1.3) (CDC, 2009). However, the drug resistant TB strains emerged since the mid-1980s with the co-infection by HIV (Human immunodeficiency virus), the major risk factor

for LTBI to progress into an active infection. The rise in MDR and XDR cases results mainly due to poor or non-compliance of patients (owing to the long treatment duration and side effects) (Lipsitch & Levin, 1998) and the characteristic ability of *Mtb* to go into non-replicating or dormant state (Gengenbacher & Kaufmann, 2012). The situation is further exacerbated by the increase in co-infection with HIV (Schluger *et al.*, 2013). Together these factors present a major challenge to TB control and urge for the identification of new anti-TB entities (O'Brien & Nunn, 2001).

1.1 Tuberculosis: etiology and epidemiology

In 1882, Robert Koch demonstrated *Mtb* as the etiologic agent of TB (Barnes, 2000). *Mtb* are rod-shaped, non-motile, acid-fast bacilli and belongs to the *Mycobacterium tuberculosis* complex (MTBC) which consists of other *Mycobacterium* species that cause animal and human tuberculosis. *Mtb* has been evolving with its obligate human host for more than 70,000 years (Warner & Mizrahi, 2013). *Mtb* is an aerobic bacillus predominantly affecting the aerated organs- the lungs, however, it is known to survive anaerobically (as latent TB infection, LTBI) and harbors in one third of the world population. The replication time of *Mtb* is around 18 – 24 h (*E. coli* replication time is 20 min). The complex cell envelop consisting of high and varied lipid content in this pathogen accounts for many of its unique clinical characteristics and virulence (Espinosa-Cueto *et al.*, 2015). *Mtb* evades the host macrophage defense mechanism by preventing its

integration into lysosomes aiding in the survival of *Mtb* (Pieters, 2001). These intrinsic characteristics of this unique bacterium thus pose a blockage to the development of effective therapeutics.

TB has haunted mankind since prehistoric times. It was thought to be on the verge of eradication after the introduction of the first line anti-TB drugs (INH and RIF) in 1950s however, it resurge back in 1980s. Social change during the industrialization in the 17^{th} to 20^{th} century also contributed to increase in the TB incidence. The TB epidemics was directly proportional to the extent of urbanization; peaking at different places at different times (Lonnroth *et al.*, 2009). Currently, longer treatment duration (resultant non-compliance which is partly related to socio-economic gradient) and the co-infection with HIV are amongst the top risk factors fueling the spread of drug resistant tuberculosis (Figure 1.1).

Key 2013 TB facts: 9 million people fell ill with TB and 1.5 million died from it (among these deaths 0.36 million were people who were HIV – positive). There were an estimated 480 000 new cases of multidrug - resistant TB(2013)

In Singapore 1,533 new cases of TB were reported among the residents in the year 2011.

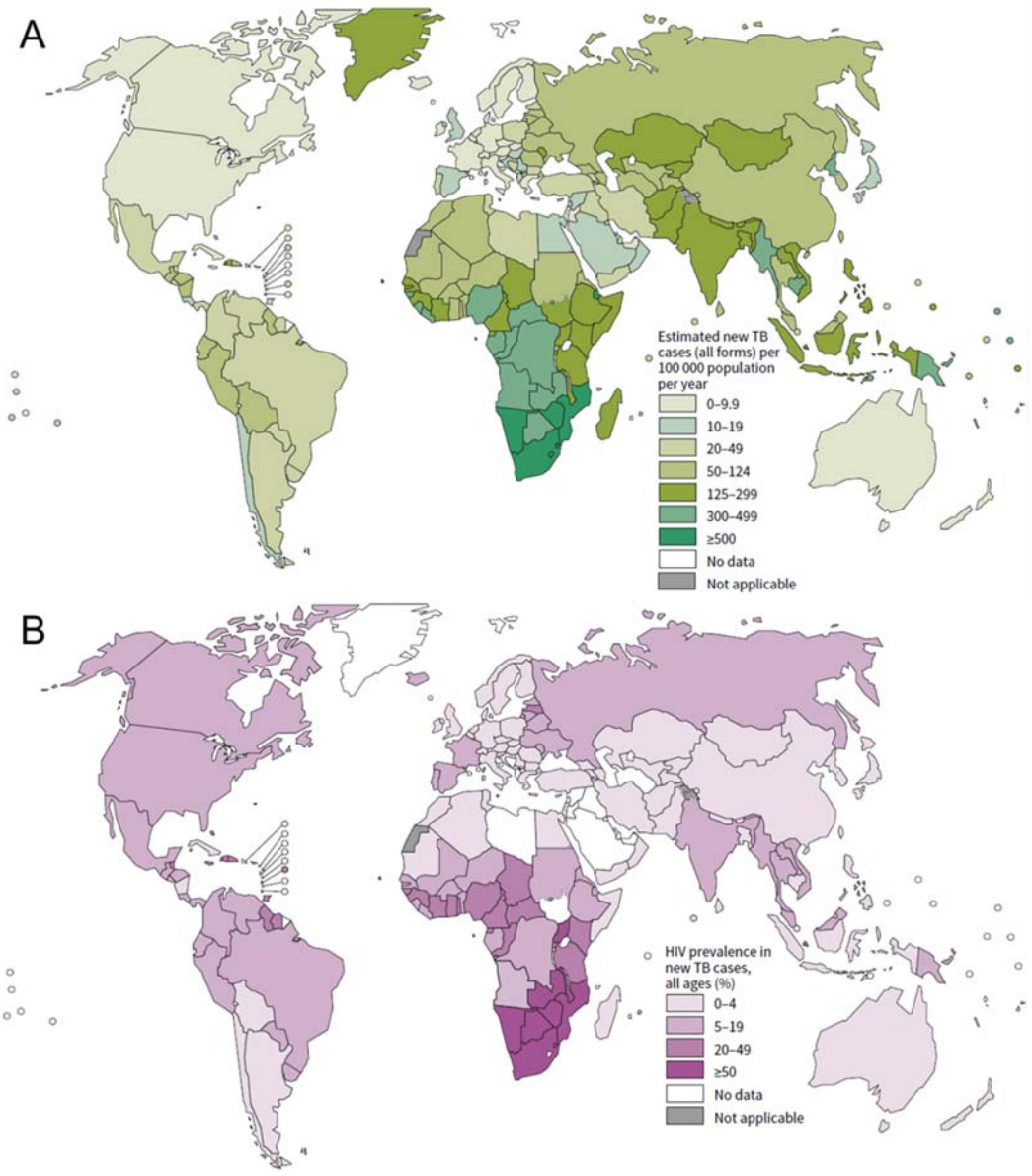

Figure 1.1 Tuberculosis epidemics according to the socio-economic status.*(A)* Estimated new TB cases per 100 000 population per year. (B) HIV prevalence in new TB cases. *(Source- WHO Global tuberculosis report 2014)*

1.2 *Mycobacterium tuberculosis* pathogenesis

Mtb is an obligate human pathogen and its transmission occurs through inhalation of aerosols from an infected person to a healthy individual. Around 10 bacteria are enough to cause the *Mtb* infection (Nikas *et al*., 2005) which, depending on the individual's immune status, progresses into an active disease or remains latent in most of the cases. *Mtb* invades the host immune system by first invading the alveolar macrophage with help of its multiple cell receptors (Ernst, 1998) which contains *Mtb* in vacuole and helps *Mtb* to be transported into deeper lung tissues. The survival strategies of *Mtb*, namely robust cell wall, upregulation of genes involved in lipid metabolism, tolerance to low pH, damage repair and detoxification, help it to combat the hostile macrophage environment (Gengenbacher & Kaufmann, 2012). The infected macrophage continues to recruit other macrophages leading to formation of granuloma. Granuloma consists of an organized aggregate of differentiated macrophages and other immune cells (Figure 1.2). Furthermore, *Mtb* has the capability to shut down its central metabolism system and enter a non-replicating stage which activates on the weakening of the host immune system.

The lipid rich *Mtb* cell envelope provides lipid mediators for the survival during replication and persistence (Glickman & Jacobs, 2001). The genes in these pathways could be explored as novel targets for development of novel TB therapeutics.

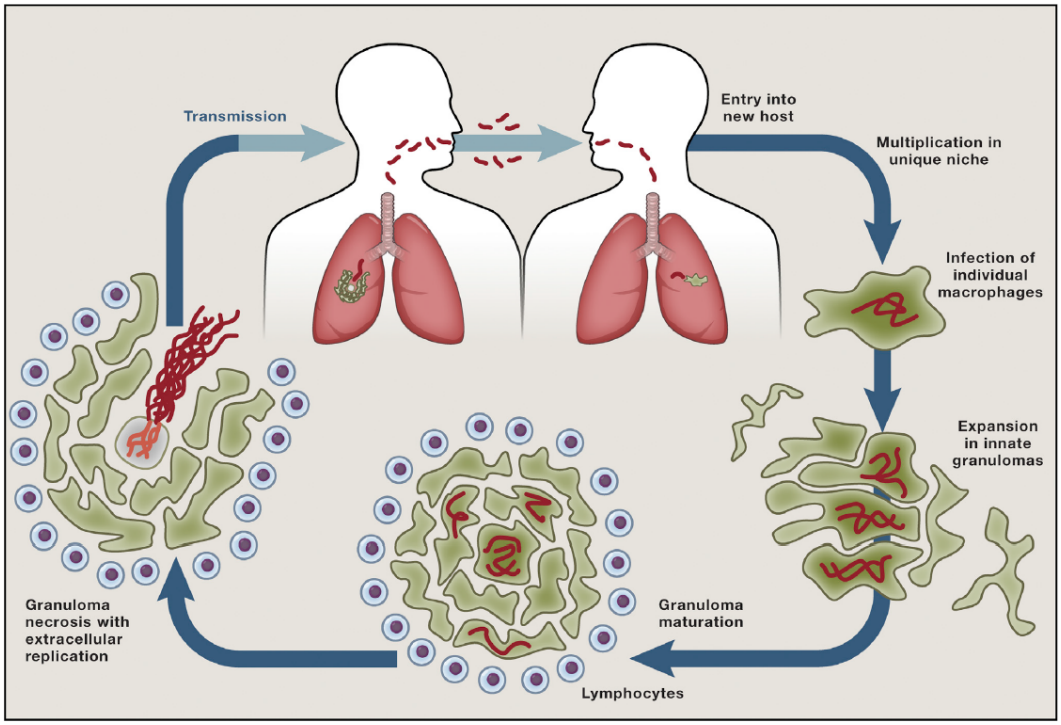

Figure 1.2 Pathogenesis of Mycobacterium tuberculosis *(Cambier et al., 2014). Aerosol particles containing active bacteria help the spread of TB. These bacteria infect the macrophages in lungs which transport the bacteria to deeper tissues where new macrophages are infected. This leads to formation of the granuloma, consisting of differentiated macrophages and other immune cells. A result of which is expansion of infection. The granuloma undergoes necrosis (necrotic core) which aids further growth and transmission active bacteria.*

1.3 Prevention of tuberculosis

The live *M. bovis* Bacillus Calmette-Guerin (BCG)vaccine is the only available preventive measure against TB since 1921 (Stefanova, 2014) and will remain as golden standard while the new anti-TB vaccine development is in progress (WHO). However, it provides protection in only some populations and with compromised efficacy. Thus, BCG vaccination alone is not adequate for protection against active TB and calls for improved vaccination strategy (Hawn *et al.*, 2014). Several clinical trials are ongoing to either boost the BCG immunization or evaluate the novel vaccines (Rowland & McShane, 2011).

1.4 Diagnostics

Few of the symptoms for suspected TB patients are coughing for more than 3 weeks, weight loss, night sweats and fever. Such patients are referred to carry out the TB diagnostic tests which comprise of phenotypic and genotypic analysis.

The conventional diagnostic tools: The preliminary diagnostic tool used to detect the presence of pulmonary TB lesions is a chest X-ray; however the technique can detect the infection only in the advanced stage. Sputum smear microscopy of stained acid-fast-tubercle bacilli is another conventional and commonly used technique. The false positive result due to presence of other acid-fast bacilli is the drawback of this technique and thus complemented by culturing the samples in liquid or on solid media, called drug susceptibility testing (DST). DST provides information on effectiveness of treatment administered by

monitoring the culture conversion. DST is also useful to detect and monitor drug resistance. Nonetheless, culturing requires weeks before the result is acquired and is undesirable in high TB and HIV incidence setting. These diagnostic tools are century old and are associated with limitations and thus inefficient for the effective control and spread of TB (Perkins & Cunningham, 2007).Advances in liquid cultures systems have led to reduction in result obtaining time to days with the developments of BACTEC and MGIT automated liquid culture systems (Becton Dickinson).

Advances in active TB diagnosis include improvement in the existing DNA amplification and immunological assays (Pai *et al.*, 2006b). Nucleic acid amplification tests (NAAT) directly amplify the nucleic acid specific region from *Mtb* complex; however it is associated with low sensitivity and requires trained personnel. Immunological assays detect the humoral immune response that relies on antibody detection, however, currently only active TB can be detected with this technique. Another technique that detects growing bacteria colorimetrically is the TK medium (Salubris, Inc., MA, USA). This rapid culturing technique allows early detection than the conventional culturing technique and can be used for DST.

Active TB also develops on reactivation of the LTBI. Until recently, LTBI could be quantified by the immunological Mantoux tuberculin skin test (TST) by injecting tuberculin purified protein derivative (PPD) intradermally in the forearm. The dimension of the hardened and elevated area at the injection spot is recorded for verifying the TB infection. However, low specificity is the limitation

of this test; it could be either positive (if the person was exposed to non-tuberculous bacteria or BCG vaccination) or negative (due to inability to react to skin test due to weakened immune system) (CDC factsheets 2012).

Advances in LTBI diagnosis: The specificity for accurate detection of *Mtb* is now possible due to the introduction of *Mtb* specific antigens (e.g. early secreted antigenic target (ESAT)-6, culture filtrate protein (CFP)-10 and TB7.7 (Rv2654)) in the interferon-γ release assays (IGRAs). These antigens sensitize the *Mtb* T-cells which is measured *in vitro* by the IGRAs. IGRAs show lower cross reactivity to BCG vaccination than the TST(Andersen *et al.*, 2000). Currently 2 commercial IGRAs are available 1) QuantiFERON®-TB Gold In-Tube test (QFT-GIT) and 2) T-SPOT®.*TB* test (T-Spot). The limitation of this technique is its inability to distinguish between active and latent TB and also, due to the fact that only limited data is available on 1) prediction of relapse of TB and 2) TB detection in children and HIV/ immunocompromised patients (Pai *et al.*, 2006a).

Diagnosis of drug resistant TB: GenoType MTBDRplus and GenoType MTBDRs by Hain are the commercial NAAT-based line probe assays used for the detection of 1st and 2nd line drugs. With simultaneous detection of *Mtb* infection these assays amplify the regions of drug resistance with a sensitivity and specificity of 98.4 and 98% respectively for rifampin resistance (Ling *et al.*, 2008). However, only the predominant mutational sites (high-level resistance mutations; selected at higher drug concentration) are evaluated. Studies show that, low-level resistance mutations have the capacity to progress into increased resistance (Baquero, 2001). Capturing such mutations at the first step of resistance

diagnosis would aid in the further limit the emergence of resistance. Consequently, examining the resistance level offered by these low-level mutations forms one of the objectives of this thesis.

An alternative cost effective technique is the microscopic-observation drug-susceptibility assay (MODS), which uses sputum sample cultured in anti-TB drugs to detect cord formation using an inverted light microscope within 7 days (Nyendak *et al.*, 2009). WHO recommends automated liquid culture systems as the 'gold standard' for first-line and second-line DST. However, the latter (second-line DST) is complex and expensive. Molecular line probe assays for first-line DST is another gold standard recommended by WHO.

In parallel, for HIV endemic regions, the HIV infection test is recommended for rational formulation of both TB and HIV drug regimens.

All the diagnostic tools are associated with drawbacks and are encouraged to be used in combination. However, the endemic countries mostly rely on the conventional tools for identification of resistant TB. Thus, in spite of the current advances in diagnostics the detection rate is still lower in the endemic countries in part, due to the inefficiency of the diagnostic tools (Wallis *et al.*, 2010) and in part, due to the unavailability of the tools. Modeling studies show that 22% of global TB deaths can be averted with development of diagnostic tools that are unaffected by HIV status and have a sensitivity of at least 85% for smear positive and smear negative cases (Keeler *et al.*, 2006). Additionally, XDR diagnosis still remains unstandardized due to involvement of more drugs and inadequate

information on the mutations associated with the drug resistance (Pai & O'Brien, 2008).

Comprehensive molecular genetics for all drugs is hence essential to efficiently design the diagnostic tools which would aid in the appropriate formulation of treatment strategy for resistant strains. The study of molecular genetics of resistance in one of the chemical class of compounds, the FQs (some of which are currently used for MDR-TB treatment), is one of the major aims of this thesis.

1.5 Treatment

Implementation of several treatment strategies by WHO in the past decades have contributed to considerable TB control. The strategies include DOTS (Directly Observed Treatment Short-course) and several version of DOTS (For example, RNTCP in India), Stop TB (WHO, 2006-2015), and End TB (WHO, 2015).

Treating new TB cases

Multidrug therapy is used to treat TB to avoid the emergence of resistance. Currently the first line drug regimen includes INH (H) (300 mg), RIF (R) (600 mg), PZA (Z) (25 mg/kg), and EMB (E) (15 mg/kg) for 2 months (daily, intensive phase) and INH (300 mg), RIF (600 mg) for 4 months (daily or 3 times weekly by DOTS, continuation phase) (Table 1.1) (WHO, 2015). Overall, daily dosing is recommended and the sputum is monitored during the treatment duration. For treating populations with high INH resistance, EMB is suggested to be included in the continuation phase of the TB regimen.

Table 1.1 Standard regimen and dosing frequency for new TB patients (2010).

Intensive phase	Continuation phase	Comments
2 months of HRZE	4 months of HR	
2 months of HRZE	4 months of HRE	Applies only in countries with high levels of isoniazid resistance in new TB patients, and where isoniazid drug susceptibility testing in new patients is not done (or results are unavailable) before the continuation phase begins.

Treating resistant TB

Controlling resistant TB is a major hurdle to the global TB control program. For previously treated patients (high likelihood of MDR-TB) DST (at least for INH and RIF) is recommended before formulation of treatment strategy which is thus individualized based on the DST results. For MDR-TB, patients are treated with the first line drug to which the *Mtb* is susceptible in combination with the second line drugs- ρ-aminosalicylic acid (PAS), cycloserine, FQs, aminoglycosides, polypeptides and ethionamide. Treating the resistant strains (MDR and XDR) requires expensive and toxic drugs with longer treatment duration which leads to patient non-compliance and further emergence of highly resistant strains.

Treating latent TB

The standard treatment for latent TB treatment is INH for 6 to 9 months. Most of the anti-TB drugs work on actively growing bacteria. Recent studies show that treating latent TB bacteria could play a major role in halting the progression into active TB infection. Exploring targets in latent stag e of TB could help in development of chemical entities that could potentially inhibit the growth of latent TB strains. Correspondingly, the second aim of this thesis was to partially validate a probable target in *Mtb* which is also known to be active in the dormant stages of other organisms.

Treating TB-HIV co-infection

The standard regimen, 2HRZE/4HR, is administered daily irrespective of HIV status followed by HIV serology test. TB-HIV coinfection is recommended to be managed by experts in both diseases due to the pharmacological interaction between rifampicin and 2 groups of drug that are used in highly active antiretroviral therapy (HAART).

1.6 Drug resistance: Challenge in TB control

Penicillin was the first antibiotic discovered by Alexander Fleming in 1928 (Florey, 1944). It was one of the successful antibiotics in the golden era of novel antibiotic classes to treat infectious diseases. However, penicillin-resistance occurred within 4 years of its mass production (Aminov, 2010) in spite of the warning against the use of sub-therapeutic doses or non-lethal quantity of antibiotics (when bought without prescription). There are 3 possible mechanisms for bacterial resistance to occur: by adaptation (robustness of cells), by spontaneous mutations prior to exposure of antibiotics or by induced mutations on exposure to antibiotics. Resistance can also occur by horizontal transmission of resistance genes which is not observed in *Mtb*. Spontaneous mutations constantly occur in prokaryotes at a rate of 0.0033 mutations/ DNA replication. Induced mutations in *Mtb* arises due to several factors including misuse of drugs from the TB drug regimen, exposure of immunocompromised patients or by direct exposure to drug resistant TB.

Misuse of drugs in TB treatment could arise due to the following reasons:

1) Long duration of treatment (6-9 months) causing patient to leave treatment halfway.
2) Exposure of *Mtb* to sub-optimal concentrations of drugs and thus unknowingly selecting for low-level resistant *Mtb* strains. (FQs are also used in treatment of other infectious diseases)

3) Dosing strategy rendered inefficient due to limited information of type of mutant strain selected.
4) Very few drugs are available for treating latent TB, which harbors in one third of the world population.

Weakened immune system due to other clinical conditions and medications leads to ineffective host defense (such as co-infection by HIV, diabetes, cancer, malnutrition, etc.). In addition, incompatibility of the treatment drugs and hence manipulation of the standard therapeutic strategy also leads to emergence of drug resistance. For example, the retroviral drugs interact with the anti-tuberculous drugs, particularly rifamycins. In such cases experts are required to design the appropriate therapy, which in many cases (developing countries with high TB and HIV burden) is not feasible.

In addition, overpopulating metropolitan cities provide the niche for direct spread of resistant strains in healthy individuals (Figure 1.3). Negligence of evaluation of the resistance status in such cases, partly due to lack of appropriate and convenient diagnostic tools further burgeons the emergence of resistance

1.6.1 MDR, XDR and TDR

Drug resistance in TB is characterized as MDR, XDR and more recently TDR (Totally Drug Resistant).The definitions of some terms used in drug resistance as mentioned by Jeon *et al.* are quoted in Table 1.2.

The spread and emergence of resistance globally are depicted in Figure 1.3. As can be seen from the figure, complete picture of the spread of resistance is yet, either not available or only subnational data is available, for most of the developing (resource limited) countries. Convenient and inexpensive diagnostics are thus an immediate need to control the spread of resistance.

Table 1.2 Definitions of drug resistance*(Jeon, 2015)*

Drug-resistance	Definition
Mono-resistance	Resistance to one 1st-line anti-TB drug only.
Polydrug resistance	Resistance to more than one 1st-line anti-TB drug (other than both INH and RIF)
Multidrug resistance	Resistance to at least both INH and RIF
Extensive drug resistance	Resistance to any FQ and to at least one of three 2nd-line injectable drugs (capreomycin, kanamycin and amikacin), in addition to multidrug resistance
Rifampicin resistance	Resistance to RIF detected using phenotypic or genotypic methods. It includes any resistance to rifampicin, whether monoresistance, multidrug resistance, polydrug resistance or extensive drug resistance

A rapid diagnosis of drug resistance and the subsequent initiation of an appropriate treatment are crucial in the management of drug-resistant TB. Using current recommendations, drug-resistant TB can be largely cured with the right combination and use of available anti-TB drugs provided efficient diagnostic tools are available (Jeon, 2015).

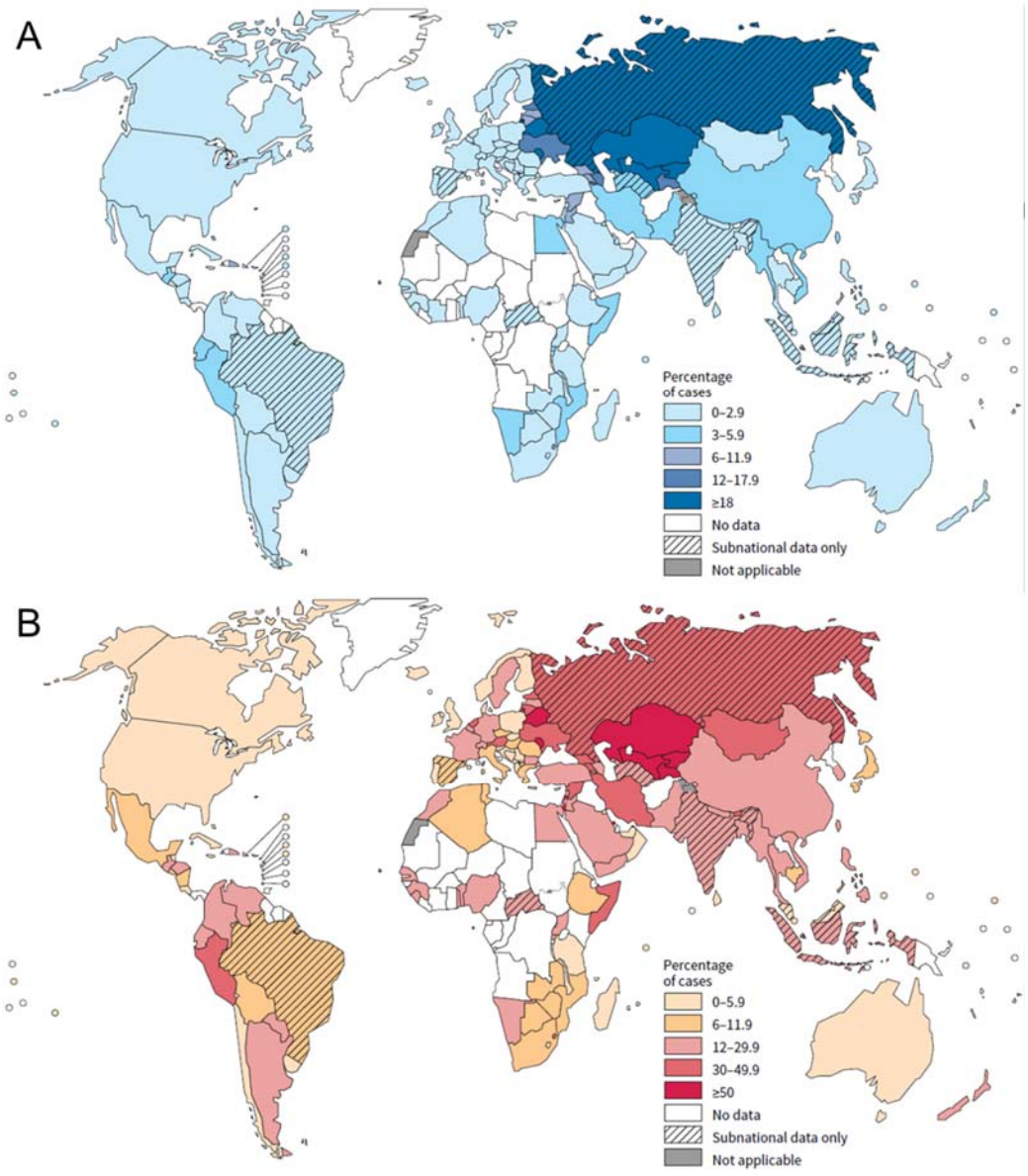

Figure1.3 (A) Percentage of new TB cases with MDR-TB (B) Percentage of previously treated TB cases with MDR-TB. *(Source- WHO Global tuberculosis report 2014)*

1.6.2 Fluoroquinolones for drug resistant TB

The very low minimum inhibitory concentration (MIC) of FQs and their potential to shorten TB therapy make them attractive candidates to counterbalance the failing TB therapy. FQs are nalidixic acid derivatives with broad spectrum anti-bacterial activity particularly against resistant *Mtb* (Figure 1.4) (Drlica & Malik, 2003). FQs belong to the quinolone family discovered in 1962; since then there has been no new structural class of antibiotics for four decades (Walsh, 2003a). Of importance is the ability of chemical modifications to the quinolones that have led to development of second generation of quinolone derivatives with increased potency and wider spectrum of antibacterial activity, for instance, the FQs-levofloxacin (LVX) and ofloxacin (OFX), which are currently used to treat resistant TB (Beena & Rawat, 2012). FQs also show limited activity against some non-replicating mycobacteria, but activity against latent TB remains to be determined.

Newer generation FQs, moxifloxacin (MXF) and gatifloxacin (GFX) were recently evaluated in phase III clinical trials to access their efficacy in the first line TB drug regimen to shorten the treatment duration from 6 to 4 months. The MXF containing regimen which replaced either INH or EMB exhibited rapid reduction in the bacterial load in the initial phase of treatment (Conde *et al.*, 2009), however, the shortened regimen was not observed to be non-inferior to the standard 6 month treatment and resulted in relapse (Gillespie *et al.*, 2014). Similar results were obtained with GFX (Merle *et al.*, 2014, Jawahar *et al.*, 2013). Nevertheless, FQs are used in first-line treatment for multi-drug resistant (MDR)

TB and to treat patients with drug intolerance (Moadebi *et al.*, 2007). Resistance to these valuable drugs is inevitable if their inappropriate use is not controlled (Moellering, 2005). Therefore, understanding the molecular mechanism of FQ resistance has received considerable attention in the scientific community since the development of these antibiotics. Correspondingly, evaluation of molecular genetic basis of resistance of the clinically used FQs is one of the main objectives of this thesis.

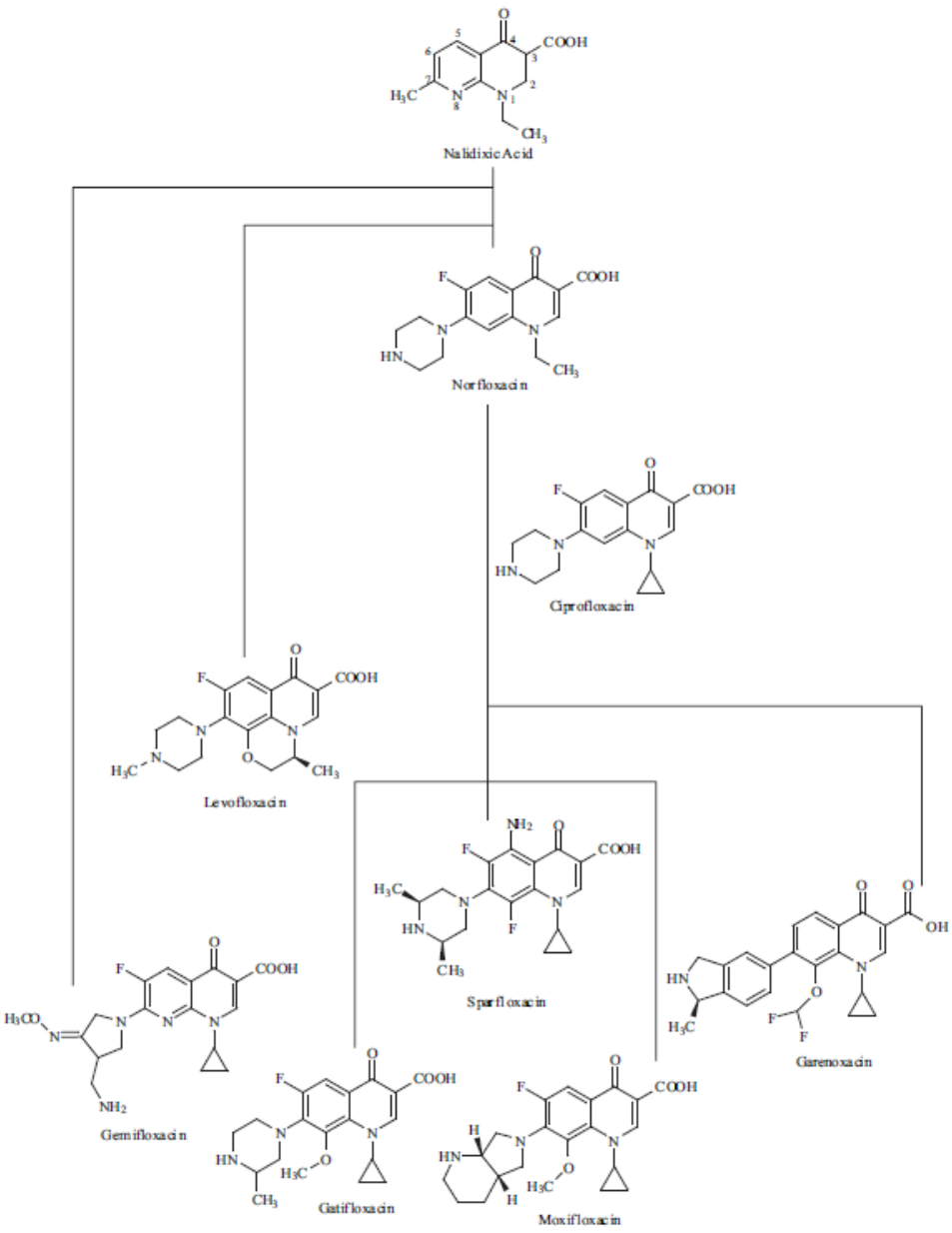

Figure 1.4 Evolution of fluoroquinolones from nalidixic acid *(Drlica & Malik, 2003). Fluoroquinolones share the common core quinolone structure and have a fluorine atom at carbon 6 position which influences gyrase potency.*

1.6.3 Molecular genetic basis of drug resistance

In their original work, Luria and Delbruck suggest that if the number of mutants in multiple experiments is the same, then it is adaptive mutagenesis (Luria & Delbruck, 1943). In contrast, if the numbers differ it is spontaneous mutagenesis. However, experimental data since has shown that only extensive mathematical analysis using multiple data points can truly distinguish adaptive from spontaneous mutagenesis. We believe that this comprises a mixture of both adaptive and spontaneous.

1.7 TB drug development- Progress and strategies

The pace of antibiotic development has reduced dramatically; for instance, there has been no new structural class of antibiotics for four decades after the introduction of quinolones in 1962 (Figure 1.5) (Walsh, 2003a, Barry & Cheung, 2009). Nevertheless, past decade has witnessed a few drugs from 6 chemical classes that entered the clinical development pipeline (Figure 1.6) (Zumla *et al.*, 2013). Amongst the Phase III drugs, 3 are repurposed TB drugs: rifapentine and 2 FQs (GFX and MXF). However, randomized clinical trials of 4 month regimen containing GFX and MXF were not found to be non-inferior to the current 6 month regimen (Jawahar *et al.*, 2013). Nevertheless, these are promising drugs against MDR TB, and given that the older generation FQs are already in use against other clinical conditions (mostly bacterial infections), emergence of *Mtb* resistance to the newer FQs (GFX and MXF) is inevitable. Understanding the mutant prevention ability and the resistance mechanism of these FQs would greatly aid in the rational dosage formulation strategies and molecular diagnostics against resistant *Mtb* strains. Correspondingly, this thesis delves into the comprehensive understanding of molecular genetics resistance of six FQs in the first part.

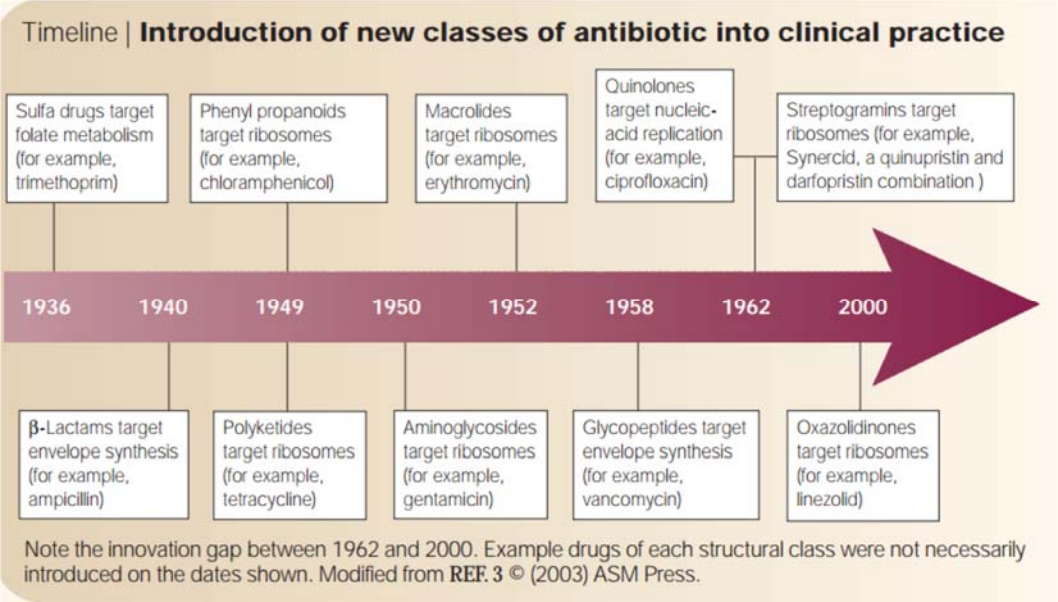

Figure 1.5 Innovation Gap, in introduction of new antibiotic class between 1962 and 2000 (Walsh, 2003a).

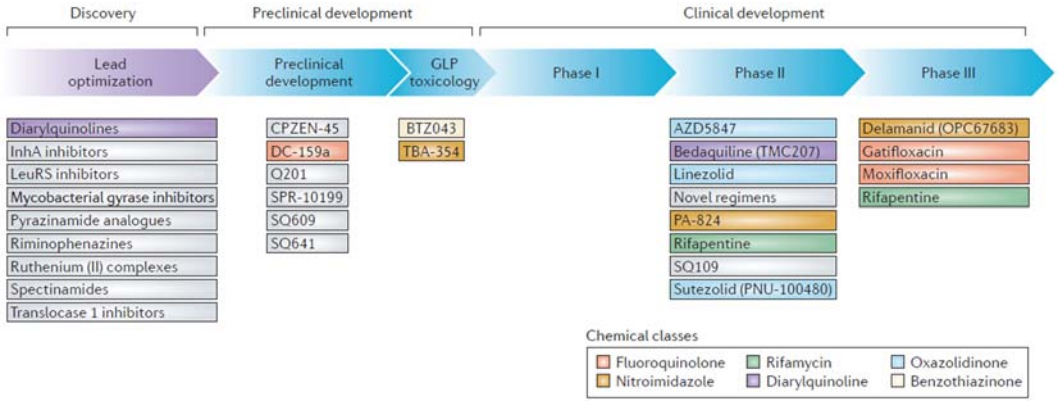

Figure 1.6 Current global pipeline of new tuberculosis drugs (Zumla et al., 2013). *Out of the 4 foremost drugs in the clinical development, 2 are FQs.*

Nonetheless, the promising FQs are still at risk of emerging with resistance due to either misuse or cross resistance (owing to the identical mechanism of action as that of the older FQs). Thus, concomitant, identification of new drug targets (unique mechanisms of action) in *Mtb* is another promising approach to control TB (Beena & Rawat, 2012).

One third of the world population is infected by dormant TB. Consequently, relapse in treated patients with the emergence of drug resistance as a result of (mostly) reactivation of dormant *Mtb* is a major concern. *Mtb* attains this latency by shutting down the central metabolism and replication; while at same time initiating the energy saving pathways for survival (Gengenbacher & Kaufmann, 2012). Thus, genes involved in these metabolic pathways of non-replicating or dormant bacteria are attractive anti-tubercular drug targets .Also, taking into account the fast evolving *Mtb*, repurposing of drugs is an excellent approach for accelerated drug development with the possibility to discover new targets.

1.7.1 Repurposing of drugs for TB treatment: 5-fluorouracil and its analogues

Developing an entirely new drug requires detailed information on pharmacokinetics, toxicity and formulation which is usually time consuming and expensive (Kale *et al.*, 2015). Repurposing of drugs holds promise to deliver faster and safer drugs, due to in-advance availability of such information (Ashburn & Thor, 2004). Correspondingly, 5-fluorouracil **(**5FU) is a clinically validated anticancer drug and recently being investigated for its mechanism of action in *Mtb* (Singh *et al.*, 2015). The mechanism of 5FU resistance in *Mtb* was

demonstrated to be associated with mutations in the two enzymes with uracil phosphoribosyltransferase activity (UPRTase; EC 2.4.2.9). The enzymes are uracil phosphoribosyltransferase (*Mt*UPRT) and pyrimidine operon regulatory protein (PyrR), encoded by the *upp* and *pyrR* genes respectively.

Antitubercular activity of 5FU is known since 1979 (Tsukamura, 1979), however, it was not pursued as a potential TB drug given the toxic side effects of 5FU. Although, 5FU cannot be repurposed as an anti-TB drug, its analogues (on chemical modifications) can be evaluated in a target based drug discovery approach (Duncan, 2004), provided, structural insights into 5FU interactions with *Mt*UPRT and PyrR are available. Subsequently, the understanding of these interactions with the help of molecular genetics approach (spontaneous mutants generated against 5FU) and structure determination of the enzymes involved forms the basis of second half of this study and is discussed in the latter part of this thesis.

1.7.2 Identification of novel targets for TB drug development

Essential biological pathways associated with DNA/RNA synthesis are often interrogated for favorable drug target enzymes (Duncan, 2004). There is ongoing research on *Mtb* metabolic pathways to understand this adaptation to persistence however, its complex nature makes the discovery of potential regulators evasive (Manabe & Bishai, 2000).

In our previous study, *Mtb* H37Rv spontaneous mutants obtained on 5 µM and 20 µM 5FU were screened for nucleotide polymorphisms in the pyrimidine synthesis

and salvage pathway enzymes- PyrR and *Mt*UPRT respectively (Mathys *et al*., unpublished data). Intriguingly, all resistant alleles selected on 5 μM and20 μM of 5FU had mutations on *upp* and *pyrR* respectively. In addition to the above observation, the expression of these two enzymes in different stages of *Mtb* makes it compelling to understand the underlying mechanism and to thereby progress one step further in their validation as potential *Mtb* targets. Structural insights into 5FU interactions with these two enzymes form the basis of the study discussed in chapters 4 and 5.

The two main objectives of this research work are based on the two backbones (1 and 3) of the End TB strategy (2015) (WHO). The backbones of the End TB strategy are quoted as below:

1) "Early diagnosis and treatment of all kinds of TB patients.

2) Policies for political and community commitment towards TB care and prevention, including the universal health coverage policies.

3) Intensified research and innovation for drug or target discovery, development of new tools, interventions and strategies."

1.8 Overall objectives

Part I- Molecular genetics of fluoroquinolone resistance

Irrespective of the effectiveness of combination therapy, emergence of resistance continues to pose a major challenge to TB control. One of the two main purposes of this study was to evaluate the potential of chemical genetics in our understanding of mechanisms of resistance and drug discovery. Six different FQs were used as model drugs in this study and their evaluations are discussed in chapter 3.

The specific objectives in the first part of this study were as follows:

1 To understand the molecular genetics of fluoroquinolones resistance

1.1 To determine mutation frequency and frequency of mutation type selected on different clinically used FQs at varying concentrations.

1.2 To determine the MICs of all FQs and the level of resistance exhibited by various mutant types.

1.3 To determine cross resistance patterns exhibited by different mutants types selected on different FQs and at different concentrations

1.4 To evaluate the mutant prevention concentration (MPCs) for the six FQs.

Part II- Structural studies of two key pyrimidine biosynthesis enzymes

The second purpose of this thesis was to utilize chemical genetics to identify new mechanisms of resistance or targets for existing drugs. In this study we investigated the mechanism of resistance or targets of the anti-cancer drug 5-

fluorouracil (5FU) in *Mtb* the findings of which are discussed in chapters 4 and 5 respectively.

The specific objectives in the second part of the study were as follows:

2 To explore and validate new mycobacterial targets for TB drug development.

2.1 To determine the structure of *Mt*UPRT.

2.2 To determine the co-crystal structure of PyrR-5FU complex.

2.3 To establish the correlation between the spontaneous mutational sites of *Mt*UPRT and PyrR with the 5FU resistance.

Schematic representation of the present study is shown in Figure 1.7.

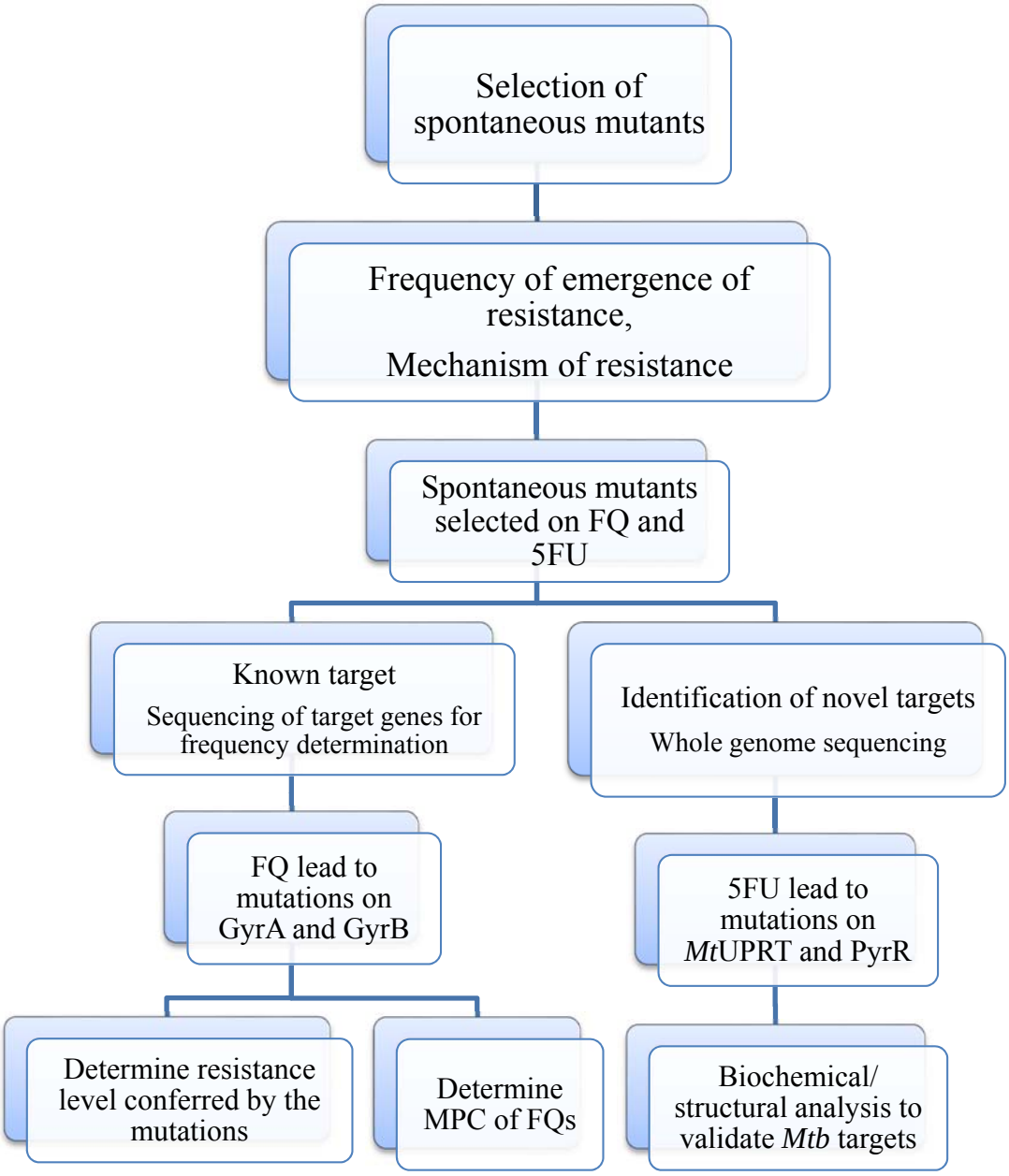

Figure 1.7 Schematic representation: Objectives and experimental approach.

2

Materials and Methods

2.1 Molecular genetics of FQ resistance

2.1.1 Mycobacterial strains and culture conditions

Liquid cultures of *M. bovis* BCG, *Mtb*- H37Rv and *Mtb*- CDC1551 were obtained in 1 liter roller bottles containing 50-100 ml Middlebrook 7H9 media supplemented with 10% ADS (Albumin Dextrose Saline), 0.05% Tween80 and 0.2% glycerol (called 7H9c). Agar plates with or without FQs prepared using Middlebrook 7H11 agar (supplemented with 10% OADC (containing Oleic acid, BSA, dextrose, Catalase powder and Sodium chloride) and 0.5% Glycerol), were used to grow the mycobacteria as colonies. The cultures were incubated at 37°C until $O.D._{600}$ = 0.6-0.8 for liquid (7H9c media) cultures or until 3-4 weeks to obtain visible colonies on agar plates. BSL-3 facility was used for culturing the *Mtb* strains.

2.1.2 Fluoroquinolones

Gatifloxacin (GFX, cat.# G7298-1G), sparfloxacin (SFX, cat. # 56968-1G-F), levofloxacin (LVX, cat. # 28266-1G-F), ofloxacin (OFX, cat. # 08757-1G) and Rifampicin (RIF, cat. # R3501-1G) were obtained from Sigma life sciences. Moxifloxacin (MXF, cat.# 32477-50mg) and ciprofloxacin (CIP, cat. # 17850-

5G-F) were obtained from Fluka analytical. Stock solutions of FQs at 10 mM were prepared in 0.1 N NaOH as required and stored at 4°C.

2.1.3 Recovery of spontaneous FQ mutants

Liquid cultures of all strains were grown to log phase, $O.D._{600}$= 0.6 to 0.8. The cultures were centrifuged at 4000 rpm for 30 min and the pellet was resuspended in 7H9 media to obtain a stock cell density of approximately 10^{10} CFU per ml. Around 10^9 and 10^7 *Mtb* cells or CFU were applied on agar plates containing 1 µg/ml Rifampicin (Control), GFX and MXF while 10^8 and 10^6 CFU were applied on SFX, LVX, CIP and OFX at varying concentrations. The plates were incubated at 37°C for 4-6 weeks before CFU counting. Dilutions of stock cultures were plated on 7H11 agar plates without antibiotics to calculate the initial CFU count.

2.1.4 Sequence analysis of *gyrA* and *gyrB* of mutants

All the colonies were picked from plates containing less than 10 colonies whereas ~5-10 colonies were picked from plates containing more than 10 colonies. Mutant colony cultures were obtained by inoculating a single colony in 30 ml sterile bottles containing 5 ml 7H9 media and incubating at 37°C on table top shaker for 2 weeks or until $O.D._{600}$ = 0.6. Mutant stocks were prepared in 1 ml 7H9c media containing 20% glycerol and stored in 2 ml screw cap tubes at -80°C.

Colony PCR: About 1 ml of mutant culture was centrifuged, resuspended in 100 µl of sterile water and heat-killed at 95°C for 20 min. The supernatant after

centrifugation was used as genomic DNA template for the PCR reaction to amplify the *gyrA* and *gyrB* genes of the mutants and sequenced.

The DNA Gyrase- Subunits A and B encoding genes *gyrA* (2517 bp) and *gyrB* (2145 bp) were amplified using 3 sets of primers each as follows:

Table 2.1 Primers for whole gene (gyrA and gyrB) sequencing

Primer	Sequence
GyrAF1	5’ gat gggcgaggacgtcgacgc 3’
GyrAR1	5’ gccgtctcggacctgttcggc 3’
GyrAF2	5’ ccc gcggtcgtacctcgctgg 3’
GyrAR2	5’ cgcaccctgcacgcccttgcc 3’
GyrAF3	5’ gcccgc gag gacgtcgttgtc 3’
GyrAR3	5’ gta ccc ggctgccgagcc tag 3’
GyrBF1	5’ cggatccgtatgccggacgtc gg 3’
GyrBR1	5’ ggcgacgtcgctgaccacttc g 3’
GyrBF2	5’ cgccggctgcaa gag atggcg 3’
GyrBR2	5’ gcc cag cgccgt gat gatcgc 3’
GyrBF3	5’ ctggcc gat tgccgttccacg 3’
GyrBR3	5’ ccggtc gag cgagtcgtcagg 3’

2.1.5 Characterization of fluoroquinolone resistant mutants

Minimum inhibitory concentration (MIC) (Pethe et al., 2010)

a) Determination of MIC_{99}:agar plates

MIC_{99} is determined by visually analyzing the mycobacterial pellet formation in broth or colonies on agar. **Agar plate MIC** was determined for FQ resistant spontaneous mutants on 24-well agar plates with FQs at concentrations ranging from 0.1 μM – 50 μM. RIF plates were used as control antibiotic. ~$5x10^4$ cells were inoculated on the wells and incubated for 3 to 4 weeks at 37°C. The plates were visually analyzed for bacterial growth. The lowest concentration at which no growth was observed was noted as the MIC_{99}.

b) Determination of MIC_{50}/ MIC_{90}: Microplate dilution assay

1ml of frozen mycobacterial stock at $O.D._{600}$ = 1.0 was inoculated in 50ml of 7H9c media. The culture was incubated at 37°C until the $O.D._{600}$ reached 0.2 to 0.3. Flat-bottom 96-well assay plates were spotted with FQs, RIF and streptomycin in the 2nd lane to give final concentration of 40 μM, 2 μM and 10 μM in 200 μl of 7H9 respectively. This was further diluted 2-fold in the subsequent wells until concentration of 0.04 μM, 0.002 μM and 0.01 μM was reached for the above drugs respectively. The mycobacterial cultures were diluted to $O.D._{600}$ = 0.04 and 100 μl was inoculated in the assay plate. The plates were incubated under humid condition at 37°C for 5 days. SpectraMax M2 was used to read the absorbance at 600 and the data was plotted to get the MIC_{50}/ MIC_{90} values.

2.1.6 Mutant prevention concentration (MPC)

Liquid cultures of the *Mtb* strains were grown to stationery phase, pelleted and resuspended in fresh 7H9c media to obtain ~$1x10^{10}$ CFU/ ml. Approximately $2x10^{10}$ cells were applied to agar plates containing varying concentrations of GFX, MXF SFX, LVX, CIP and OFX. RIF plates were used as control with a inoculum of $1x10^{9}$ CFU/ ml. Around 20 plates for each concentration for all FQs were used. The plates were incubated at 37°C for 4-6 weeks before CFU counting. The concentration of a given FQ at which no colonies were seen on all the 20 plates was recorded as the MPC for that FQ.

2.2 Structural basis of mapping the spontaneous mutations with 5FU in MtUPRT

2.2.1 Cloning, expression and purification of *Mt*UPRT

A 624 bp DNA fragment consisting of the *upp* gene was amplified by *Taq* polymerase using *Mtb* H37Rv genomic DNA as the template in a PCR reaction. The cloning primers contained the restriction sites BamHI and HindIII and were as follows: uppF 5' GGA TCC GTG CAG GTC CAT GTC GTT GAC 3' and uppR 5' AAG CTT TCA GCG CGG GCC GAA CTG GCG 3'. The purified PCR product was subcloned into pCR 2.1-TOPO vector and transformed in the chemically competent One shot TOP10 cells (Life technologies).

Gateway cloning system (Life technologies) modified in house was used to generate the final expression vectors. The plasmid, isolated from the cells and the entry vector, pNAT745 (with attL1 and 2 sites) were digested with the restriction enzymes BamHI and HindIII and run on a 1% agarose gel. The digested gene fragment and the pNAT745 bands on the gel were purified using gel extraction kit (Qiagen) and ligated using the DNA ligation kit (Roche) followed by transformation into TOP10 cells. The pNAT745-*upp* plasmid was isolated and subjected to LR recombination reaction to clone the gene into four destination vectors, having the attR1 and 2 sites and with different affinity purification tags (His-S, MBP-His-S, NusA-His-S and Trx-His-S) followed by transformation into Tuner (DE3) competent cells (Novagen) *E. coli* cells to yield N-terminal tagged proteins. Transformed cells were grown in LB to a log phase culture ($O.D_{600}$= 0.6

to 0.8) at 37°C in the presence of 30 μg/ml kanamycin, and then induced with 0.2 mM isopropyl β-D-1-thiogalactopyranoside at 18°C for 20 h. Small scale expression and purification of the protein showed that the vector pNAT80 (His-S tag) expressed the protein with least impurities and was further used for large scale protein production.

The purification protocol used was a modified version of the protocol described by Villella *et al.* (Villela *et al.*, 2013). The overexpressed cells were harvested by centrifuging at 7500 g for 30 min. The cell pellet was resuspended and incubated in lysis buffer consisting of Buffer A (20 mM Tris pH 7.5, 300 mM NaCl) and lysonase (Merck) followed by sonication. The cell lysate was collected and treated with 1% (w/v) streptomycin sulphate for 30 min at 4°C and dialyzed overnight with 20 mM Tris (pH 7), 100 mM NaCl at 4°C. The lysate was then subjected to gradient elution on a MonoQ HR 16/10 column followed by affinity purification on HiTrap column. The eluted fractions were then applied to gel filtration column- HiLoad 16/600 Superdex 200 prep grade and eluted with Buffer A to get the isolated *Mt*UPRT protein (The purification columns used were from GE-Amersham). The purity of *Mt*UPRT was analyzed using Novex 4–12% Bis-Tris gels from Invitrogen (Carlsbad, CA, USA) and quantified using a standard Bradford assay. The eluted fractions were concentrated using Vivaspin concentrators (5 kDa cutoff) (Viva Products, Littleton, MA, USA).The aliquots of the protein were stored at -80°C.

2.2.2 Dynamic light scattering (DLS) of *Mt*UPRT

The homogeneity of *Mt*UPRT during concentrating was assessed intermittently using DLS. DLS measurements were performed at room temperature (298 K) on a DynaPro (Protein Solutions) DLS instrument (Wyatt Technology Corp., Santa Barbara, CA, USA). All samples were centrifuged at 18,000 g for 20 min prior to the experiments. Measurements were recorded at 18°C.

2.2.3 Crystallization of *Mt*UPRT

The crystallization of *Mt*UPRT was carried out at 8mg/ml concentration. Crystallization screening was done using the Phoenix Liquid Handling System (Art Robbins Instruments) with the high throughput reagent screens by Hampton and Qiagen. The ratio of protein to crystallization reagent in the crystallization drop was 1:1 (0.2µl each) and it was equilibrated with 40 µl of the reservoir reagent at 25°C. Crystals were observed in the Crystal screen I (Hampton Research, USA) condition number C10 (#34) consisting of 0.1 M sodium acetate trihydrate (pH-4.6) and 2 M sodium formate. However, owing to the smaller crystal size (<0.05mm) optimization of the precipitant concentration, reservoir: protein solution ratio and equilibration temperature were carried out. Grid screen with the above condition was manually set up with the precipitant, sodium formate, ranging from 1.5 to 3 M using the sitting drop vapour diffusion technique. The crystal drops were set up in duplicates in the following reservoir: protein solution ratios- 1:1, 1:2 and 2:1. The plates were equilibrated at 25°C and 16°C. Macro- and micro-seeding techniques were also used during the further optimization of the crystals. Although the crystal could not be reproduced in the

manual grid screening, the micro-seeding (using cat whisker) technique was useful for reproducing the crystals. The initially obtained crystals were diluted 10 times with the reservoir solution and crushed using MicroSeed Beads (Molecular Dimensions) to generate microseeds or microcrystals. A fresh aforementioned grid screen was set up and several tiny microcrystals were streaked onto the new drops using a cat whisker. Notably, bigger and diffraction quality crystals were obtained using this technique with 2 M precipitant and drop ratio of 1:2 at 25°C.

2.2.4 Data collection and structure determination

*Mt*UPRT crystals were soaked in a cryo-protectant solution consisting of the crystallization condition supplemented with either 50% glycerol or perfluoropolyether oil to optimize the cryo condition. The crystals were mounted on nylon loops and flash-cooled at -180°C in the nitrogen cold stream. The complete data set for *Mt*UPRT was collected using the in-house Rigaku rotating anode generator (Microfocus rotating anode X-ray generator Rigaku MicroMax(tm)-007 HF). Two complete data sets consisting of 120 and 180 images were collected with a 1° oscillation range at a wavelength of 1.5418Å. The data collection statistics are provided in Table 1. The data was processed with HKL 2000.

2.2.5 *Mycobacterium bovis* BCG culture conditions, selection of spontaneous mutants against 5-fluorouracil and sequencing of *upp*

Mtb surrogate, *Mycobacterium bovis* BCG, was used to select for the spontaneous mutants with 5FU. *Mt*UPRT from both strains are 100% identical. Liquid culture

of *M. bovis* BCG was obtained in 1 liter roller bottles containing 50-100 ml Middlebrook 7H9 media supplemented with 10% ADS (Albumin Dextrose Saline), 0.05% Tween80 and 0.2% glycerol. Middlebrook 7H11 agar plates, with or without 5FU were used to grow *M. bovis* BCG as colonies. The liquid cultures were incubated at 37°C until $O.D._{600}$ =0.6-0.8 (~1×10^8 CFU/ml; colony forming units). Around 1×10^8 CFU were applied on agar plates containing 5 and 20 µg/ml 5FU. The plates were incubated at 37°C for 4 to 6 weeks. Mutant subcultures were obtained by inoculating a single colony in 30 ml sterile bottles containing 5 ml 7H9 media and incubating at 37°C on table top shaker for 2 weeks or until $O.D._{600}$ = 0.6.

Sequence analysis of *Mtb upp*: About 1 ml culture of mutant culture was centrifuged and the pellet was resuspended in 100 µl of sterile water and heat-killed at 95°C for 20 min. The supernatant after centrifugation was used as genomic DNA template in the PCR reaction to amplify the *upp* gene of the mutants followed by sequencing. Following primers were used for PCR reactions and sequencing:

SuppF 5’ ggacgcacccgtatcagcccc3’

SuppR 5’ cgcagcgaatctccaagtagc 3’

2.2.6 5FU susceptibility of 5FU resistant mutants with *Mt*UPRT mutations

MIC_{50} were determined for the 5FU resistant mutants to evaluate their susceptibility to 5FU (Refer to section 2.1.5 (b) for the experimental procedure).

2.3 Structure and mapping of spontaneous mutational sites of PyrR from Mtb

2.3.1 Cloning expression and purification of *Mtb* PyrR

pyrR-pET28b construct (codon optimized for *E. coli)* was ordered from Genscript and was transformed in Tuner (BL21 DE3) competent *E. coli* cells (Novagen) to yield N-terminal His-tagged protein. The transformed cells were grown in Luria-Bertani medium to a log phase culture ($O.D._{600}$= 0.6 to 0.8) at 37°C in the presence of 30 μg/ml kanamycin, followed by induction with 0.5 mM isopropyl β-D-1-thiogalactopyranoside at 18°C for 20 h.

The overexpressed cells were harvested by centrifugation at 7500 × g for 30 min. The cell pellet was resuspended in lysis buffer consisting of Buffer A (20 mM Bis-Tris pH 6.5, 200 mM NaCl, 5% Glycerol and 1mM DTT) followed by sonication. The lysate was first processed by affinity chromatography using a HiTrap column (GE-Amersham). Subsequently, the eluted sample was applied to the HiLoad 16/60 Superdex 200 prep-grade gel filtration column (GE-Amersham), and eluted with Buffer A. The purity of PyrR was analyzed using Novex 4–12% Bis-Tris gels which showed a single band at approximately 25 kDa (Invitrogen Carlsbad, CA, USA) and quantified using a standard Bradford assay. The eluted fractions were pooled and concentrated to 4 mg/ml using Vivaspin 20 concentrators (5 kDa cut-off) (Viva Products, Littleton, MA, USA). The homogeneity of PyrR was further confirmed by Dynamic light scattering (DLS) experiments as mentioned in section 2.2.2.

2.3.2 Crystallization of PyrR-5FU complex

The crystallization screening of PyrR (4 mg/ml) in the presence 5FU (ratio-1:100) was carried out manually. The ratio of protein to crystallization solution (Hampton Research, USA) in the crystallization drop was 1:1 (1 µl each); the drop was equilibrated with 450 µl of reservoir solution at 25°C using hanging drop method. The PyrR-5FU complex crystals were observed in the crystal screen I condition consisting of0.1 M imidazole pH 6.5, 1.0 M sodium acetate trihydrate. The above condition was optimized in grid screening combined with additive screen. Diffraction-quality crystals were obtained with the above condition in the presence of 10% v/v 1,2-Butanediol at 25°C.

2.3.3 Data collection and structure determination

The PyrR-5FU complex crystals were briefly soaked in 50% glycerol (cryo-protectant) before they were mounted on nylon loops and flash-cooled at -180°C in a nitrogen cold stream. The complete dataset for *Mtb* PyrR-5FU was collected using the in-house Rigaku rotating anode generator (Microfocus rotating anode X-ray generator Rigaku MicroMax-007 HF) using the Saturn 944+ detector. The data collection and structure statistics are provided in Table 1. The data was processed with HKL 2000 (Otwinowski & Minor, 1997). The *Mtb* PyrR structure solutions were obtained through molecular replacement method using Phaser program (McCoy *et al.*, 2007). The coordinates from PDB: 1W30 were used as the starting search model. Six molecules of PyrR were observed in the asymmetric unit. The PyrR model was examined and built in COOT (Emsley & Cowtan, 2004). Phenix-refine was used for further refinement (Adams *et al.*,

2010). The PyrR was modeled to fit in its substrates and 5FU followed by the refinements using the COOT and Phenix programs, respectively. The final structure was refined up to 2.6 Å resolution with an R-factor of 0.19 (R_{free} 0.23) (Table 5.1) The overall geometry of the final model was analyzed by Ramachandran plot with the program (Chen *et al.*, 2015).

2.3.4 *Mycobacterium bovis* BCG culture conditions, selection of spontaneous mutants against 5FU and sequencing of *pyrR* gene

As mentioned earlier *Mtb* surrogate, *Mycobacterium bovis*BCG, was used to select for the spontaneous mutants with 5FU. PyrR sequence from both strains are 100% identical. Selection of spontaneous mutants on 5FU was carried out as mentioned in section2.2.5.

Sequence analysis of *Mtb pyrR*: About 1 ml culture of mutant culture was centrifuged and the pellet was resuspended in 100 µl of sterile water and heat-killed at 95°C for 20 min. The supernatant after centrifugation was used as genomic DNA template in the PCR reaction to amplify the *pyrR* gene of the mutants followed by sequencing. The primers listed below were used for PCR reactions and sequencing:

SpyrRF1	5’ cgtgcgagtgctacgctgccg 3’
SpyrRR1	5’ ggtcggcgtcgtcgaggatgg 3’

2.3.5 5FU susceptibility of 5FU resistant mutants with PyrR mutations

MIC_{50} were determined for the 5FU resistant mutants to evaluate their susceptibility to 5FU (Refer to section 2.1.5 (b) for the experimental procedure).

3
Molecular genetics of fluoroquinolone resistance

Inappropriate use of drugs selects for bacteria with new types of mutations resulting in inevitable emergence of resistance to antibiotics. Comprehensive information of molecular genetics of drug resistance mechanism is essential for appropriate formulation of dosing strategy, for the development of efficient diagnostic tools and for the development of new drugs or drug derivatives (Ramaswamy & Musser, 1998). Introduction of newer generation FQs was being considered recently to evaluate their efficacy to shorten the current 1st line anti-TB therapy to 4 months (Bryskier & Lowther, 2002). FQs show broad spectrum anti-bacterial activity against both replicating and non-replicating mycobacteria. FQ mechanism of action involves inhibiting the DNA gyrase enzyme, resulting in the interruption of DNA replication (Drlica, 1999).

3.1 DNA gyrase- Fluoroquinolone target

DNA gyrase is a heterotetramer composed of two subunits of GyrA and two subunits of GyrB subunits (Blanchard, 1996). The catalytic core of DNA gyrase comprises of the C-terminal domain of GyrB and N-terminal domain of GyrA. DNA gyrase is an essential enzyme required in relaxation of supercoiled DNA during the process of replication, transcription and recombination. DNA gyrase accomplishes this function by generating double strand breakage in the DNA strands for strand passage followed by re-ligation of the strands (Figure 3.1).

3.2 Mechanism of action of fluoroquinolones

FQ mechanism of action involves interruption of DNA replication by inhibiting the DNA gyrase. FQs interact with the quinolone-binding pocket (QBP) of DNA gyrase within the catalytic core of the enzyme by forming a ternary complex with the DNA-DNA gyrase assembly (Figure 3.2) (Piton *et al.*, 2010). This halts the re-ligation of the DNA strands leading to the inhibition of replication consequently resulting in cell death due to double-strand breaks (DSBs) in the DNA. The QBPs or the quinolone resistance determining regions (QRDRs) of the GyrA (QRDR-A; amino acids 74 to 113) (Takiff *et al.*, 1994) and GyrB (QRDR-B; amino acids 500 to 538) (Cole *et al.*, 1998) are conserved regions. Mutations in these regions confer resistance to FQs (Takiff *et al.*, 1994).

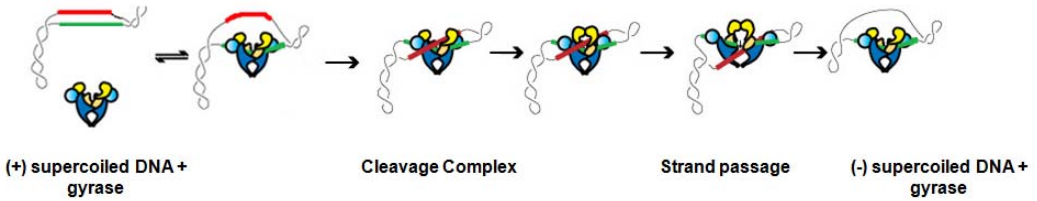

Figure 3.1 DNA gyrase function and the mechanism of FQ action. *(Piton et al., 2010). The FQs covalently bind to the DNA gyrase cleavage complex thereby inhibiting the gyrase function to re-ligate the DSBs in the DNA. Bacterial cell death results due to occurrence of several DSBs throughout the chromosome.*

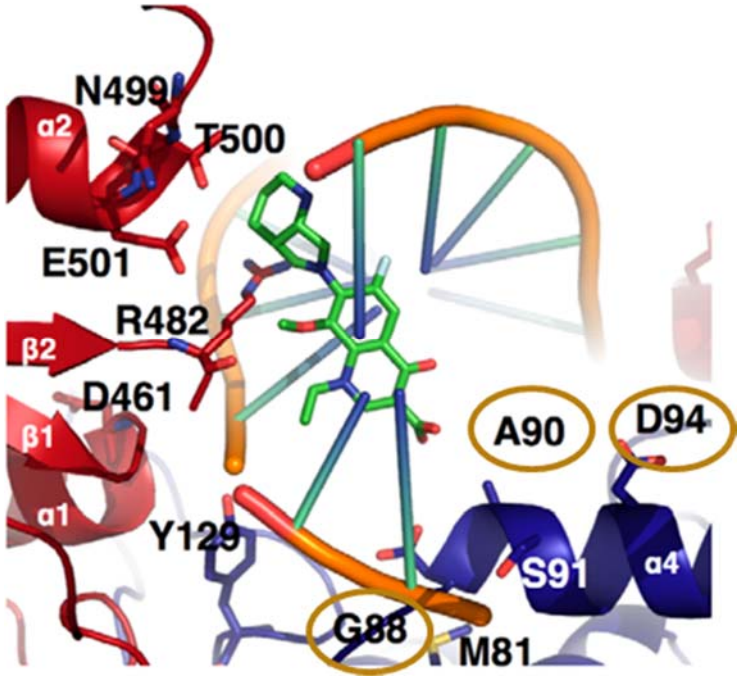

Figure 3.2 Moxifloxacin interacting with Quinolone Binding Pocket (QBP) of DNA gyrase *(Piton et al., 2010). (The above GyrB residue numbering: D461, N499, T500 and E501 correspond to D500, N538, T539 and E540 in Mtb as described by Cole et al., 1998)*

3.3 Fluoroquinolone resistance

The introduction of FQs in the 1st line TB drug regimen is of concern due to emergence of resistance in *Mtb* particularly due to its wide use for treatment of other infections, for example urinary tract infections, community acquired pneumonia, typhoid fever and ocular infections (Singh *et al.*, 2012, Field *et al.*, 2012). Mycobacteria are known to be intrinsically less susceptible to FQs; therefore acquired resistance is the only kind that can be controlled by rational formulation and use of these antibiotics. Understanding the molecular genetics of FQ resistance before designing treatment regimens and formulation strategies are hence critical for the clinical laboratories and the TB control program (Sun *et al.*, 2008, Drlica & Malik, 2003).

3.4 Molecular genetics of fluoroquinolone resistance

It is known that most mutations (approximately 90%) associated with FQ resistance map to the QRDR-A and QRDR-B (Antonova *et al.*, 2008, Mokrousov *et al.*, 2008, Sekiguchi *et al.*, 2007, Kocagoz *et al.*, 1996). Consequently, majority of the studies are focused on the mutations located within the QRDR-A (Zhou *et al.*, 2000, Devasia *et al.*, 2012) and only recently, some investigations include those in QRDR-B (Pantel *et al.*, 2012, Malik *et al.*, 2012). Earlier reviews also revealed considerable discrepancies in the reported percentages of GyrA mutations ranging from 11% to 90%, while the GyrB mutations were not taken into account by most of the studies (Pitaksajjakul *et al.*, 2005, Huang *et al.*, 2005, Cheng *et al.*, 2004, Yew *et al.*, 2000, Giannoni *et al.*, 2005). Additionally, the

mutations outside the QRDRs were not identified. Recent findings, indicating that mutations outside the hotspot (QRDR) confer resistance in clinical isolates (Devasia *et al.*, 2012, Ginsburg *et al.*, 2003, Pantel *et al.*, 2012) calls for detailed assessment of these mutations. Such information would be useful in designing molecular diagnostic tests with better sensitivity and specificity. For the assessment of resistance and to get a comprehensive picture of all possible mutations on the DNA gyrase, we sequenced the entire *gyrA* and *gyrB* genes for 318 *Mtb*- H37Rv and 351 *Mtb*- CDC1551 laboratory-generated FQ spontaneous mutants.

Although newer FQs (MXF and gatifloxacin (GFX)) are generally more potent, their structures are based on the same scaffolds of existing FQ (example ciprofloxacin (CIP)) with minor changes (Figure 3.3); thus the inherent risk of cross-resistance remains a hindrance to proper treatment (Walsh, 2003a). In addition, there is a possibility of FQs been used in the treatment of other infectious diseases (for example, urinary tract infections and enteric fever) in patients prior to the activation of TB (Dalhoff, 2012). This prior exposure of *Mtb* to sub-optimal dose of other FQs leads to selection of low level resistance through cross-resistance to FQs used in TB treatment (Baquero, 2001). This mandates the understanding of cross resistance patterns amongst the FQs which will allow for rational formulation of an anti-TB drug regimen (Malik *et al.*, 2012, Caminero, 2006, Alangaden *et al.*, 1995, Sirgel *et al.*, 2012).

Researchers have examined this significant aspect of cross resistance for the FQs. However, these studies included only a few of the clinically used FQs, for

instance, study done by Alangaden *et al*. included only CIP, levofloxacin (LVX), and sparfloxacin (SFX) (Alangaden *et al.*, 1995). Also, collective inferences from these studies could be biased, as these studies used different *Mtb* strains namely clinical isolates (Sirgel *et al.*, 2012), pathogenic or the attenuated laboratory strains (Kocagoz *et al.*, 1996) by different research groups. Moreover, cross-resistance patterns for the newer FQs- MXF and GFX (developed in 2000-2005) remain to be evaluated.

Sindelar *et al.* proposed a significant approach to limit emergence of resistant strains due to selective drug pressure called the mutant prevention concentration (MPC) (Sindelar *et al.*, 2000). Their study showed that FQ concentrations in serum could be reached above the MPC and thus useful in designing effective dosing strategies that would limit emergence of resistant strains. These MPCs, however, have not been considered by most of the studies or have been reported for only one clinically used FQ (Zhou *et al.*, 2000).

FQ resistant strains or mutants emerge due to spontaneous mutations or SNPs (single nucleotide polymorphism) on the DNA gyrase when subjected to sub-optimal or intermittent exposure to FQ concentrations (Drlica, 1999). Thus, molecular genetic studies and determining minimum inhibitory concentrations of these resistant strains are paramount to evaluate FQ resistance mechanism and selection of mutant types and thus under critical investigation (Xu *et al.*, 1996). In this regard, we initially evaluated the effect of MXF selected *M. bovis* BCG mutants on the FQ resistance mechanism. Later we extended this study to examine FQ resistance mechanism in the *Mtb* strains- H37Rv and CDC1551 with

six clinically used FQs. The structures of the FQs used in this study are mentioned in Figure 3.3.

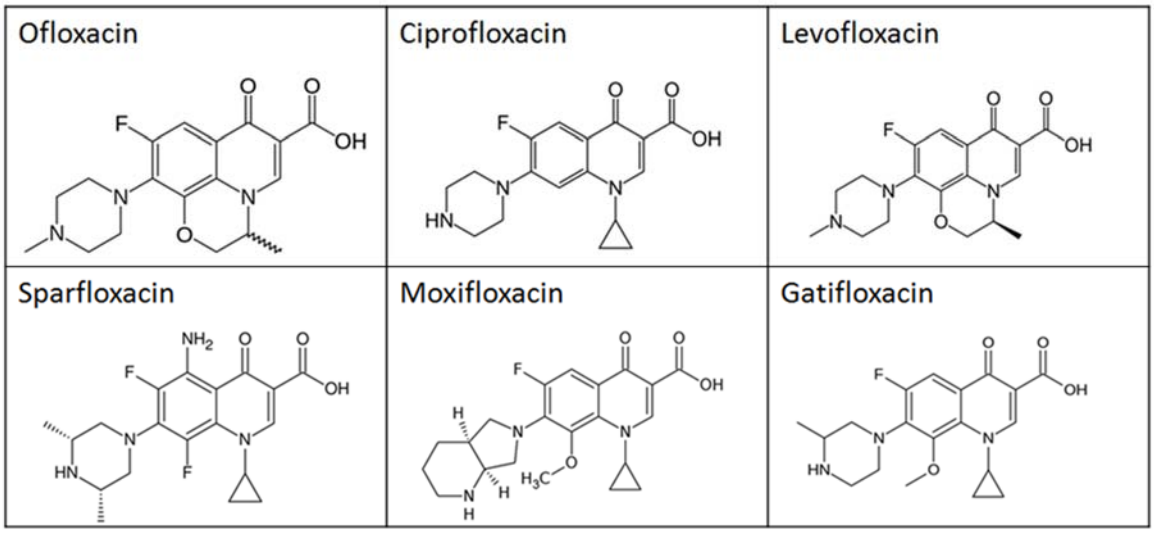

Figure 3.3 Fluoroquinolones used in this study.

3.5 Objectives

The specific objectives for the first part of the study were as follows:

1) To determine mutation frequency and frequency of mutation type selected on different clinically used FQs at varying concentrations.
2) To determine the MICs of all FQs and the level of resistance exhibited by various mutant types.
3) To determine cross resistance patterns exhibited by different mutants types selected on different FQs and at different concentrations
4) To evaluate the MPCs for the six FQs.

3.6 Results

MXF is under evaluation ever since its inclusion in the 1st line therapy for TB has been considered (Blanchard, 1996). One way to assess this issue is to select for spontaneous mutants with MXF to identify and analyze the mutations that confer the low- to high-level resistance. Formulation of dosing strategies utilizes such information to determine the concentration that can maintain lowest or no mutational levels. It has been observed previously and in this study that, with increasing drug concentration (selection pressure) the type of mutation selected varies until specific variants that confer the highest resistance are selected with very low mutation frequency, while at low concentration various types of low-level resistance mutants are selected (Zhou *et al.*, 2000).

3.6.1 Selection and sequence analysis of *M. bovis* BCG spontaneous mutants at 1.25 µM and 5 µM MXF

In our initial experiment we determined mutation frequency of *M. bovis* BCG against 1.25 µM and 5 µM of MXF (2.5 and 10 times MIC_{99} respectively). The mutants were sequence analyzed to evaluate the different alleles of DNA gyrase that were selected. The mutation frequency was found to be 1×10^{-9} at 1.25 µM while there were no mutants recovered at 5 µM of MXF. In total, twelve mutants were recovered on 1.25 µM. Sequencing their QRDR-A and QRDR-B regions resulted in identification of SNPs only in QRDR-A at 2 positions, Gly88 and Asp94 (Table 3.1).

Table 3.1 GyrA alleles selected at 1.25 µM MXF

SNP's in QRDR-A	No. of mutants
G88C	4
D94G	6
D94N	1
D94Y	1
Total	12

Cross resistance is another important challenge when drugs belonging to the same class are used in treatment regimens. Therefore, in our pilot study, we also sought to evaluate this phenomenon for the MXF resistant strains harboring the mutations- D94G, D94N, D94Y and G88C by determining the MIC_{99} of other FQs on agar plates. The six FQs used were as follows: GFX, MXF, SFX, CIP, LVX and OFX. The aforementioned MIC_{99} result showed that above MXF resistant strains were cross resistant to all the FQs and a slight shift towards higher MIC_{99} observed was in the order as follows: GFX < MXF/SFX/CIP < LVX < OFX (Table 3.2). Interestingly, MIC_{99} shift was also observed within the strains depending on the resistant allele. MIC_{99} for the G88C variant was higher than the D94G/N/Y variants.

Table 3.2 MIC_{99} of FQs against M. bovis BCG MXF resistant alleles.

FQ (µM)	WT-BCG	D94G	D94N	D94Y	G88C
GFX	0.2	5	5	5	5
MXF	0.5	10	10	10	20
SFX	0.5	10	10	10	20
LVX	0.5	20	20	20	20
CIP	1	10	10	10	20
OFX	2	50	50	50	50

3.6.2 Frequency of mutation and mutation types of *M. bovis* BCG against the six FQs at 5 µM- Preliminary data

The mutation frequency of *M. bovis* BCG was found to be at 1×10^{-8} for OFX, CIP and LVX; 1×10^{-9} for MXF; between 1×10^{-8} and 1×10^{-9} for SFX. There were no mutants recovered on GFX above 5 µM. Interestingly, predominance of mutation type selected was dependent on the type of FQ used for selection (Table 3.3). For instance, MFX only selected the G88 variant, LVX selected mostly the D94 variants whereas, OFX also selected the A90 variant along with D94. To analyze this phenomenon that the genotype (amino acid mutation in DNA gyrase) and the resistance phenotype (mutation frequency) depend on the type of FQ we selected for FQ spontaneous mutants in *Mtb*.

Table 3.3 Mutation frequency and mutation types of M. bovis BCG selected against FQs at 5 µM

FQ	FQ generation	Mutation frequency	G88C	D94Y	D94N	D94G	A90V	S91P	**Total**
GFX	4th	$<1.0\times10^{-9}$	-	-	-	-	-	-	-
MXF	4th	1.1×10^{-9}	27	-	-	-	-	-	**27**
SFX	3rd	1.6×10^{-9}	-	-	4	-	-	-	**4**
LVX	3rd	1.0×10^{-8}	4	5	7	4	-	-	**20**
CIP	2nd	1.3×10^{-8}	3	14	9	5	-	-	**31**
OFX	2nd	3.0×10^{-8}	5	12	10	11	33	3	**74**
Total			**39**	**31**	**30**	**20**	**32**	**3**	**156**

It has been shown in CIP and its analogs that, apart from dependence of genotype or phenotype of mutants selected on these FQs, their concentration also affects the selection of mutant alleles (Zhou *et al.*, 2000). Due to the broad-spectrum antimicrobial activity of FQs, they are widely used in treatment of other infectious pathogens at various concentrations. Therefore, we extended our study to comprehensively evaluate the drug concentration, mutation-type and frequency relationship amongst FQs in *Mycobacterium* strains. *Mtb* strains H37Rv and CDC1551 were used in a single experimental setup to recover spontaneous mutants on FQs to access the possibility of different strains harboring diverse mutation spectrums. FQ concentrations ranging from 0.1 μM to 50 μM were used.

H37Rv is a virulent laboratory strain, whereas CDC1551 is a recent clinical isolate responsible for the TB outbreak during 1994 to 1996 with virulence comparable to H37Rv (Valway *et al.*, 1998, Manca *et al.*, 1999). CDC1551 has undergone several passages in laboratory since then. The proteome of these two strains was found to be highly similar (Betts *et al.*, 2000). The GyrA protein sequence of both these strains is identical except at 3 residues (Glu21Gln, Ser95Thr and Gly668Asp) whereas the first 28 amino acids from the CDC1551 GyrB are either missing or it could be an annotation artifact.

3.6.3 Frequency of spontaneous mutations at varying FQ concentrations

The mutation frequency of the *Mtb* strains and *M. bovis* BCG was ~1×10^{-8} at 0.5 to 2 μM and 0.5 to 1 μM of GFX respectively, while no mutants were recovered above 5 and 2 μM respectively (Table 3.4). A similar mutation frequency (1×10^{-8}) of the *Mtb* and BCG strains was obtained at 1 to 5 μM and 0.5 to 2 μM of MXF respectively. Similar mutation frequency was observed with SFX. For LVX the above frequency was observed at higher concentrations- 5 to 10 μM and 2 to 10 μM respectively for the *Mtb* strains- CDC1551 and H37Rv, whereas, for CIP and OFX these concentrations further increased to 5 to 20 μM and 5 to 10 μM respectively for the *Mtb* and BCG strains.

Table 3.4 Frequency of mutation at increasing FQ concentrations, at cell density 1×10^8 CFU.

a. *M. bovis* BCG

µM	GFX	MXF	SFX	LVX	CIP	OFX
50	0	0	0	0	0	0
20	0	0	0	0	0	0
10	0	0	0	0	3.5	0.25
5	0	0	0	2	11	1.25
2	0	1	1	2.75	46	6.75
1	1	2.3	4	4	149	DL
0.5	1.75	2.5	7	DL	L	L
0.2	17.75	11.5	DL	L	L	L
0.1	L	L	L	L	L	L

b. *Mtb*-H37Rv

µM	GFX	MXF	SFX	LVX	CIP	OFX
50	0	0	0	0	0	0
20	0	0	0	0	0.27	0.33
10	0	0	0	0.33	1.83	3.36
5	0	0.62	0.44	4.21	4.24	4.05
2	2.18	2.72	1.36	-	-	-
1	2.32	6.1	4.75	-	L	L
0.5	-	-	-	L	L	L
0.2	L	L	L	L	L	L
0.1	L	L	L	L	L	L

c. CDC1551

µM	GFX	MXF	SFX	LVX	CIP	OFX
50	0	0	0	0	0	0
20	0	0	0	0	0.75	1
10	0	0	0	2.75	1.75	2.75
5	0	2.5	2.25	2	2	4
2	3	2.5	2.75	5.5	9.5	21.5
1	3.4	3.25	4.5	16	L	L
0.5	5	12.75	6.25	L	L	L
0.2	L	L	L	L	L	L
0.1	L	L	L	L	L	L

[Note: Bacterial growth- L= Lawn or Confluent; DL= dispersed lawn or semi-confluent]

3.6.4 Distribution of SNPs across DNA gyrase of the FQ resistant *Mtb* strains- H37Rv and CDC1551

To obtain a statistically significant data, 318 H37Rv and 351 CDC1551 mutants were selected for sequencing the *gyrA* and *gyrB* genes. Sequencing was not done in the *M. bovis* BCG. Table 3.5 summarizes the distribution of mutants according to the mutation location (on or outside of QRDR-A and QRDR-B).

Table 3.5 gyrA and gyrB sequencing summary for H37Rv and CDC 1551 mutants

Mutants	No. of variants		% of variants	
	H37Rv	CDC	H37Rv	CDC
QRDR-A	280	255	88.05	72.64
QRDR-B	18	30	5.66	8.54
Outside-QRDR-A	1	16	0.31	4.55
Outside-QRDR-B	8	32	2.51	9.11
WT DNA gyrase	11	18	3.45	5.12
Total	318	351	100	100

FQs selects for alterations mostly on QRDR-A of Mtb strains

Sequencing of the H37Rv and CDC1551 mutants revealed that 88% and 72% respectively had a SNP within the QRDR-A and around 5% and 8% within the QRDR-B (Table 3.5). These numbers also correspond to the percentages observed in the clinics (Cui *et al.*, 2011). GyrA mutations at 3 positions (G88, A90 and D94) alone made up to 96% of the total QRDR-A mutations in both strains (Table 3.6). Mutants with these SNPs have highest MICs and are considered as the high-level resistance mutants. Given their high prevalence and impact on drug resistance, they are frequently analyzed for the detection of MDR TB. However, recent studies indicate that the high-level resistance could also arise from the generally overlooked, low level resistant mutants in events when FQ dose is inadequate or compromised. In our study ~3.8% of such mutations were observed on the QRDR and ~2.8% outside the QRDRs of both the genes (Tables 3.6 and 3.7). We report here 2 new variants of GyrA recovered from this study; A126E and A288D, which exhibited lower MICs (Figure 3.7).

The QRDR-B region should be redefined

A significant percentage of mutations were observed outside the QRDRs of both the genes. Around 8% H37Rv mutants and 18% CDC1551 mutants had SNPs on the GyrB. Amongst these GyrB mutations, the SNPs at T539 and E540 occurred in $1/4^{th}$ and $1/3^{rd}$ of the total H37Rv and CDC1551 GyrB mutants respectively (Table 3.5). Four novel GyrB variants namely T539I, T539A, E540A and S486Y were recovered from our study.

Table 3.6 Frequency of FQ resistant GyrA alleles of Mtb strains

GyrA	Mutation	H37Rv	CDC	Total
QRDR-A	G88C	20	154	174
	A90V	80	68	148
	D94G	102	7	109
	D94H	35	5	40
	D94N	24	4	28
	D94Y	6	4	10
	S91P	3	4	7
	D89N	8	4	12
	D94A	1	2	3
	D94V	1	0	1
	A74S	0	2	2
	S95A	0	1	1
Outside QRDR-A	A126E	0	12	12
	A126D	1	0	1
	A288D	0	4	4
Total	15	281	271	552

Table 3.7 Frequency of FQ resistant GyrB alleles of Mtb strains

GyrB	Mutation	H37Rv	CDC	Total
QRDR-B	N538K	1	19	20
	N538D	10	4	14
	N538S	1	2	3
	N538Y	0	2	2
	N538T	5	0	5
	D500N	0	1	1
	G509S	0	1	1
	L518F	1	1	2
Outside QRDR-B	R485C	0	9	9
	T539T	0	5	5
	T539I	1	3	4
	T539A	3	2	5
	E540D	0	3	3
	E540V	2	4	6
	E540A	0	1	1
	S486Y	0	2	2
	S486F	0	2	2
	A543V	2	1	3
Total	19	26	62	88

[Note: The GyrB numbering system is according to Cole *et al*. (Cole *et al.*, 1998, Maruri *et al.*, 2012)]

Predominance of particular gyrase alleles is concentration dependent

In general, at higher concentrations of FQs, lesser mutants and with high level of resistance were selected for both H37Rv and CDC1551 strains (Figure 3.4 and 3.5). The SNPs at position D94 and G88 were predominantly selected at all FQ concentrations in the H37Rv and CDC1551 strains respectively. The SNPs at position A90 was predominantly selected at 5 μM and 2 μM of FQs in the H37Rv and CDC1551 strains respectively. SNPs in GyrB mostly occurred at lower FQ concentrations in both the strains.

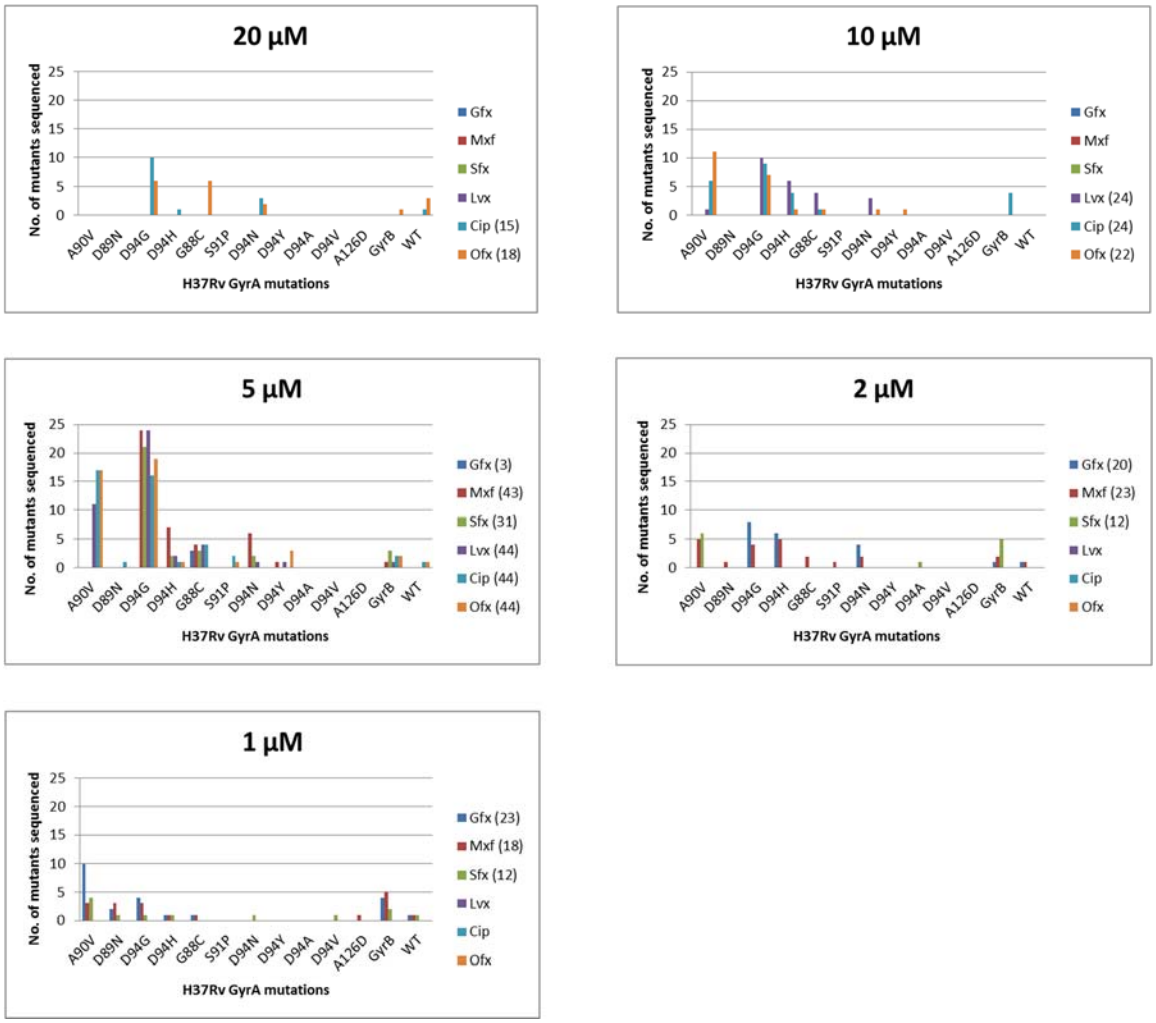

Figure 3.4 Spectrum of DNA gyrase alleles of H37Rv selected by different concentrations of FQs. *At higher concentrations of FQs mutations conferring high-level resistance were specifically selected while at lower concentrations wide range of DNA gyrase alleles selected. (The digits in brackets indicate number of mutants selected on the FQ for sequencing.)*

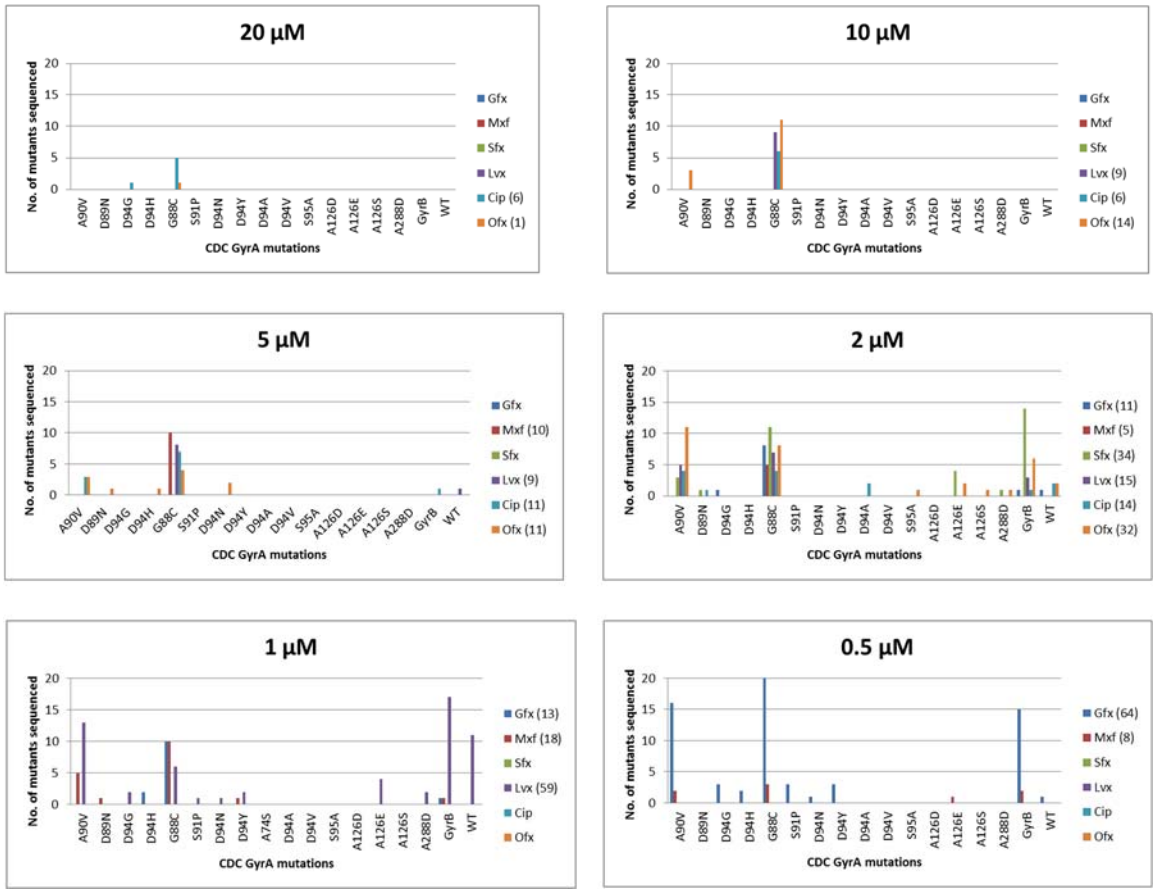

Figure 3.5 Spectrum of DNA gyrase alleles of CDC1551 selected by different concentrations of FQs. *At higher concentrations of FQs mutations conferring high-level resistance were specifically selected while at lower concentrations wide range of DNA gyrase alleles selected. (The digits in brackets indicate number of mutants selected on the FQ for sequencing.)*

3.6.5 Comparison of frequency of mutant types selected at varying FQ concentrations

To analyze the effect of FQ type on the selection of spontaneous mutants we separately plotted the spectrum of DNA gyrase alleles selected at varying concentrations of each FQ. Figures 3.6 and 3.7 summarize the spectrum of GyrA alleles in the FQ resistant H37Rv and CDC1551 strains respectively. Figures 3.8 and 3.9 summarize the spectrum of GyrB alleles in the FQ resistant H37Rv and CDC1551 strains respectively.

Variants of GyrA in H37Rv and CDC1551

In the H37Rv strain, D94G was the most abundant SNP selected by all concentrations of FQs followed by A90V, several variants of D94 (D94H, D94N, D94Y, D94A and D94V) and G88C (Figure 3.6). The aforementioned SNPs were also the most predominantly selected SNPs at higher concentrations of all FQs (below the concentration where no mutants are selected called MPC; MPC varies amongst the FQs) and are associated with high level of resistance. For example, only D94 variants (with a few exceptions) were selected at 5 μM of MXF and SFX and 20 μM of CIP and OFX.

In contrast to H37Rv, the most abundant SNP in the CDC1551 strain was G88C followed by A90V (Figure 3.7). Nevertheless, similar to H37Rv, they were also associated with high level of resistance. Three new SNPs-A74S, A126E and A288D were recovered in the CDC1551 strain. All these new variants occurred at lower concentrations of FQs.

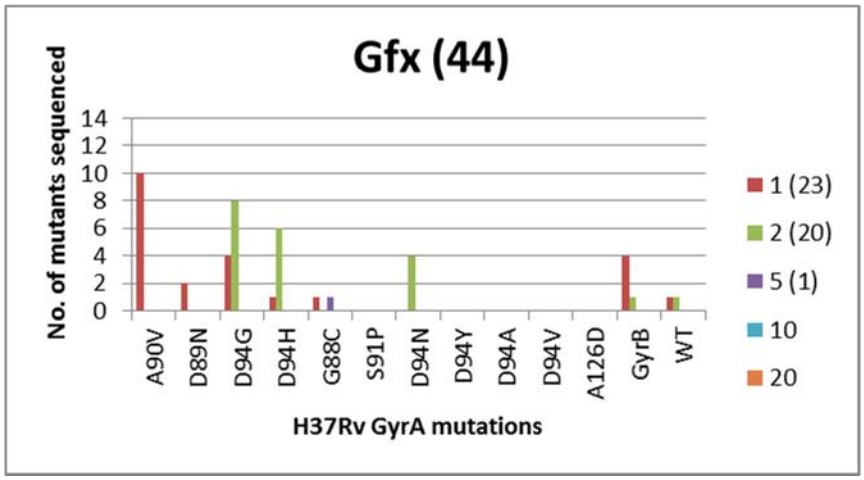

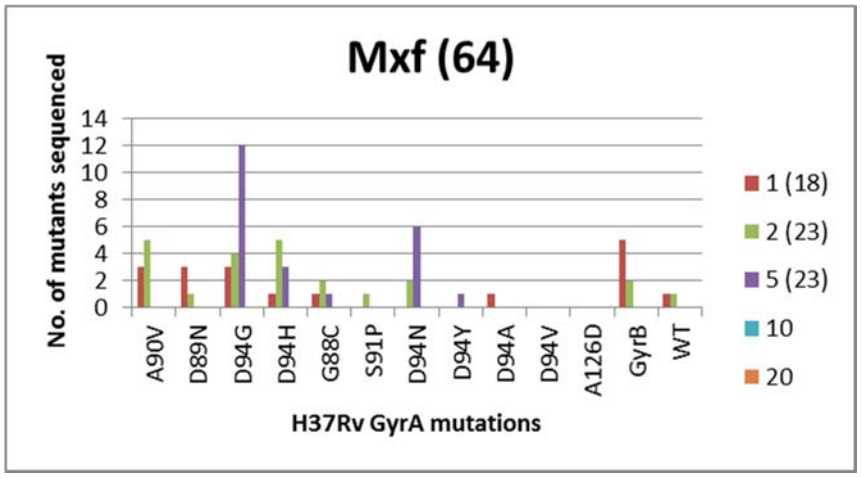

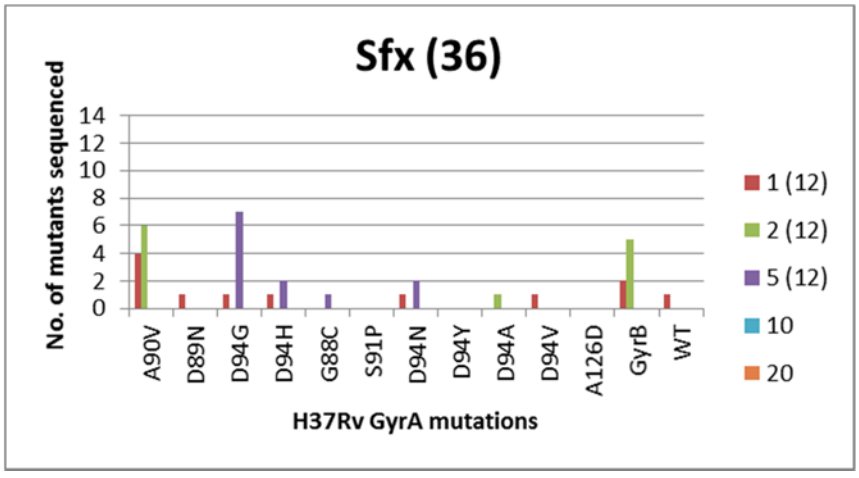

Figure 3.6 Effect of FQs and their concentrations (μM) on the spectrum of GyrA alleles of FQ resistant H37Rv. *(The digits in brackets indicate number of mutants selected at that concentration for sequencing.) (Figure continued on next page)*

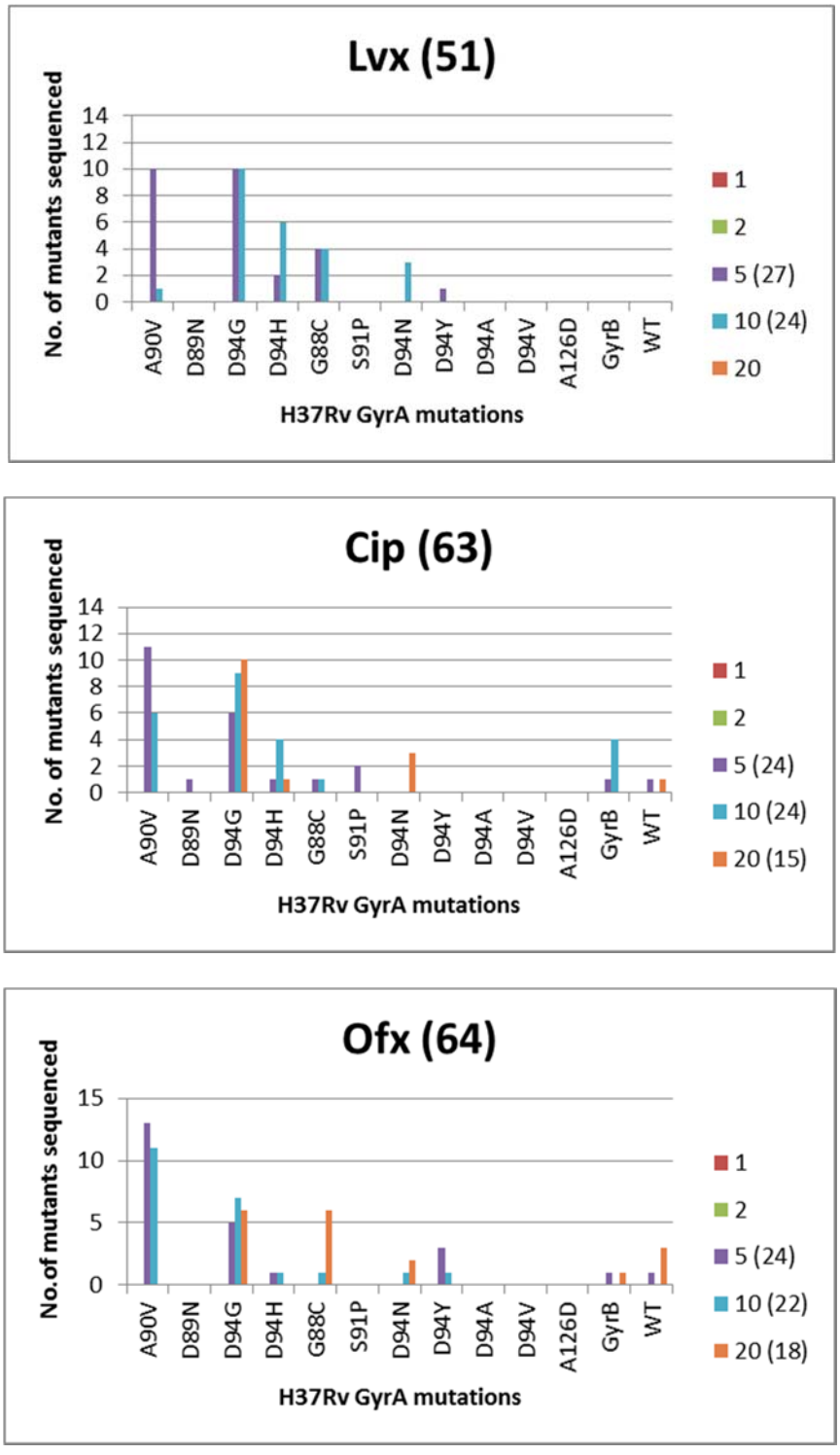

Figure 3.6 Effect of FQs and their concentrations (µM) on the spectrum of GyrA alleles of FQ resistant H37Rv. *(The digits in brackets indicate number of mutants selected at that concentration for sequencing.) (Figure continued from previous page)*

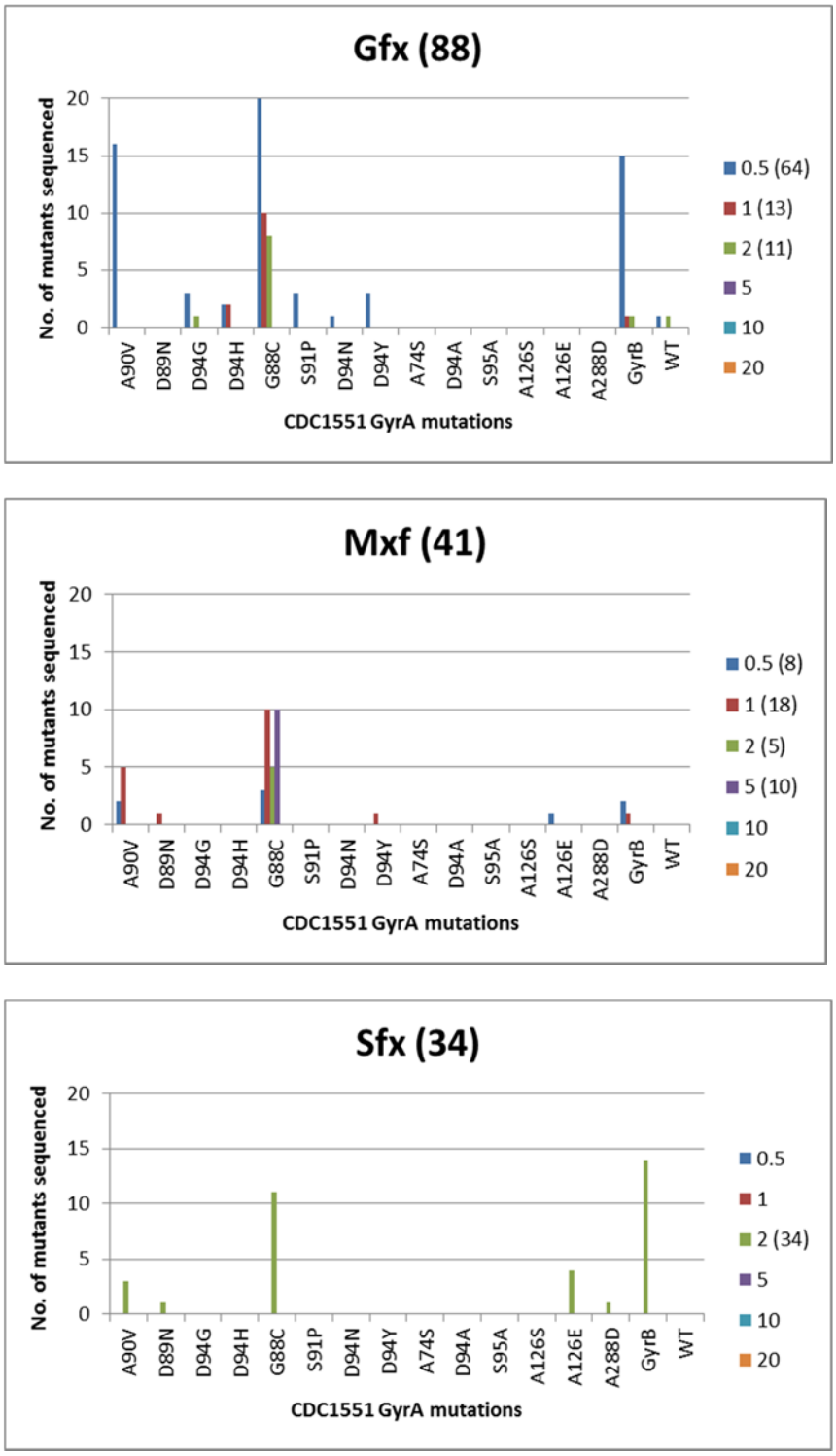

Figure 3.7 Effect of FQs and their concentrations (μM) on the spectrum of GyrA alleles of FQ resistant CDC1551. *(The digits in brackets indicate number of mutants selected at that concentration for sequencing.)**(Figure continued on next page)*

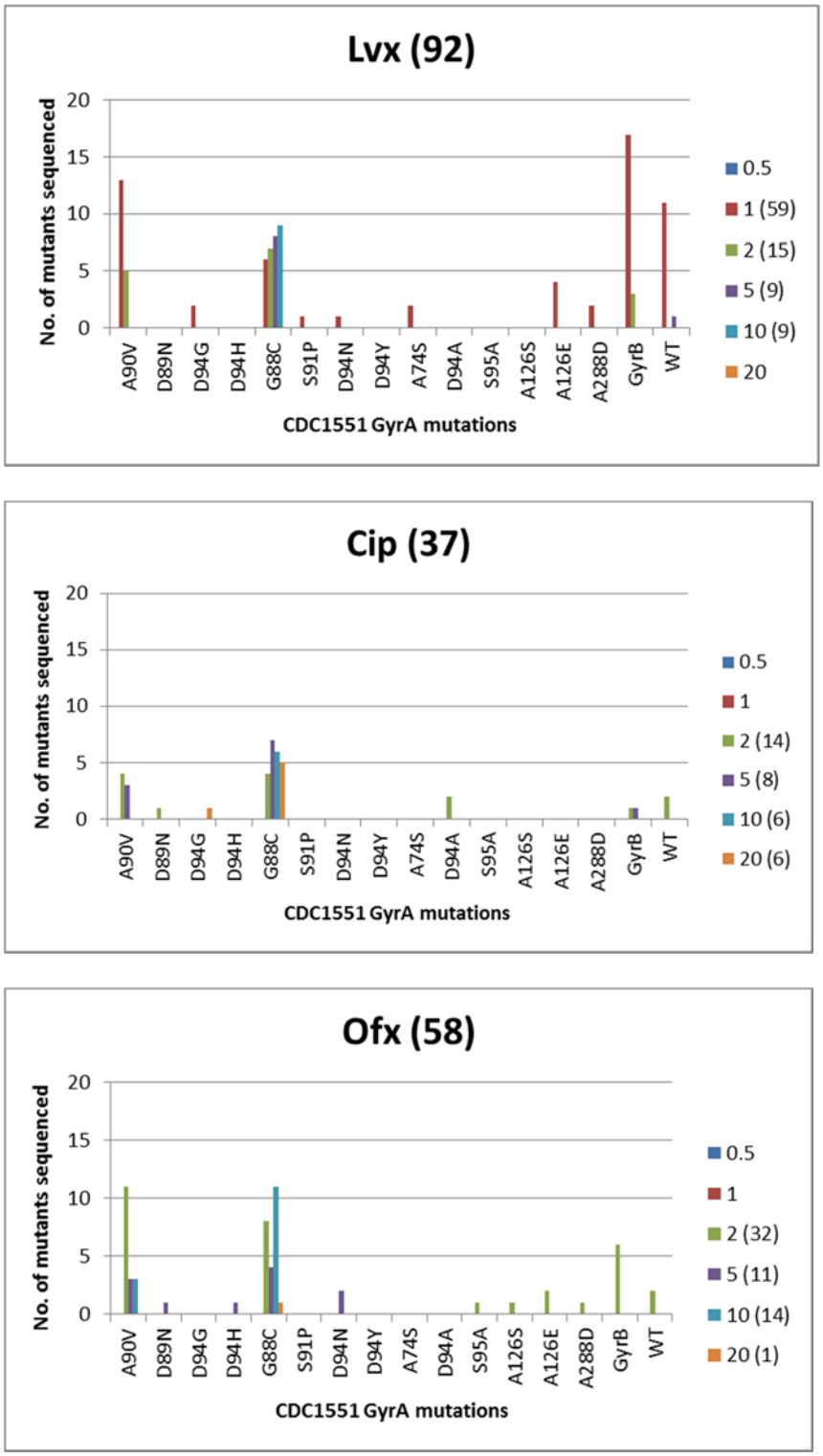

Figure 3.7 Effect of FQs and their concentrations (µM) on the spectrum of GyrA alleles of FQ resistant CDC1551. *(The digits in brackets indicate number of mutants selected at that concentration for sequencing.)(Figure continued from previous page)*

Variants of GyrB in H37Rv and CDC1551

The GyrB alleles of H37Rv were predominantly selected at lower concentrations of all FQs in contrast to GyrA. Yet, within the lower concentration range, the high-level resistant GyrB variants were selected at higher concentration. The SNPs at N538 and T539 were more common (Figure 3.8). At 1 μM, MXF and SFX selected GyrB alleles that were located outside the QRDR-B. All the five H37Rv mutants selected at 2 μM SFX harbored the mutation N538T. The new H37Rv GyrB variants: L518F, T539A and T539I, were found in this study and reported for the first time.

GyrB variations were observed to a greater extent in CDC1551 than in H37Rv. The number of distinct GyrB variants in H37Rv and CDC1551 was 9 and 17 respectively (Table 3.7). Several new variants of GyrB were recovered with the CDC1551 strain, namely, R485C, S486Y, G509S, N538Y and E540A in addition to the above mentioned new variants in H37Rv (L518F, T539A and T539I).

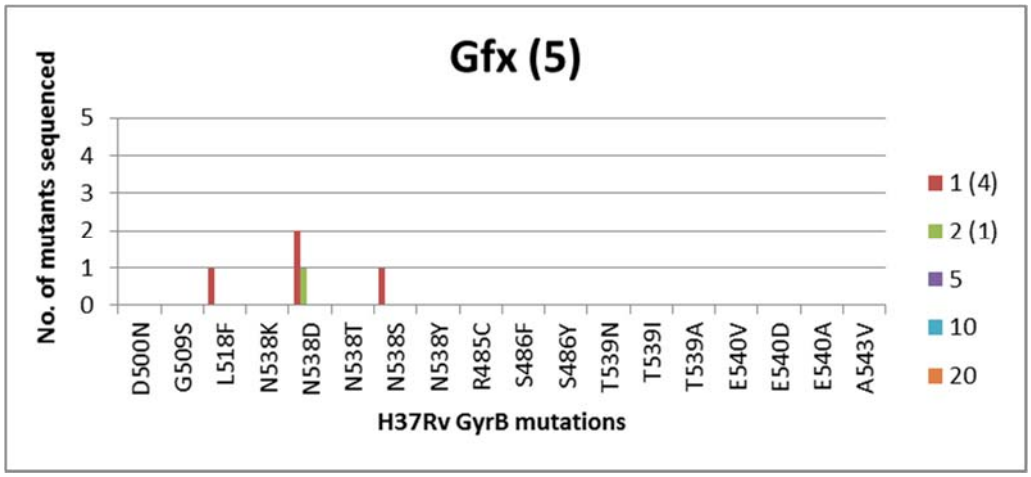

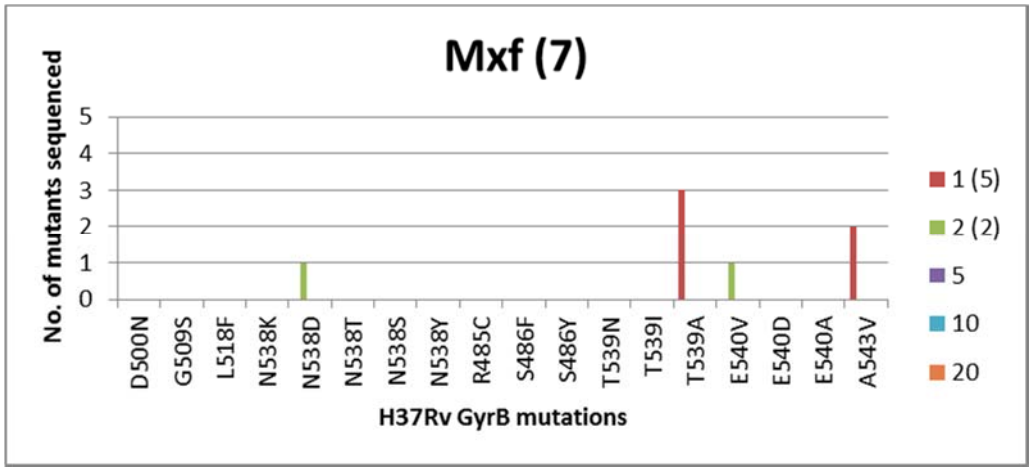

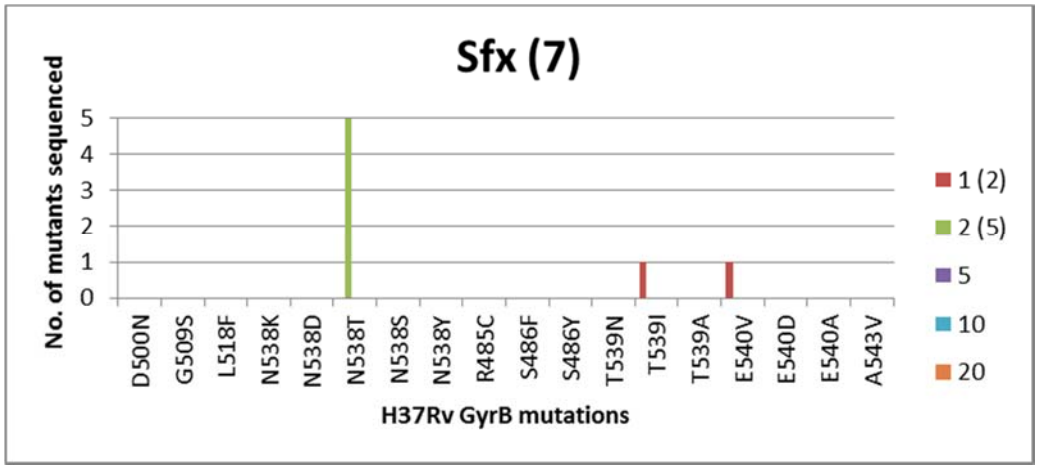

Figure 3.8 Spectrum of recovered H37Rv GyrB alleles. *(The digits in brackets indicate number of mutants selected at that concentration for sequencing.) (Figure continued on next page)*

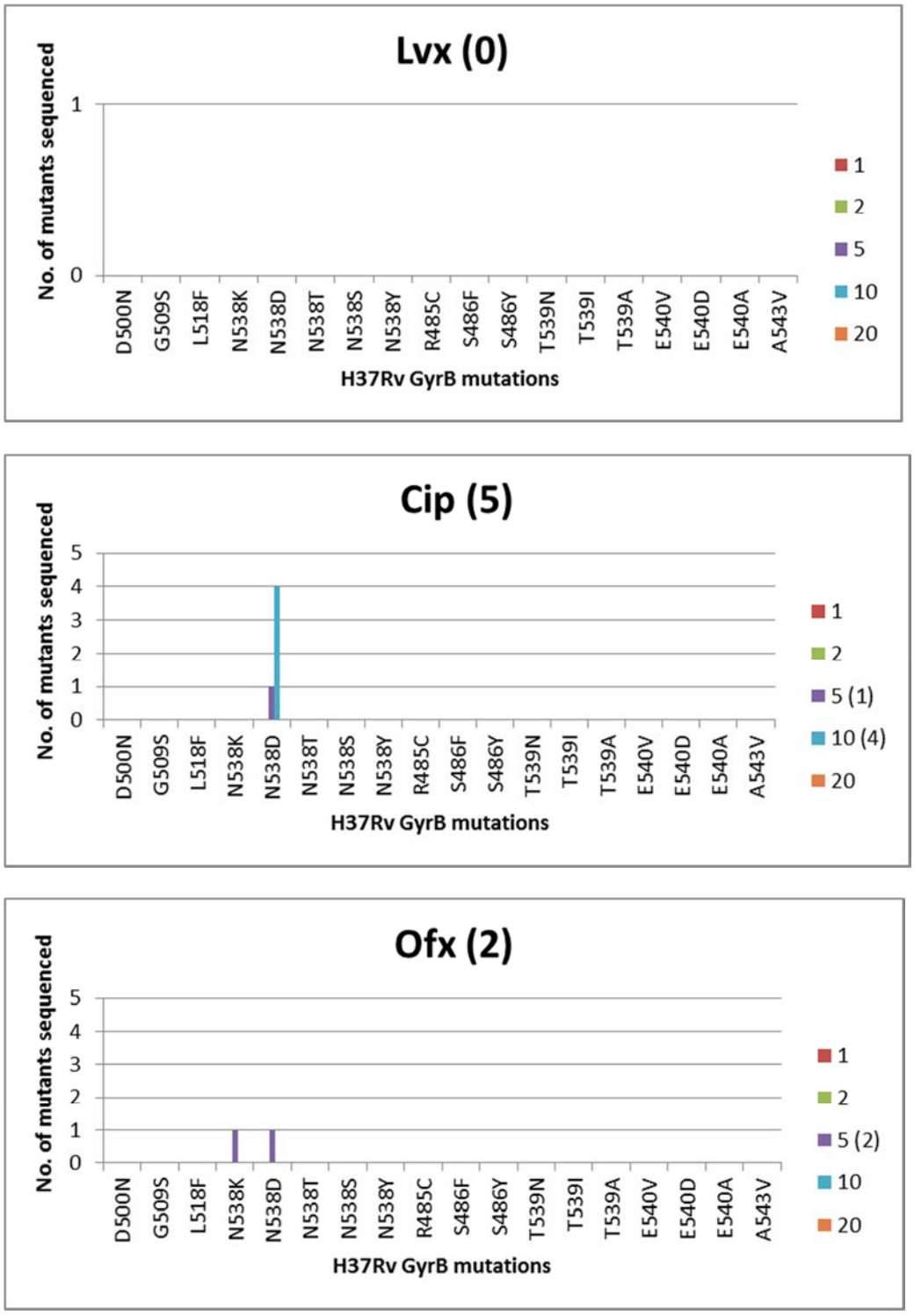

Figure 3.8 Spectrum of recovered H37Rv GyrB alleles. *(The digits in brackets indicate number of mutants sequenced) (Figure continued from previous page)*

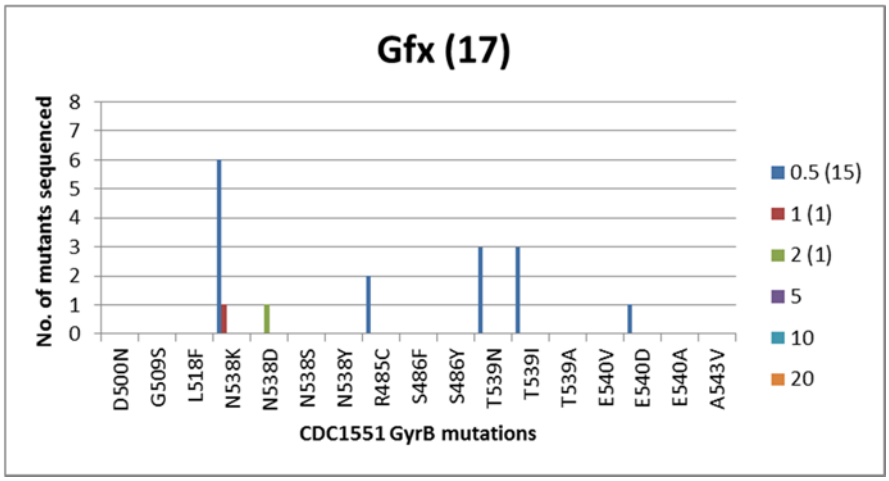

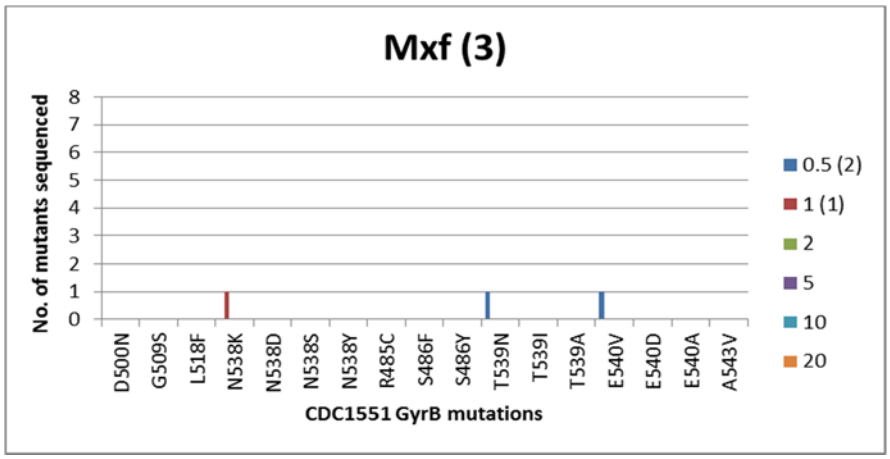

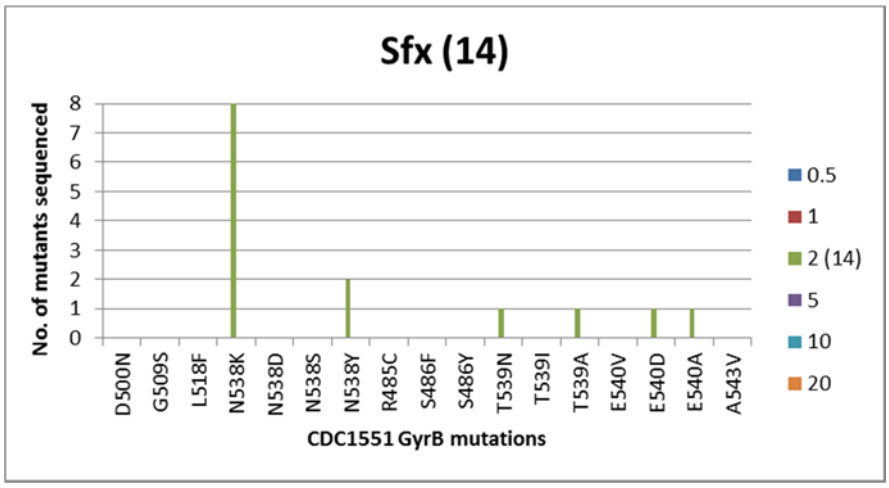

Figure 3.9 Spectrum of recovered CDC1551 GyrB alleles. *(The digits in brackets indicate number of mutants sequenced) (Figure continued on next page)*

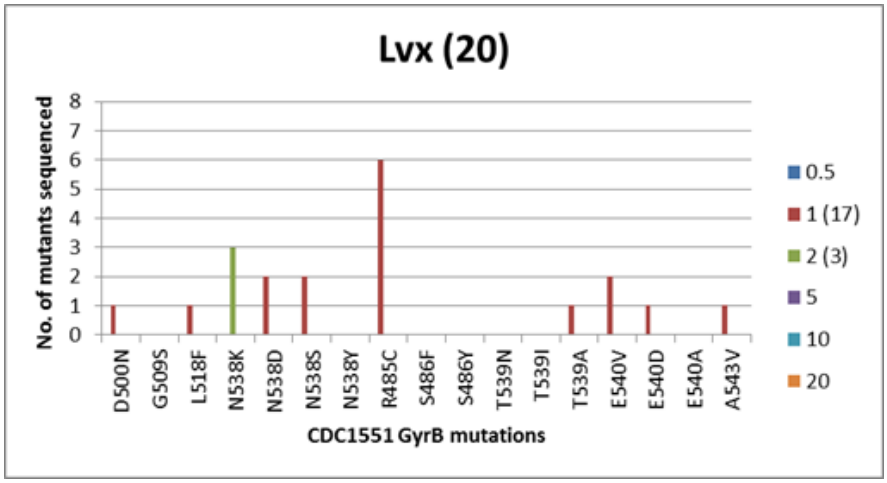

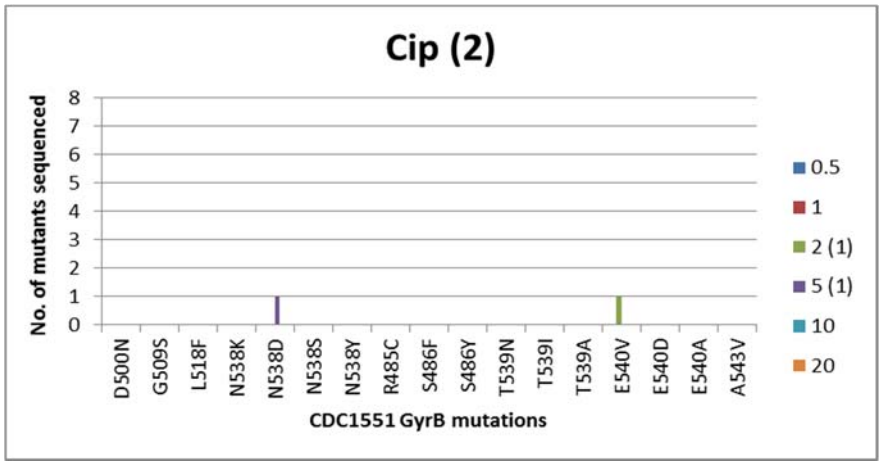

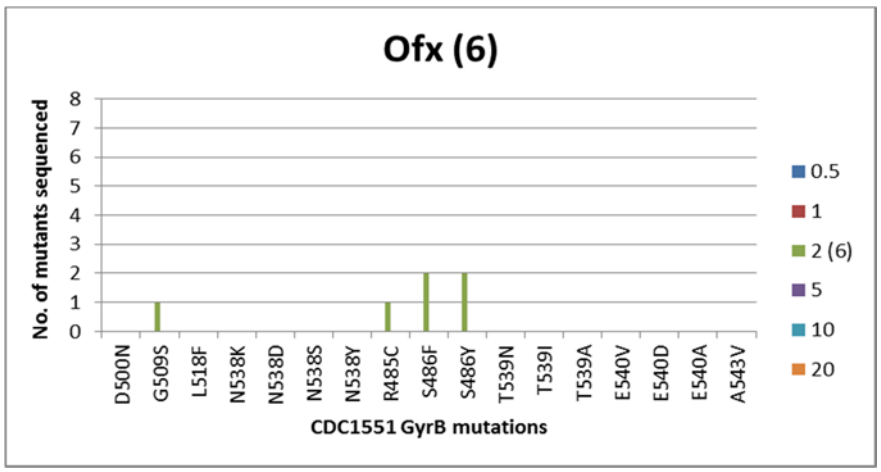

Figure 3.9 Spectrum of recovered CDC1551 GyrB alleles. *(The digits in brackets indicate number of mutants selected at that concentration for sequencing.) (Figure continued from previous page)*

3.6.6 Cross resistance- susceptibility of DNA gyrase alleles to FQs

As mentioned earlier a shift in MIC was observed in *M. bovis* BCG with the FQ resistant mutants in the order GFX < MXF/SFX/CIP < LVX < OFX. Similar trend was observed with the DNA gyrase variants of the CDC1551. GFX was the most active and exhibited least MICs for all the CDC1551 mutants used in the experiment. When the FQ MICs in a few GyrA variants were measured, G88C was found to be the least susceptible followed by A90V. The GyrB variants N538K and E540V were also less susceptible to the FQs, and thus require higher drug concentration to restrict their growth into colonies (Figure 3.10).

When the MICs FQs in the mutant strains were compared with the wild type (WT) CDC1551 strain (Table 3.8), the GyrB mutants with alterations in the non - QRDR- T539N and R485C showed susceptibility to GFX, MXF and SFX but resistance to LVX, CIP and OFX. The GyrA variants with non-QRDR alterations exhibited similar MICs as WT. Interestingly, for GyrB variant N538K exhibited around 3 fold increase in MIC with GFX and MXF whereas only by 2 fold with OFX.

Table 3.8 FQ MIC_{99} in Mtb strains - H37Rv and CDC1551.

FQ	H37Rv (μM)	CDC1551 (μM)
GFX	≤0.7	≤0.7
MXF	≤0.7	≤0.7
SFX	≤0.7	≤0.7
LVX	1.25	1.25
CIP	2.5	2.5
OFX	2.5	2.5

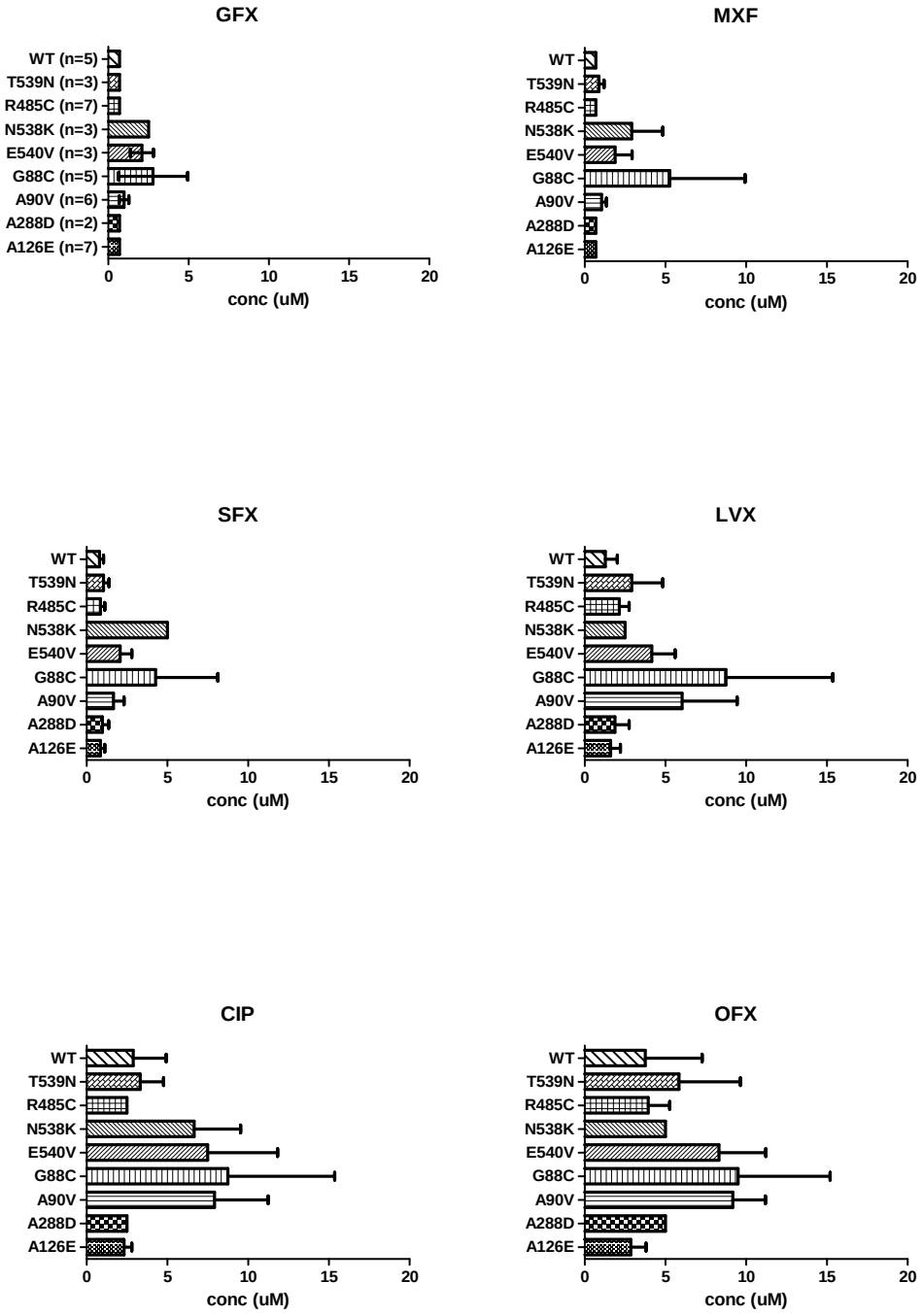

Figure 3.10 Cross resistance: Susceptibility of DNA gyrase variants of CDC1551 to fluoroquinolones. *(The "n=" values on y-axis of GFX indicate number of mutants selected to test against all FQs; WT= Mutants having WT sequence for GyrA and GyrB)*

3.6.7 Mutant prevention concentration of FQs

No mutants were selected above 5 μM of GFX in an inoculum of approximately 2×10^{10} CFU (Figure 3.11). Selection of no mutant could be achieved at 10 μM of MXF and SFX and 20 μM of LVX. Whereas, more than 20 μM of CIP and OFX was required for limiting the emergence of resistant mutant. MPC for CIP and OFX is attainable as shown previously, however experiments with higher than 20 μM was not possible in our study.

GFX MPC (5 μM) is below its C_{max} (10.15 μM) while both the values for MFX are similar (Table 3.8). (C_{max} values in pharmacokinetics are defined by the maximum concentration a drug can achieve in the given test area of the body). Both, CIP and OFX, exhibit very high MPC values while their C_{max} is reached at lower concentrations. MPCs of CIP and OFX are between 20 μM and 50 μM respectively; whereas their C_{max} is only 7.24 μM and 8.3 μM respectively.

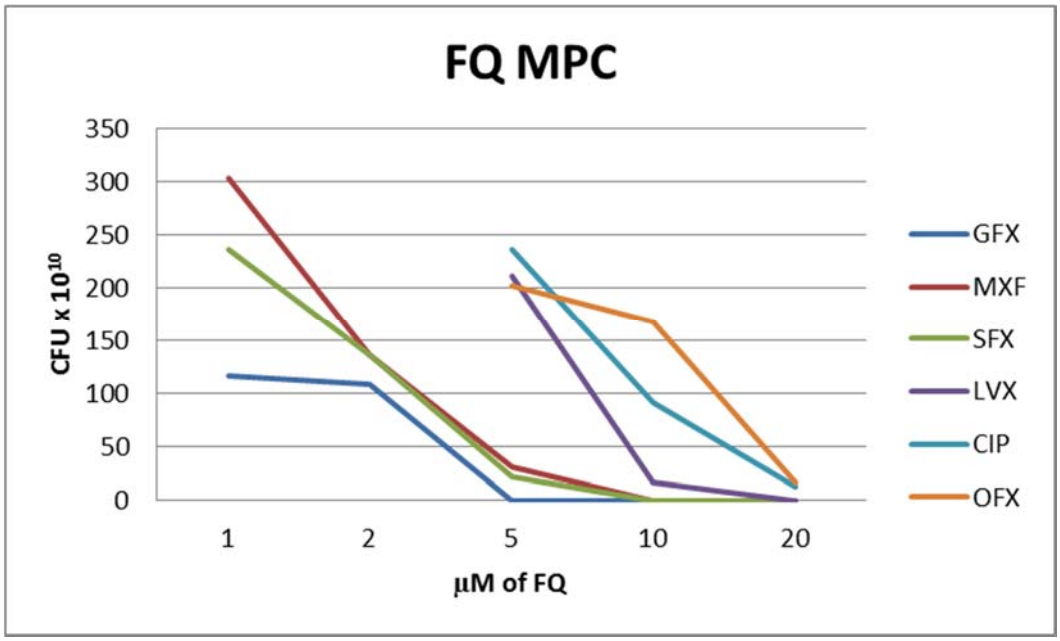

Figure 3.11 Mutant prevention concentrations of Fluoroquinolones.

Table 3.9 Mutant prevention pharmacodynamics for commercial FQs (Brennan & Young, 2008, Nuermberger & Grosset, 2004)

FQ	Mol. wt.	Dose Mg	Cmax µg/mL	AUC µg*h/mL	Cmax µM	MPC (µM)	AUC µM*h
GFX	374.42	400	3.8	33	10.15	5-10	88.14
MXF	401.11	400	4.3	36.1	10.72	5-10	90.00
SFX	392.41	200	1.1	18.8	2.80	5-10	47.91
LVX	361.38	500-750	6.2	45	17.16	10-20	124.52
CIP	331.35	250-750	2.4	11.6	7.24	20-50	35.01
OFX	361.38	1000	3	24	8.30	20-50	66.41

[Note: C_{max}- maximum concentration a drug can achieve in the given test area of the body

AUC- Area under the curve or actual body exposure to drug after administration of a dose of drug.

MPC- Mutant prevention concentration]

3.7 Discussion

Our results indicate that newer generation FQs namely GFX, MXF and SFX are the most potent FQs against *Mtb.* While, similar potency with CIP, LVX and OFX could be achieved only at 4-5 times the concentration of GFX, MXF, and SFX, suggesting that these are less potent against *Mtb*. Secondly, as compared to GFX, MXF and SFX, 2 and 4 fold higher concentration of CIP, LVX and SFX was required to limit the emergence of *M. bovis* BCG and *Mtb* mutants respectively. These findings suggest that different generation antibiotics could have different frequencies of mutation which is attributed to the potency of the newer generation compounds. However, the cross-resistance still remains an issue for drugs from the same class of compounds.

The data presented above also emphasizes that commercially available FQs used for treatment of tuberculosis differ with respect to enrichment of resistant mutants. The 318 H37Rv and 351 CDC1551 spontaneous mutants obtained in this study were analyzed to evaluate the frequency of occurrence of different mutation types or gyrase variants by sequencing the target genes- *gyrA* and *gyrB*. Interestingly only single nucleotide polymorphism were observed unlike the occasional double mutations observed in the clinics (Cui *et al.*, 2011). Increasing concentrations of the FQs selected for the mutant strains with mutations that confer higher-level of resistance and a concentration could be reached where no mutant was recovered. This data resonates with the results obtained by Zhou *et al*. with CIP and its analogues. We also observed that, some mutations were predominantly selected by a specific FQ, for instance, the newer FQ, MXF,

selected most mutants that harbored high-level resistance mutations of *gyrA* (except at lower concentrations) while LVX, CIP and OFX selected wide variety of variants on both *gyrA* and *gyrB*. Interestingly, selection of variants also demonstrated dependence on FQ concentrations, for instance, lower FQ concentrations primarily selected variants (low-level resistant mutants) with mutations mostly on *gyrB* and outside of the QRDR-A/B. These results show that, the resistance genotype (amino acid mutation in DNA gyrase) and phenotype (mutation frequency) depends on the type of FQ as and resonates with the results reported by Zhou *et al*. (Zhou *et al.*, 2000). Interestingly, higher concentration of MXF was observed to overcome the low level resistance and corresponds with observation reported by Poissy *et al*. (Poissy *et al.*, 2010).

Sequencing statistically significant number of mutants allowed us exhaustive scrutiny of those low-level resistance mutations that are conventionally ignored, owing to the fact that most (85-90%) occur on the hotspot QRDR regions of *gyrA* and *gyrB*. It is known that, low-level resistance increases probability of clinical resistance, and thus, if ignored (in the light of wide use of FQs at lower concentrations to treat other infectious diseases) could lead to dire consequences (Baquero, 2001). Subsequently, MIC_{99} determination of the selected mutants shows that the level of resistance is often higher than the concentration used for selection. This result suggests that appropriate assessment of these mutations in TB patients is crucial while the formulation of drug-regimen and has valuable contribution towards limiting emergence of resistance.

Sequencing the entire *gyrA* and *gyrB* gene revealed a significant percent (2.82% in H37Rv and 13.66% in CDC1551) of SNPs on the outside of their QRDRs. Ignoring these SNPs could cause considerable difference while reporting their percentage of mutations on DNA gyrase and probably a hindrance to FQ resistance mechanism studies. Moreover, our results support the recent suggestion made to include codons 539 and 540 in the QRDR-B (Maruri *et al.*, 2012) taking into account that, 25% H37Rv and 33% CDC1551 of GyrB mutations occurred in these two codons (current QRDR-B: codon 500-538). Also, mutants with alterations at these two codons are known to have higher MIC values and also as seen in our cross resistance study (Figure 3.7).

The cross-resistance patterns exhibited by FQ resistant DNA gyrase variants assessed in our study strengthens the argument and significance of understanding patient history of FQ usage, prior to the administration of the anti-TB treatment. Our results show that the variants selected on one FQ were resistant to all other FQs used in this study. Of importance was the differential degree of shift in MIC that was observed amongst the FQs in the order of GFX < MXF < SFX < LVX < CIP < OFX. GFX and MXF, the newer FQs, had the least shift in MIC which reinforced their potency. Interestingly, MIC shift was also observed within the variants depending on the type of mutation it harbors; MIC for the G88C variant was higher than the D94G and A90V variants of *M. bovis* BCG and A90V variant of CDC1551. The QRDR-B variants N538K and E540Vexhibited increased MIC with all the FQs while the non-QRDR-B variants exhibited increased MIC with LVX, CIP and OFX. Interestingly, for N538K, the fold increase in MIC with

GFX and MXF was higher than OFX. This observation suggests that N538 is more susceptible to OFX than GFX or MXF, as reported previously for this GyrB variant (Malik *et al.*, 2012) and other GyrB variant N533 (Von Groll *et al.*, 2009) reiterates the consideration of analysis of GyrB alterations while investigating the FQ resistant clinical isolates. The 2 to 3 fold increase in MIC of the non-QRDR-B variants-T539N and E540V emphasize their inclusion in the QRDR-B as suggested by Maruri *et al*. Overall, these MIC values demonstrate their potential application in the formulation of drug concentrations in clinical trials.

The lowest MPC of GFX once again suggests that it is the most potent of all FQs followed by MXF and SFX. There seems to be no probability of emergence of mutants with GFX, since its MPC is at 5 μM while its C_{max} reaches as high as 10.15 μM at the current GFX dosage. In contrast, CIP and OFX seem to be undesirable to limit the emergence of resistant *Mtb* strains. The MPC experiments show that maximum CIP concentration achieved in human body with the current dosage is much lower than the concentration required to limit the emergence of *Mtb* resistance. This result support the suggestion made by Field *et al.* to avoid CIP in the TB drug regimen (Field *et al.*, 2012). In sum, with the currently recommended dosages CIP and OFX would certainly lead to resistance, while GFX and MXF would prevent resistance. Thus, it is critical to understand the MPC of FQ.

Together, our results suggest consideration of re-designing current FQ formulations, re-defining the QRDR region for GyrB and 'not to' underestimate the significance of low-level resistant mutations. Overall, our study evaluated the

determinants necessary to understand the genetics of FQ resistance which would be useful in the efforts made to limit the emergence of resistance, thereby aiding the TB control program.

3.8 Future directions

Cross resistance and MICs were evaluated for only a few DNA gyrase variants. Examining these aspects for all the variants and particularly low-level resistant mutants would help in better understanding their resistance level. As some of these mutations exhibit susceptibility to older FQs but not the more potent newer FQs. Such information could be useful in dosing strategies for resistant TB cases.

Around 3 to 5 percent of the strains had WT DNA gyrase sequencing suggesting other mechanisms of FQ resistance, for instance, efflux pumps. Whole genome sequencing of these strains would help to acquire this information.

Although the results obtained here resembles the data observed in the clinics, further studies in animal models need to be carried out to validate the findings.

4

Structural basis of mapping the spontaneous mutations with 5-fluorouracil from Mycobacterium tuberculosis

Dormant or non-replicating *Mtb* harbors in one third of the world population which results in latent TB infection (LTBI); 5 – 10% of which, if untreated, has a probability to develop active TB infection. Thus, effective diagnosis and treatment of LTB infection is one of the goals of the TB control program. As mentioned earlier, molecular genetics could also be utilized in the identification of novel *Mtb* drug targets thereby providing insights into the development of new class of compounds. As such, 5FU showed antitubercular activity and whole genome sequencing of 5-fluorouracil (5FU) resistant mutants led us to the identification of uracil phosphoribosyltransferase (*Mt*UPRT) and pyrimidine operon regulatory protein (PyrR) as the probable targets in *Mtb* (Mathys *et al*., unpublished). In the light of its involvement in the energy saving salvage pathway, which is possibly active in dormant *Mtb*, *Mt*UPRT is an attractive *Mtb* target. However, 5FU is highly toxic and cannot be used in TB treatment. Nevertheless, structural insights of this protein would help in understanding its functional implications in *Mtb* and facilitate the screening for novel anti-TB chemical entities.

4.1 Role of MtUPRT in pyrimidine biosynthesis - Salvage pathway

The enzyme uracil phosphoribosyltransferase (UPRTase; EC 2.4.2.9) which is explored as drug target in several clinical conditions (Hughes *et al.*, 2005, Dong & Zhang, 2014, Villela *et al.*, 2013, Sunamura *et al.*, 2002, Switzer *et al.*, 1999) is involved in the low energy-requiring pyrimidine salvage pathway. As such, it is known to be active during the energy-saving seedling (dormant) stage in plants (Bressan *et al.*, 1978) and in the absence of *de novo* pyrimidines in bacteria (Martinussen & Hammer, 1994). UPRTases catalyses the conversion of uracil and 5'-phosphoribosyl-α-1'-pyrophosphate (PRPP) to pyrophosphate (PPi) and uridine 5'-monophosphate (UMP, the only precursor of all pyrimidine nucleotides) (Figure 4.1) (Villela *et al.*, 2011).

Mechanism of action of 5FU involves formation of toxic metabolites (FUMP-fluorouridine monophosphate) that inhibit the DNA/RNA replication (Figure 4.1).

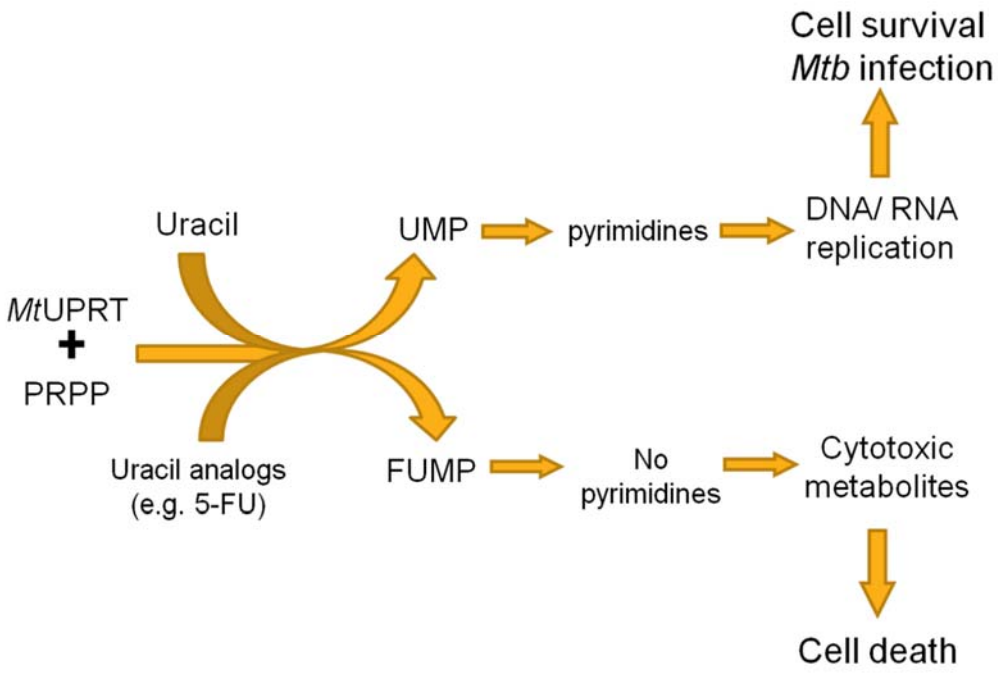

Figure 4.1 MtUPRT function in salvage pathway of pyrimidine biosynthesis and probable action of 5FU. *MtUPRT catalyses the conversion of PRPP and uracil to UMP (the precursor of pyrimidines). Uracil analogs (example, 5FU) disrupt this MtUPRT function by formation of FUMP and cytotoxic metabolites leading to cell death. With availability of MtUPRT structure and the target based drug discovery approach the screening of MtUPRT inhibitors would be greatly facilitated.*

[MtUPRT- Mycobacterium tuberculosis uracil phosphoribosyltransferase; PRPP- 5'-phosphoribosyl-α-1'-pyrophosphate; 5FU- 5-fluorouracil; UMP- Uridine monophosphate; FUMP- fluorouridine monophosphate); DNA- Deoxyribonucleic acid; RNA- Ribonucleic acid]

4.2 MtUPRT as a potential target in Mtb

The *Mt*UPRT was indicated as an anti-TB target and probably has activity in the LTBI bacteria (Villela *et al.*, 2013). In addition, the anticancer drug 5FU was recently shown to target the *Mt*UPRT (Singh *et al.*, 2015). Simultaneously, generation of spontaneous mutants against 5FU in our previous study also led to identification of mutations in this protein. To validate and access the potential of *Mt*UPRT as a target in *Mtb* it is necessary to determine the structure of *Mt*UPRT. Structural insights into the interactions of 5FU with *Mt*UPRT would aid in synthesizing 5FU analogues with minimal toxicity.

4.3 Objectives

The objectives for this part of the study were firstly to elucidate the crystal structure of *Mtb* UPRT (*Mt*UPRT) and *Mt*UPRT in complex with 5FU to understand their interactions. Secondly, to establish the correlation between the spontaneous mutational sites of *Mt*UPRT (selected in the presence of 5FU) and their structural interactions with 5FU.

4.4 Results

4.4.1 MtUPRT purification and characterization

The *upp* gene was cloned and overexpressed in BL21*E. coli* to yield the recombinant *Mt*UPRT protein. The protein was purified to homogeneity in three step purification by chromatography. The 27.4 kDa *Mt*UPRT eluted in tetrameric form at a volume corresponding to 120 kDa (Figure 4.2). In addition, the Dynamic Light Scattering (DLS) measurements confirmed the protein to be in a homogeneous, tetrameric form; consistent with the gel-filtration result (Figure 4.3)

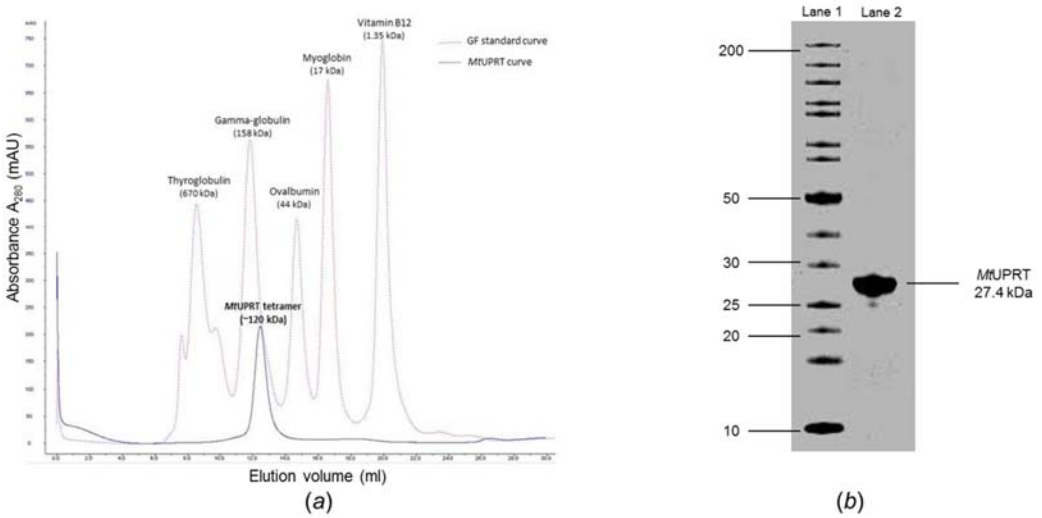

Figure 4.2(a) Gel-filtration chromatography elution profiles of MtUPRT and the protein standard. *MtUPRT and the protein standard were eluted from an analytical column (Superdex 200 10/300 GL). The MtUPRT eluted at 12.8 ml, which is consistent with a tetrameric association in solution as observed in DLS data.*

(b) The purity of MtUPRT (27.4 kDa) characterized by 4–12% SDS-PAGE. *The gel was stained followed by Coomassie staining. Lane 1 contains the protein molecular weight standard marker (in kDa). Lane 2 contains the purified MtUPRT.*

Msr#	Time(s)	Temp(C)	Count Rate	Ampl	Diff Coeff	Radius(nm)	Polyd(nm)	PolydIndx	MW(KDa)	%Mass	Baseline	Sos Error
1	10.0	20.1	387582	0.767	503.	4.26	0.684	0.03	100.	100.0	1.000	2.38
2	20.0	20.1	378603	0.799	490.	4.38	0.631	0.02	107.	100.0	1.000	1.69
3	30.0	20.0	382816	0.780	470.	4.55	0.166	0.00	117.	100.0	1.000	2.82
4	40.0	20.0	393239	0.786	454.	4.71	0.856	0.03	126.	100.0	1.000	1.76
5	50.0	19.9	390976	0.751	451.	4.73	1.52	0.10	128.	100.0	1.000	5.06
6	60.0	19.9	395247	0.780	442.	4.83	0.878	0.03	134.	100.0	1.001	3.06
7	70.0	19.9	402572	0.760	434.	4.92	0.743	0.02	140.	100.0	1.000	5.47
8	80.0	19.9	389954	0.725	434.	4.92	0.718	0.02	140.	100.0	1.001	3.02
9	90.0	19.9	381132	0.765	432.	4.93	1.68	0.12	141.	100.0	1.000	3.90
10	100.0	20.0	378405	0.773	421.	5.08	1.54	0.09	151.	100.0	1.000	9.63
11	110.0	20.0	373748	0.770	428.	5.00	0.456	0.01	145.	100.0	1.000	5.61
12	120.0	20.0	366447	0.763	439.	4.88	0.622	0.02	137.	100.0	1.000	2.34
13	130.0	20.0	369617	0.760	433.	4.94	0.760	0.02	142.	100.0	1.001	4.97
14	140.0	20.0	370772	0.751	442.	4.84	1.67	0.12	135.	100.0	1.000	4.16
15	150.0	20.0	363146	0.756	444.	4.82	1.08	0.05	134.	100.0	1.000	2.34
16	160.0	20.0	368548	0.762	443.	4.83	0.673	0.02	134.	100.0	1.000	1.18
17	170.0	20.0	370715	0.748	443.	4.83	0.734	0.02	134.	100.0	1.001	1.83
18	180.0	20.0	372734	0.739	438.	4.88	1.06	0.05	137.	100.0	0.999	2.25
19	190.0	20.0	366513	0.756	442.	4.84	0.675	0.02	135.	100.0	1.000	1.48
20	200.0	20.0	386327	0.747	423.	5.06	1.15	0.05	150.	100.0	1.002	5.31
Aves:												
Mono		20.0	379454	0.762	445.	4.81	0.915	0.04	133.	100.0	1.000	3.51
Bi-1		0.0	0	0.000	0.000	0.000	----	----	0.000	0.0	0.000	0.000
Bi-2				0.000	0.000	0.000			0.000	0.0		

Figure 4.3 Dynamic light scattering (DLS) data of MtUPRT. *The DLS result shows the apparent molecular weight of MtUPRT (27.4 kDa) which is close to its tetrameric form.*

[Note: The polydispersity index (PolydIndx) values smaller than 0.05 indicate highly monodisperse standards. Sos error (sum of squares) represents the quality of data. Sos error less than 20 are good and less than 5 are considered negligible.]

4.4.2 Structure of MtUPRT

The structure of *Mt*UPRT was solved by molecular replacement method and refined up to 3Å resolution (Table 4.1, PDB code: 5E38) (Ghode *et al.*, 2015). The *Mt*UPRT molecule consists of a β-sheet sandwiched by 6 α-helices (including 2 single-turn helices). In all the monomers, a part of the β-arm region (Arg55-Ser64) had no interpretable electron density and were not modeled. There are four molecules in the asymmetric unit (Figure 4.5) and are consistent with the in solution studies.

A sequence homology search of the GenBank/EMBL/DDBJ database for *Mt*UPRT was conducted using BLAST (Altschul *et al.*, 1990). The result showed that *Mt*UPRT sequence is highly conserved in bacterial species. Although the gene encoding UPRTase is present in human, it does not have any detectable activity (Schumacher *et al.*, 1998). Also, the *Mt*UPRT protein sequence alignment with its human analogue shows no consensus and hence might prove to be an attractive target in *Mtb*. (Figure 4.4). *Mt*UPRT and its homologs share a highly conserved PRPP binding 12-residue sequence and the uracil binding residues (Schumacher *et al.*, 1998). A search for structurally similar proteins within the PDB database was performed using the DALI server (Holm & Rosenstrom, 2010) which revealed several structurally similar proteins that includes UPRTases from bacteria with a sequence identity ranging from 48% to 37% and RMSD of less than 2.1Å. These structural similarities indicate that, despite being from various

species with varying sequence identity, the structures of the UPRTases are similar and conserved.

*Mt*UPRT is a dimer of dimer similar to several of its homologs (Figure 4.5). The four molecules of the asymmetric unit are identical with an RMSD less than 1Å for the pairwise comparison of Cα atoms. The total buried area of a monomer in the asymmetric unit is approximately1600Å^2. There are nine hydrogen bonding contacts between the monomers of the tetramer, besides the several hydrophobic interactions.

In order to understand the substrate specificity, we briefly attempted to crystallize *Mt*UPRT along with uracil and 5FU. However, no interpretable density was observed for these ligands. This led us to model the ligand-*Mt*UPRT complex using the UMP-UPRT homolog complex structure from *Thermotoga maritime* (PDB code 1O5O). The superposition of homolog complex onto *Mt*UPRT inferred the UMP binding pocket of *Mt*UPRT. The UMP binding pocket of *Mt*UPRT consists of Arg102, Met131, Thr134, Gly135, Ser137, Tyr191 and Asp198 (Figure 4.6). Out of the four spontaneous mutational sites identified and mapped on the *Mt*UPRT structure (discussed in section 4.4.3), two were conserved amongst the other UPRTases (Figure 4.6)

Table 4.1 Data collection and structure refinement statistics of MtUPRT

Space group	$P3_2$
a, *b*, *c* (Å)	118.09, 118.09, 77.8
α, β, γ (°)	90, 90, 120
Resolution range (Å)[a]	33.0 – 3.0
Total No. of reflections	134623
No. of unique reflections	22764
Completeness (%)	97.1 (99.3)
Redundancy	6.0 (5.1)
$\langle I/\sigma(I)\rangle$	9.5 (3.2)
R_{merge}[b]	0.21
Refinement and quality of model	
R_{work}[c]	0.24
R_{free}[c]	0.27
Bond length (Å)[d]	0.004
Bond angle (°)[d]	0.908

[a]Data for the highest resolution bin is in parentheses.
[b]$R_{merge} = \Sigma|Ii - Im|/\Sigma Ii$, where Ii is the intensity of the measured reflection and Im is the mean intensity of all symmetry-related reflections.
[c]$R_{work} = \Sigma| |F_{obs}| - |F_{calc}| |/\Sigma|F_{obs}|$, where F_{obs} and F_{calc} are observed and calculated structure factors, respectively. $R_{free} = \Sigma_T| |F_{obs}| - |F_{calc}| |/\Sigma_T|F_{obs}|$, where T denotes a test data set of about 5% of the total reflections randomly chosen and set aside prior to refinement.
[d]RMSD = root-mean-square deviation.

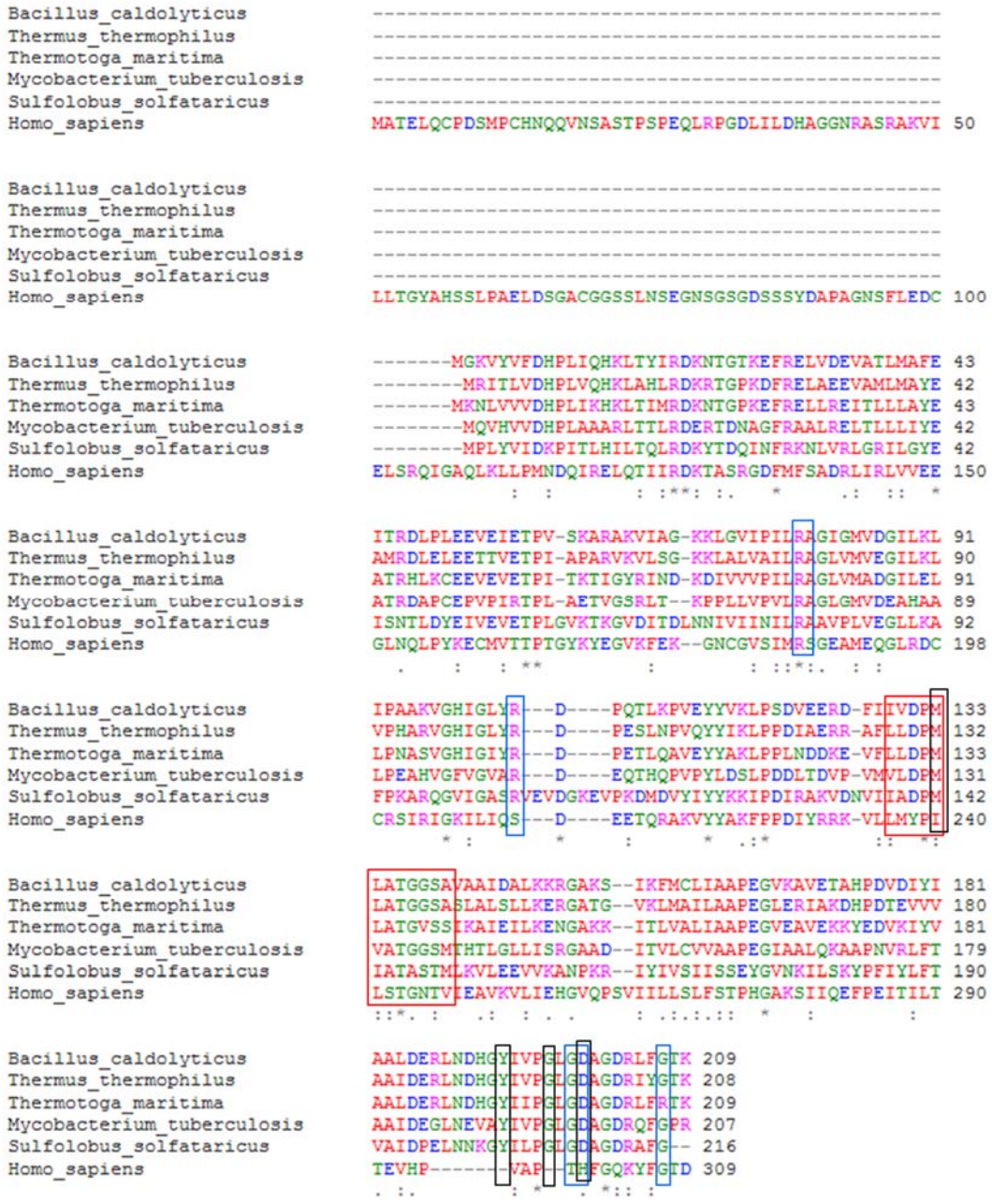

Figure 4.4 Multiple sequence alignment between human and bacterial UPRTases. *The identical conserved residues are indicated by stars. The highly conserved PRPP binding domain is marked in red box (Villela et al., 2013). The residues implicated for uracil binding in B. caldolyticus are shown in black box (Kadziola et al., 2002). The blue box indicates the proposed Mtb residues involved in catalysis. The multiple sequence alignment was carried out using ClustalW2 software.*

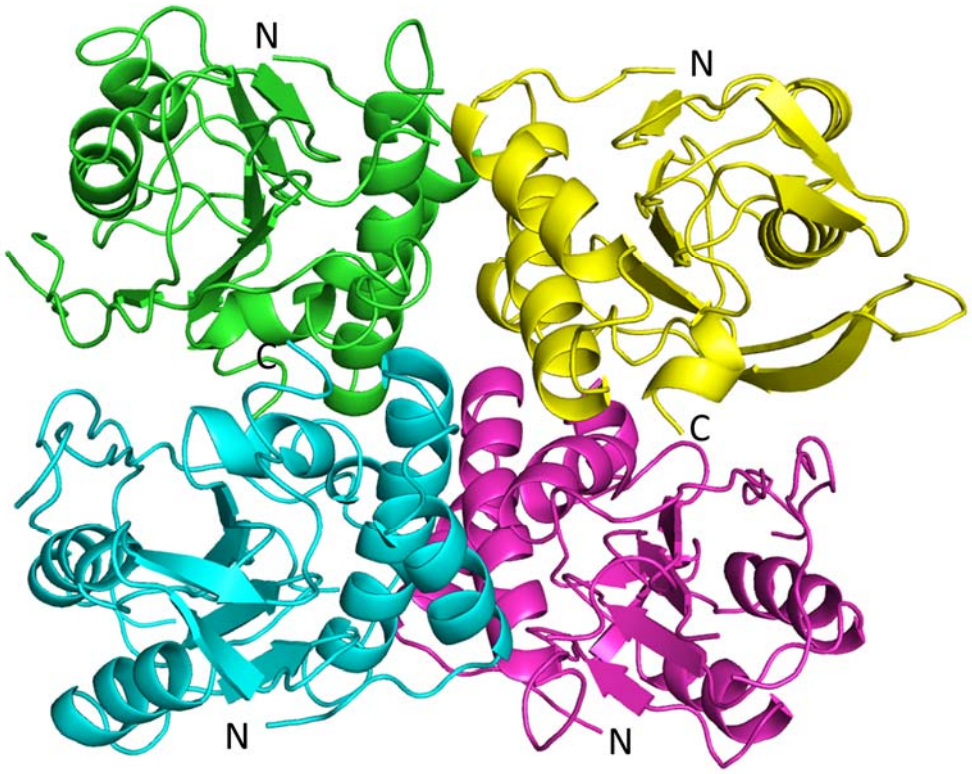

Figure 4.5 Structure of MtUPRT tetramer in an asymmetric unit of the crystal. *Each monomer is shown in different color. (The N and C terminals of the protein are indicated in the monomer unit figure 4.6)*

4.4.3 Mapping of spontaneous mutations, that confer 5FU resistance in *Mtb*, on the *Mt*UPRT

To understand the implication of *Mt*UPRT in the 5FU resistance, we selected spontaneous mutants with 5 and 20 μg/ml 5-FU (12 and 25 times the MIC_{90} respectively) using the *M. bovis* BCG strain. *Mt*UPRT encoding *upp* gene was sequenced for 42 independent isolates, eight of which contained polymorphisms on *upp* (Table 4.2). Here, we report four distinct single nucleotide polymorphisms (SNPs) and two distinct deletions (2 mutants contained the same deletion) that were observed in the *upp* gene of the 5FU resistant mutants for the first time. The four SNPs resulted in mutated residues namely Arg45Pro, Gly63Arg, Gly81Val and Cys157Tyr which were mapped on the *Mt*UPRT structure (Figure 4.6). The closest of them, Cys157Tyr is at a distance of approximately 10Å from the UMP. Apart from Cys157Tyr, the other three mutated residues were exposed on the surface.

Table 4.2 Polymorphisms observed in upp gene of spontaneous 5FU mutants of M. bovis BCG

Amino acid change	Nucleotide change	5FU (µg/ml)	Frequency
Single nucleotide polymorphisms			
Arg45Pro	g134c	5	1
Gly63Arg	g187c	20	1
Gly81Val	g470a	5	1
Cys157Tyr	g242t	20	1
Nucleotide deletions/ Frameshift			
Leu32Cys	c94 deleted	5	1
Tyr105Pro	a316 deleted	5 (2), 20 (1)	3
Total	6	-	8

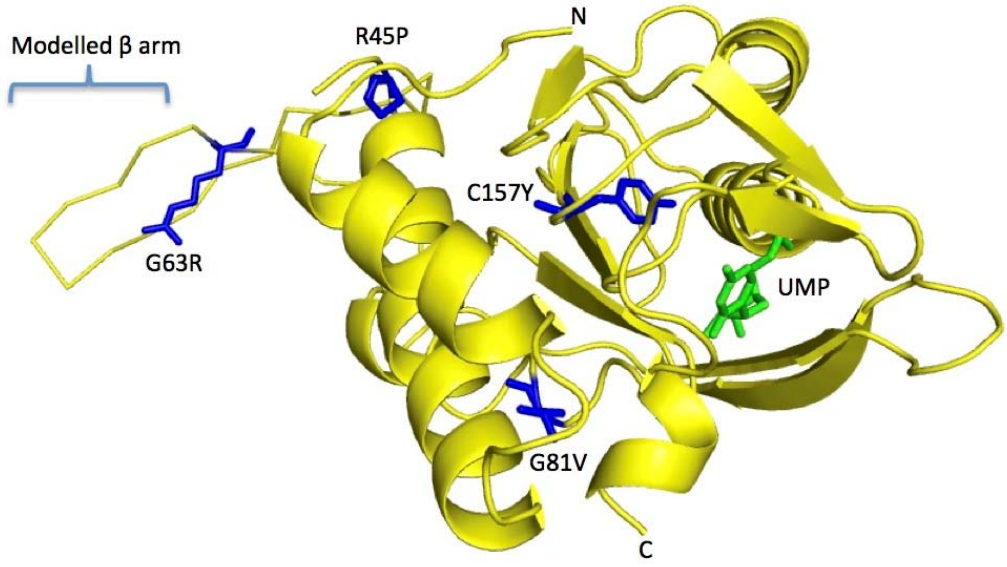

Figure 4.6 Cartoon representation of the MtUPRT-UMP complex structure along with mapping of mutational sites. *MtUPRT structure was modeled on the homologous structure from Thermotoga maritima UPRT (PDB 1O5O). 5FU spontaneous mutations are shown in stick representation in blue and the UMP is shown in green. (N and C indicate the N and C terminals of the protein respectively).*

4.4.4 5FU Susceptibility of 5FU resistant mutants harboring alterations on *Mt*UPRT

The susceptibility of the 5FU mutants was compared against wild type *M. bovis* BCG by evaluating the MIC_{50} of the strains. A decrease in susceptibility from 5- to 20- fold was observed in the mutant strains. The mutant Gly63Arg showed the least susceptibility to 5FU with 20-fold increase in MIC50, followed by Arg45Pro, Cys157Tyr and Gly81Val (Figure 4.7).

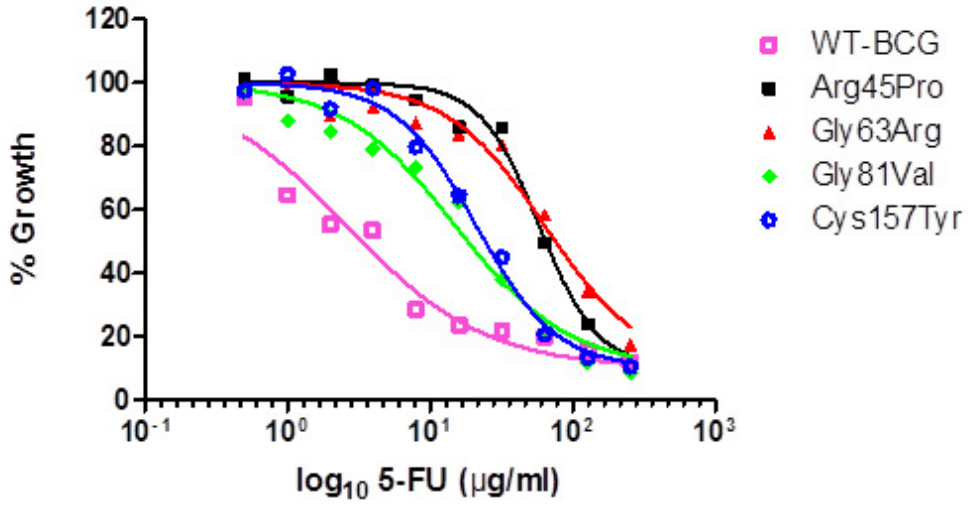

Figure 4.7 5FU concentration dependent kill of M. bovis BCG and its 5FU resistant mutants. *Gly63Arg exhibits the highest increase in MIC_{50}. MIC_{50} determination protocol was adopted from Pethe et al. (Pethe et al., 2010). Graph Pad Prism 5 software was used to plot the MIC_{50} curves.*

4.5 Discussion

No new class of chemical compounds have been developed for 4 decades in the TB drug regimen after the introduction of quinolones in the 1960's (Walsh, 2003b). New therapeutics which can offer shorter treatment duration and compatibility with HIV drugs are an immediate requirement to achieve the long term targets of the TB control program. Thus, identifying and validating new targets for developing new drugs, is of utmost priority for TB treatment and to control the emergence of resistance (WHO, 2013).

*Mt*UPRT was recently identified as a target of the anti-cancer drug, 5FU. Given that 5FU is a pyrimidine/ uracil analog, it possibly interacts directly with *Mt*UPRT as observed in other bacterial species (Schumacher *et al.*, 1998). 5FU is also known to inhibit growth in several bacteria, for example, *P. aeruginosa* and *E. coli* (Attila *et al.*, 2009, Imperi *et al.*, 2013, Rangel-Vega *et al.*, 2015). The mechanism of action of 5FU in *Mtb* was recently studied by Singh *et al*., where 5FU resistance in *Mtb* was attributed to the mutations in the genes *upp* and *pyrR* (pyrimidine operon regulatory protein) (Singh *et al.*, 2015). In their study, generation of spontaneous mutants against 5FU (at 5 times MIC_{90}) resulted in 3 out of 10 mutants with a nucleotide deletion at position 74 in the *upp* gene. Using a similar approach, we isolated 48 mutant *Mtb* colonies selected against 5FU and sequenced for the *upp* gene. In our study, 6 novel *upp* alterations in 8 independent 5FU resistant isolates (3 isolates had the same mutation) were identified. The remaining mutants with wild type *upp* sequence suggest additional targets or mechanisms of 5FU resistance; for example the pyrimidine operon regulatory

protein (PyrR) as indicated by Singh *et al*., and as discussed in chapter 5. In this study, we report the crystal structure of *Mt*UPRT for the first time along with mapping of the novel spontaneous mutational sites of *Mt*UPRT obtained in this study.

Although the four mutational sites identified were located away from the proposed *Mt*UPRT catalytic or uracil binding site, three of them (Arg45, Gly63 and Gly81) were either conserved in other bacterial species or belonged to the same amino acid group (Non-polar, aliphatic). This observation implies the probable role of these sites in resistance mechanism or function of the protein. Nonetheless, in the light of its involvement in energy saving salvage pathway, *Mt*UPRT is an attractive dormant *Mtb* target. The structural and functional insights of *Mt*UPRT would aid in validation of this novel TB target. Screening for the inhibitors, in a structure activity relationship approach, would greatly accelerate the development of novel anti-TB therapeutics and strategies.

4.6 Future directions

The four mutations that occurred on *Mt*UPRT on exposure to 5FU were located away from the 5FU binding site implicating they may have minimal or no impact on the interaction. To address this hypothesis, effect of 5FU interaction on the mutated *Mt*UPRT protein activity will be assessed, using the site directed mutagenesis, isothermal thermal calorimetry (ITC) and activity assays.

5

Structure and mapping of spontaneous mutational sites of PyrR from Mycobacterium tuberculosis

The ability of *Mtb* to enter into a persistent stage in the host without disease symptoms is fundamental to the pathogenic success of *Mtb* (Gengenbacher & Kaufmann, 2012). Thus, the development of new drugs with novel mechanisms of actions, that can address the above issues, is urgently needed (O'Brien & Nunn, 2001). As mentioned earlier, antitubercular activity was demonstrated by Tsukamura *et al.* in 1979. 5FU also exhibited antitubercular activity in *Mtb*-H37Rv strain in our experiments, exhibiting dose dependent inhibition. The mechanism of resistance of 5FU in *Mtb* was studied only recently by Singh *et al*., where 5FU resistance in *Mtb* was attributed to the mutations in the genes *upp* and *pyrR* encoding the ezymes *Mt*UPRT and pyrimidine operon regulatory protein (PyrR) respectively (Singh *et al.*, 2015). Structural insights of these proteins would help in understanding its functional implications in *Mtb* and facilitate the screening for novel anti-TB chemical entities.

5.1 Role of PyrR in pyrimidine biosynthesis

The gene encoding *Mtb* PyrR is located on the *pyr* operon along with the enzymes involved in the *de novo* pyrimidine biosynthesis pathway. PyrR regulates the above enzymes resulting in transcription termination (Cole *et al.*, 1998). PyrR

executes this function by binding to the *pyr* operon mRNA (conserved sequence) thereby disrupting the antiterminator. In addition to its regulatory function, PyrR is also known to have residual uracil phosphoribosyltransferase (UPRTase) activity. The UPRTase activity involves conversion of the substrates uracil and 5'-phosphoribosyl-α-1'-pyrophosphate (PRPP) to uridine 5'-monophosphate (UMP) and pyrophosphate (PPi) (Villela *et al.*, 2011). This UPRTase function was recently implicated to be disrupted by an anticancer drug 5FU (an uracil analogue) making PyrR an attractive target in *Mtb*.

5.2 PyrR as a potential target in *Mtb*

Antitubercular activity of 5FU is known since 1979, however, it was not pursued as a potential TB drug given the toxic side effects of 5FU. Nonetheless, 5FU can be chemically modified in a target based drug discovery approach (Duncan, 2004), provided structural insights into 5FU interactions with PyrR are available. To that end, we solved the co-crystal structure of *Mtb* PyrR-5FU complex for the first time. To establish the plausible interactions between PyrR residues and 5FU deduced from the previous study, we selected spontaneous mutants in the presence of 5FU. Sequencing the *pyrR* gene of these mutants led us to the identification of thirteen mutational sites of *Mtb* PyrR, four of which were located in close proximity to 5FU binding site. The knowledge on the PyrR-5FU complex structure will aid in the screening of *Mtb* PyrR inhibitors and will assist in design and development of novel TB drugs.

5.3 Objectives

The objectives for this part of the study were firstly, to elucidate the co-crystal structure of *Mtb* PyrR in complex with 5FU to understand the interactions of 5FU with PyrR. Secondly, to establish the correlation between the spontaneous mutational sites of PyrR and 5FU resistance mechanism.

5.4 *Results*

5.4.1 *Mtb* PyrR purification and characterization

The *pyrR* gene cloned in pET28b was overexpressed in *E. coli* to yield the recombinant *Mtb* PyrR protein. The protein was purified to homogeneity in two step purification by chromatography. The 22.6 kDa PyrR eluted in monomeric form at a volume corresponding to <25 kDa on a HiLoad 16/60 S200 gel filtration column. The DLS experiment carried out after protein concentration (4 mg/ml) showed an apparent molecular weight close to the hexameric form (Figure 5.2).

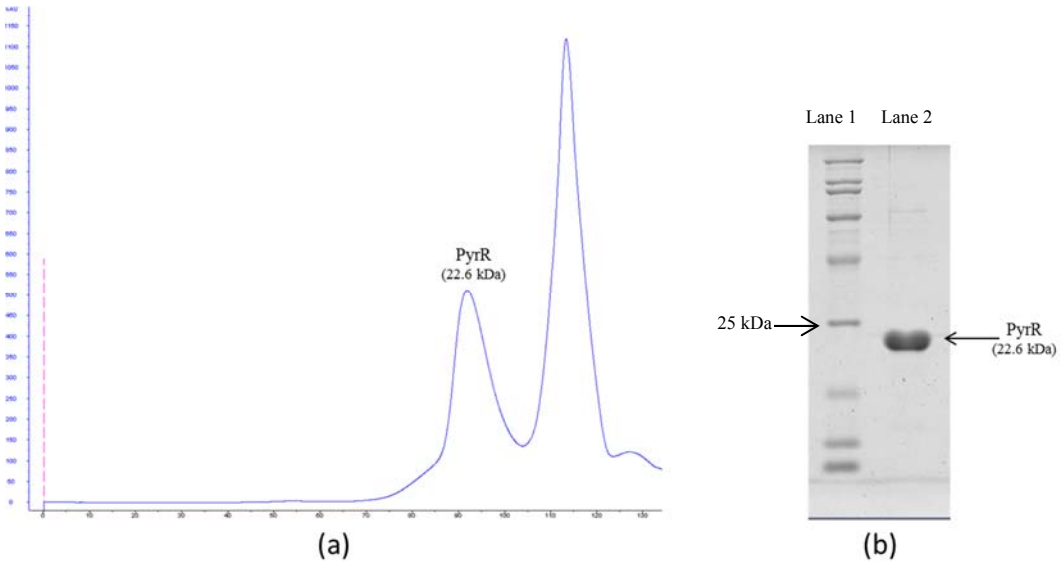

Figure 5.1 (a) Gel-filtration chromatography elution profile of Mtb PyrR. *The protein eluted at 91 ml, which corresponds to its monomeric size.*

(b) The purity of Mtb PyrR (22.6 kDa) characterised by 4–12% SDS-PAGE *followed by Coomassie staining. Lane 1 contains the protein molecular weight standard marker (in kDa). Lane 2 contains the purified PyrR.*

Msr#	Time(s)	Temp(C)	Count Rate	Ampl	Diff Coeff	Radius(nm)	Polyd(nm)	PolydIndx	MW(KDa)	%Mass	Baseline	Sos Error
1	10.0	20.0	389805	0.743	421.	4.99	1.82	0.13	144.	100.0	1.000	10.9
2	20.0	20.0	389099	0.743	417.	5.03	0.954	0.04	148.	100.0	1.000	9.78
3	30.0	20.0	389420	0.744	412.	5.09	1.74	0.12	152.	100.0	1.001	8.34
4	40.0	20.0	383911	0.704	408.	5.15	1.46	0.08	156.	100.0	1.000	9.36
5	50.0	20.0	390559	0.674	410.	5.12	1.58	0.10	154.	100.0	1.000	5.38
6	60.0	20.0	397705	0.659	407.	5.17	1.54	0.09	157.	100.0	1.000	7.19
7	70.0	20.0	387682	0.683	405.	5.18	1.99	0.15	158.	100.0	1.001	8.85
8	80.0	20.0	379147	0.678	409.	5.14	0.618	0.01	155.	100.0	1.000	7.05
9	90.0	20.0	378014	0.678	418.	5.03	1.77	0.12	147.	100.0	1.000	5.17
10	100.0	20.0	377318	0.672	417.	5.04	1.53	0.09	148.	100.0	0.999	4.41
11	110.0	20.0	382515	0.650	417.	5.04	1.34	0.07	148.	100.0	1.000	5.11
12	120.0	20.0	385368	0.639	421.	4.99	1.59	0.10	145.	100.0	0.999	5.98
13	130.0	20.0	383327	0.641	415.	5.06	1.83	0.13	150.	100.0	1.000	6.71
14	140.0	20.0	385484	0.643	418.	5.03	0.833	0.03	147.	100.0	1.001	5.99
15	150.0	20.0	385767	0.640	419.	5.01	1.61	0.10	146.	100.0	1.000	4.92
16	160.0	20.0	382010	0.653	419.	5.02	0.729	0.02	147.	100.0	1.000	4.62
17	170.0	20.0	385889	0.671	413.	5.08	0.723	0.02	151.	100.0	1.000	4.42
18	180.0	20.0	396491	0.648	413.	5.08	1.03	0.04	151.	100.0	1.000	6.07
19	190.0	20.0	393538	0.641	413.	5.08	1.31	0.07	151.	100.0	1.000	3.53
20	200.0	20.0	393760	0.634	411.	5.11	1.05	0.04	153.	100.0	1.000	5.31
21	210.0	20.0	395630	0.646	402.	5.22	1.19	0.05	161.	100.0	1.000	10.0
Aves:												
Mono		20.0	387259	0.671	414.	5.08	1.35	0.08	151.	100.0	1.000	6.62
Bi-1		0.0	0	0.000	0.000	0.000	----	----	0.000	0.0	0.000	0.000
Bi-2				0.000	0.000	0.000			0.000	0.0		

Figure 5.2 Dynamic light scattering data of Mtb PyrR. *DLS result shows the apparent molecular weight of the protein to be at 151 kDa .*

5.4.2 Structure of *Mtb* PyrR

The structure of *Mtb* PyrR was solved by molecular replacement method using PDB 1W30 as a search model and refined up to 2.6 Å resolution (Table 5.1,PDB code: 5IAO) (Ghode *et al.*, 2016). The pyrR molecule consists of an antiparallel β-sheet with three β-strands and a parallel β-sheet with four β-strands along with four α-helices (including a single-turn helix). The amino acid residues 91-101 had no interpretable electron density and were not modeled. There are six molecules (trimer of dimers) in the asymmetric unit (Figure 5.4). The dynamic light scattering experiments indicated the presence of hexamer in the concentrated protein solution consistent with the crystal structure observation. The six molecules of the asymmetric unit are identical with an RMSD less than 1Å for the pairwise comparison of Cα atoms. The total buried area of a monomer in the asymmetric unit is approximately 1500Å^2. There are ten hydrogen bonding contacts between the monomers, besides several hydrophobic interactions.

A simulated annealing map for the 5FU residue is shown in Figure 5.5. The 5FU molecule is found to form hydrogen bonds with Arg58, His177 and Arg179. Furthermore, a water molecule is found to stabilize the 5FU interaction by forming hydrogen bonds with an oxygen atom from 5FU and Asp120.

A search for structurally similar proteins within the PDB database was performed using the DALI server (Holm & Rosenstrom, 2010) which revealed several structurally similar proteins ranging from RMSD 1.1 to 3.3 (sequence identity from 58 to 18%) in the first 100 hits. The closest homologs includes, *Bacillus*

caldolyticus with RMSD of 1.1 (55% sequence identity) followed by PyrR from *Bacillus subtilis* with RMSD of 1.3 (53% sequence identity).

A sequence homology search of the GenBank/EMBL/DDBJ database for *Mtb* PyrR was conducted using BLAST (Altschul *et al.*, 1990). The result showed that PyrR homologues are present over the archaea and bacterial species. The closest homologs of *Mtb* PyrR are from other mycobacterial species and are highly conserved. The sequence alignment of *Mtb* PyrR with its homologs is shown in Figure 5.3. The figure also indicates the conserved regions of PRPP and uracil as observed in other species. The UPRTases from other species are also aligned with PyrR to indicate the conserved residues essential for the UPRTase activity in both the enzymes. Amongst the PyrR homologs, the PyrR mutational sites were either conserved or belong to the same amino acid group.

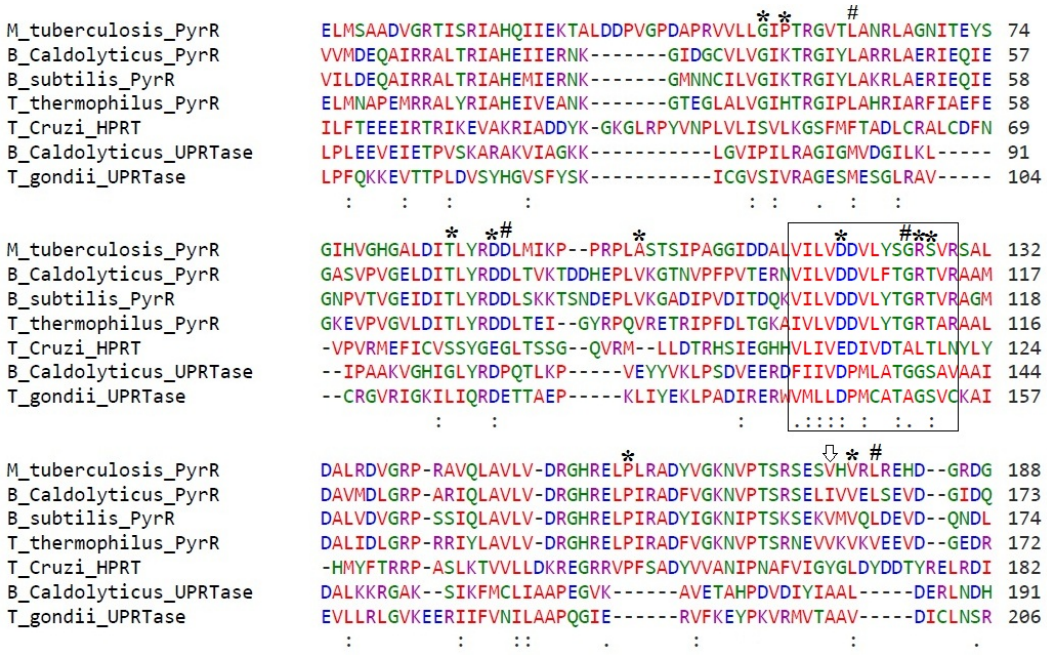

Figure 5.3 Multiple sequence alignment of Mtb PyrR with its structural homologues and UPRTases across the bacterial species. *Sites of spontaneous mutations in PyrR from Mtb are indicated by an asterisk. The residues involved in PRPP binding are highlighted by a black box. Val178, which is observed to be involved in water-mediated hydrogen bonding contact with 5-FU in our PyrR-5FU complex structure, is indicated by an arrow. Mutational sites reported by Singh et al. are indicated by "#". Multiple sequence alignment was carried out using EMBL-EBI Clustal Omega software.*

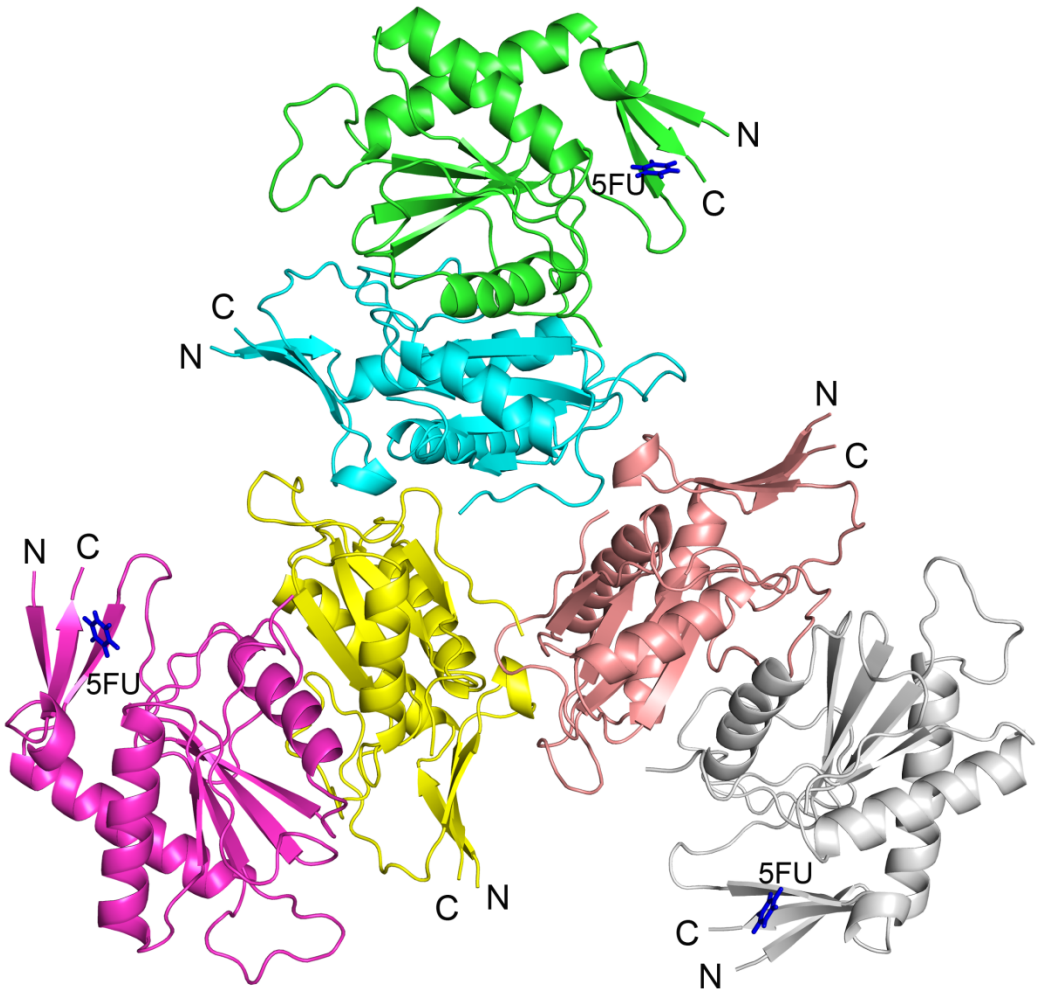

Figure 5.4 Cartoon representation of the Mtb PyrR-5FU complex. *The crystal shows hexameric association of the six PyrR monomers in one asymmetric unit which are distinctly colored. The 5FU is shown in stick representation.*

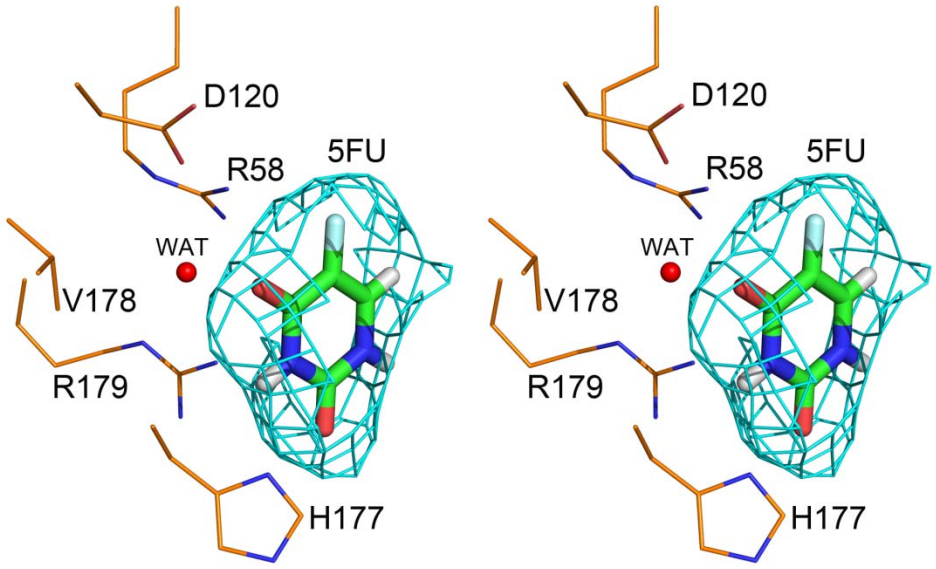

Figure 5.5 Simulated annealing omit map of the 5-fluorouracil (5FU) interacting region of Mtb PyrR. *The 5FU and 3.5Å surrounding the ligand were omitted prior to refinement and map calculation (Fo-Fc map; contoured at 3σ). For clarity, in this figure we show the density only for the ligand. Water molecule is shown as red sphere.*

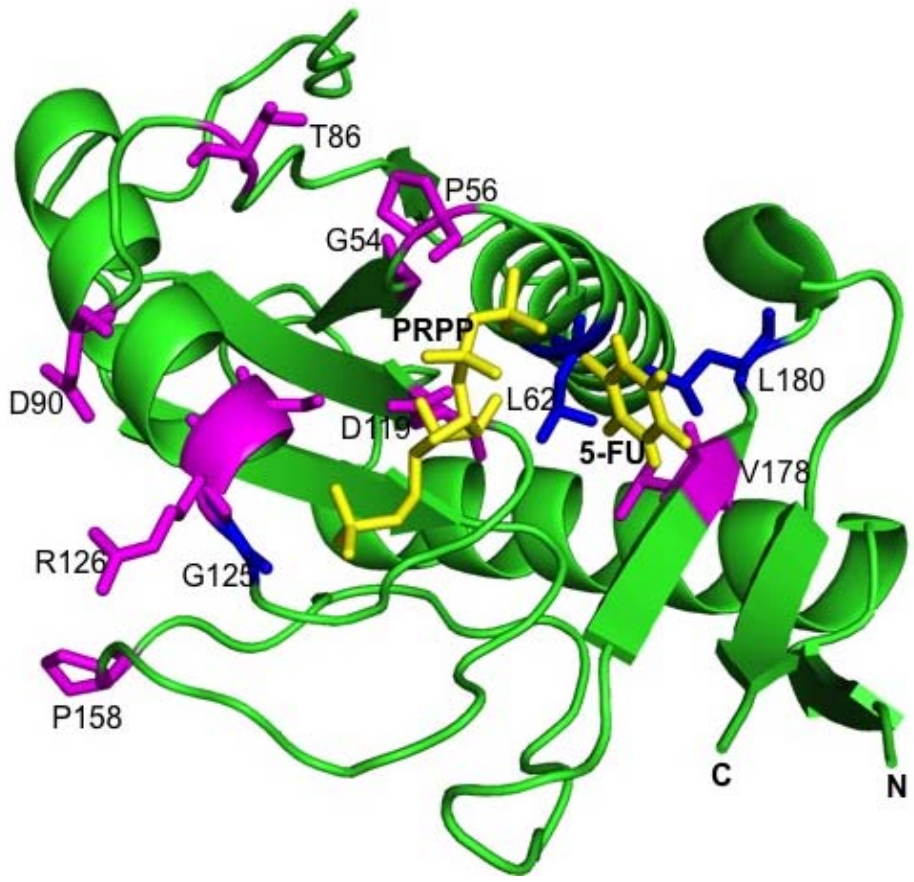

Figure 5.6(a) Cartoon representation of PyrR-5FU complex structure along with mapping of mutational sites. *PRPP was modeled on PyrR-5FU structure using the PyrR-UMP structure from Trypanosoma cruzi (PDB 1I14). 5FU spontaneous mutations are mapped on the structure. Mutations from this study are highlighted in pink. Mutations observed by Singh et al. are highlighted in blue. Most of the mutations are located around the phosphoribosyl part of the UMP binding region of PyrR. The residues Val178 is located in the 5FU binding site while two sites Leu62 and Leu180 lie in the close proximity. (N and C indicate the N and C terminals of the protein respectively)*

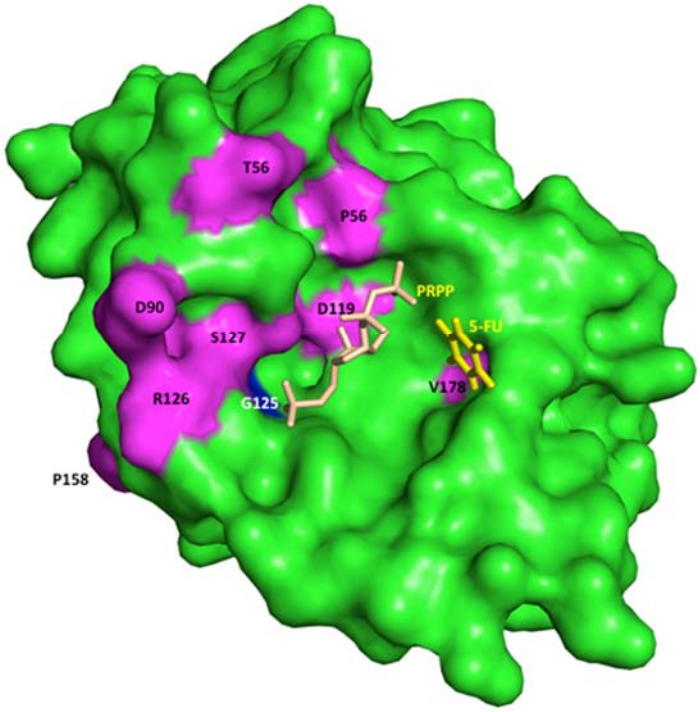

Figure 5.6(b) Molecular surface representation of PyrR-5FU complex structure along with mapping of mutational sites. *This figure is in same orientation as Figure 5.6(a) except that it shows molecular surface representation.*

Table 5.1 Data collection and structure refinement statistics for PyrR.

Space group	C2
a, *b*, *c* (Å)	142.84, 127.77, 90.78
α, β, γ (°)	90, 90.38, 90
Resolution range (Å)[a]	42.24 - 2.6 (2.7 - 2.6)
Total No. of reflections	458032
No. of unique reflections	49764
Completeness (%)	99.2 (97.2)
Redundancy	3.8
⟨*I*/σ(*I*)⟩	7.7 (6.1)
R_{merge}[b]	0.138
Refinement and quality of model	
R_{work}[c]	0.19
R_{free}[c]	0.24
RMSD bond length (Å)[d]	0.005
RMSD bond angle (°)[d]	0.860

[a]Data for the highest resolution bin is in parentheses.

[b]$R_{merge} = \Sigma|Ii - Im|/\Sigma Ii$, where Ii is the intensity of the measured reflection and Im is the mean intensity of all symmetry-related reflections.

[c]$R_{work} = \Sigma| |Fobs| - |Fcalc| |/\Sigma|Fobs|$, where Fobs and Fcalc are observed and calculated structure factors, respectively. $R_{free} = \Sigma_T| |Fobs| - |Fcalc| |/\Sigma_T|Fobs|$, where T denotes a test data set of about 4% of the total reflections randomly chosen and set aside prior to refinement.

[d]RMSD = root-mean-square deviation.

5.4.3 Mapping of spontaneous mutations that confer 5FU resistance in *Mtb*, on the PyrR structure

Mtb PyrR was recently reinvestigated as potential target of an anti-cancer drug 5-fluorouracil (5FU) (Singh *et al.*, 2015). To understand the implication of *Mtb* PyrR in the 5FU resistance, we selected for spontaneous mutants with 5 µg/ml and 20 µg/ml 5-FU (12 and 25 times the MIC_{90} respectively). *Mtb* PyrR encoding *pyrR* gene was sequenced for 45 independent isolates, 20 of which contained polymorphisms on the *pyrR* gene. Amongst these 20 mutants, 13 harbour distinct single nucleotide polymorphisms (SNPs) in the *pyrR* gene, 12 of which are novel (Table 5.2). We also identified 2 distinct nucleotide insertions and 3 distinct deletions of nucleotide(s) resulting in frameshift (Table 5.2). We mapped the above spontaneous mutational sites or residues on the PyrR-5FU complex structure to understand their implications in 5FU resistance, if any. Apart from the mutations obtained from our study, we also mapped the mutations observed by Singh *et al.* onto our structure. Further, we modeled the PRPP binding site by aligning the PDB structure 1I14. The RMSD for the alignment was observed to be 0.94. Among the 12 mutational sites mapped Val178 lie in close proximity to the 5FU binding site, whereas the residues Gly54, Pro56, Asp119, Arg126 and Ser127 were observed to be close to the binding site of modeled PRPP (Figure 5.6). The spontaneous mutations reported by Singh et al., Leu62 and Leu180, were situated close to the 5FU binding site and Gly125 lie close to the PRPP binding site.

5.4.4 5FU Susceptibility of 5FU resistant mutants harboring alterations on PyrR

The susceptibility of the 5FU mutants was compared against wild type *M. bovis* BCG by evaluating the MIC_{50} of the strains. The MIC_{50} values for the 5-FU mutants revealed a decrease in their susceptibility to 5-FU; particularly the strain bearing a mutation at the 5-FU binding site, Val178, which exhibited a 60-fold decrease. Strains with mutations in the PRPP binding sites, Asp119 and Ser127, exhibited decreases of 24- and 14-fold, respectively.

Table 5.2 Polymorphisms observed in pyrR gene of spontaneous 5FU mutants in M. bovis BCG

Amino acid change	Nucleotide change	5FU (µg/ml)	No. of mutants
Single nucleotide polymorphisms (SNPs)			
Gly54Arg	g160c	20	1
Pro56Ser	c166t	20	1
Thr86Ala	a256g	5	2
Thr86Pro	a256c	20	1
Asp90Glu	c270g	5	1
Asp90Asn	g268a	20	1
Ala101Pro	g301c	20	1
Asp119Gly	a356g	20	1
Arg126Cys	c376t	5	1
Ser127Leu	c380t	20	1
Ser127Pro	t379c	20	1
Pro158Arg	c473g	20	1
Val178Gly	t533g	20	2
Nucleotide insertions or deletions (⌂= insertion, Δ= deletion, nt= nucleotide)			
	t⌂124	20	1
	g⌂495	5	1
Frameshift	Δnt434-445	20	1
	Δnt502-515	5	1
	Δnt570-580	5	1

5.5 Discussion

TB drug pipeline has been stagnant until recently as opposed to the rapidly evolving resistant *Mtb*, the causative agent of TB (Ramaswamy & Musser, 1998). No new class of chemical compounds have been developed in the TB drug regimen after the introduction of quinolones in the 1960's (Walsh, 2003b) until the introduction of linezolid. The most effective drugs in the current TB drug regimen are decades old and are ineffective against the resistant *Mtb*. The emergence of resistance is attributed to the ability of *Mtb* to enter a persistent stage which is difficult to eradicate with the available TB drugs. Thus, identifying and validating new targets for developing new drugs (novel mechanism of action) is of utmost priority for TB treatment and control of resistance (WHO, 2013). Identification of active proteins in the essential yet, less explored biological pathways in *Mtb* persistence holds promise in identification of novel drug targets. Correspondingly, several pathways (enzymes) have been indicated to be essential for *Mtb* in the persistence (Wayne & Lin, 1982, Sherman *et al.*, 2001).

One such investigational pathway is the pyrimidine biosynthesis pathway. The pyrimidine biosynthesis mechanisms differ in mammals and bacteria making it an attractive pathway to explore for potential targets in *Mtb* (Kantardjieff *et al.*, 2005). The regulatory enzyme, PyrR, from this pathway was recently identified as a target of an anti-cancer drug, 5FU. The anti-mycobacterial activity of 5FU was demonstrated more than 3 decades ago (Tsukamura, 1979), however, its investigation as a potential TB drug had not been pursued until recently. The mechanism of action of 5FU in *Mtb* was studied by Singh *et al*., where 5FU

resistance in *Mtb* was attributed to the mutations in the genes *upp* and *pyrR* (Singh *et al.*, 2015). However, PyrR-5FU interactions are not known yet In this study the crystal structure of *Mtb* PyrR in complex with 5FU is reported for the first time. In addition we also mapped the novel spontaneous mutational sites obtained from our study and from Singh *et al.* on the *Mtb* PyrR structure to understand their functional implications in 5FU resistance.

We identified 12 novel amino acid residue changes in 15 independent 5FU resistant isolates, in addition to one previously reported mutation (Arg126Cys) (Singh *et al.*, 2015). Besides, we also observed 5 mutants with deletions or insertions of single or a few nucleotides, re-instating the availability of an alternative UPRTase in *Mtb* (Table 2). The remaining mutants with wild type *pyrR* sequence suggest additional targets or mechanisms of 5FU resistance; for example the *Mtb* uracil phosphoribosyltransferase (*Mt*UPRT) as indicated by Singh *et al*. and in our earlier study (Ghode *et al.*, 2015).

The mutational sites, Arg58, Asp120, His177, Val178 and Arg179 lie in close proximity to the 5FU binding site. Notably, a water molecule is observed to stabilize 5-FU interaction with PyrR. This water molecule mediates hydrogen bonding interaction between oxygen atom of 5-FU with Asp120 side chain and Val178 amine. Furthermore the residues Asp119, Gly125, Arg126 and Ser127 are observed to be close to the binding site of modeled PRPP. Notably, the UPRTase activity of PyrR is not critical for the survival of the *Mtb* and hence a mutation that could hinder the binding of PRPP would also result in blocking the production of toxic FUMP. The 5FU susceptibility results (increased MICs of the

mutants) also indicate the possible interactions of these sites with the substrates Uracil, 5FU and PRPP. Together these observations imply the probable roles of Uracil/ 5FU- and PRPP- binding site mutations in the 5FU resistance mechanism in *Mtb*.

5.6 Future directions

The role of the residues: Leu62, Val178 and Leu180, which lie in close proximity to the 5FU binding site of the PyrR, will be validated by site-directed mutagenesis followed by ITC and activity assays. Mapping of PyrR mutations on the PyrR-UMP structure revealed that most of the mutations were located in the PRPP binding site of the protein (Pro56, Asp119, Gly125, Arg126 and Ser127). Implications of these sites in the 5FU mechanism of action will be studied in the similar manner as discussed earlier.

6

Conclusions

Fluoroquinolones are used in the treatment of resistant TB. It is essential to understand the molecular genetics of FQ resistance before its clinical significance is challenged. As such, our study should give a snapshot of molecular genetics of resistance of the major FQs that are involved in the infectious diseases drug regimens including TB. Newer generation FQs, gatifloxacin (GFX), moxifloxacin (MXF) and sparfloxacin (SFX) were the most potent FQs against *Mtb*. Secondly, as compared to GFX, MXF and SFX, 2 and 4 fold higher concentration of ciprofloxacin (CIP), levofloxacin (LVX) and ofloxacin (OFX) was required to limit the emergence of *M. bovis* BCG and *Mtb* mutants respectively. These findings suggests that different generation antibiotics from the same class of compounds have different frequencies of mutation, which is attributed to the better structural modifications in newer generation molecules.

The evaluation of the mutation frequency and mutation type selected by different fluoroquinolones at varying concentrations in a single experimental setup should help in formulation of drug regimens. With increasing concentrations of the FQs, the mutant strains with mutations that confer higher-level of resistance were selected until a concentration reached beyond which no mutant was recovered. Lower FQ concentrations primarily selected variants (low-level resistance mutants) with mutations mostly on *gyrB* and outside of the QRDR-A/B. Some mutations were predominantly selected by a specific FQ while LVX and OFX

selected wide variety of variants on both *gyrA* and *gyrB*. Our results resonates the phenomenon that, the resistance genotype (amino acid mutation in DNA gyrase) and phenotype (mutation frequency) depends on the type of FQ (Zhou *et al.*, 2000).

The evaluation of resistance levels conferred by the generally unnoticed mutations should help in designing better resistance diagnostics tools. It is known that low-level resistance increases probability of clinical resistance and thus, in the light of wide use of FQ at lower concentrations to treat other infectious diseases, if ignored could lead to dire consequences (Baquero, 2001). Correspondingly, some rare and low-level resistance mutants recovered during our study show increased MIC to FQs, suggesting that appropriate assessment of these mutations in TB patients is crucial while deciding the drug-regime and has valuable contribution towards limiting emergence of resistance.

The cross-resistance patterns exhibited by FQ resistant DNA gyrase variants in our study strengthen the argument and significance of understanding patient history of FQ usage prior to beginning of the anti-TB treatment. The differential degree of shift in MIC was observed amongst the FQs in the order of GFX < MXF/SFX/CIP < LVX < OFX. These MIC values show their potential application in the formulation of drug concentrations in clinical trials. In addition, the results obtained in the cross-resistance studies reinforced the potency of GFX and MXF, the newer generation of FQs.

The MPC experiments carried out in our study have further established better grounds for rational formulation of anti-TB drug regimen. Our FQ MPC results suggest that, GFX with its C_{max} higher than its MPC is promising to limit the emergence of resistant mutants, while the currently used CIP dosage is insufficient to restrict mutants. These results, therefore suggest consideration of re-designing current FQ formulations for both older and newer FQs which would aid in the TB control program.

The emergence of resistant *Mtb* infection and the dearth of newer class of anti-tuberculous drugs have made identification and validation of novel targets and drugs imperative. Most of the current drugs have the limitation of cross resistance or inability to target the latent stage of TB. Combination therapy in TB treatment is the key to control the emergence of drug resistance. Thus, availability of novel targets in *Mtb* that offer distinct mechanism of resistance would be of great help in the efforts to eradicate TB. The two essential enzymes in the pyrimidine biosynthesis pathway, *Mt*UPRT and PyrR, were recently indicated to be involved in the mechanism of 5-fluorouracil (5FU) action and resistance in *Mtb*.

Consequently, our study on the structural and functional insights of *Mt*UPRT and PyrR, to elucidate the interactions between these two enzymes and 5FU are essential for understanding its implications in TB. The structure determination and mapping of spontaneous mutations on the *Mt*UPRT revealed residues located away from the substrate binding site. This result suggest that, taking into account the activity of *Mt*UPRT in the low energy requiring salvage pathway, aerobically generating the spontaneous mutants could have hampered the exact selection of

the mutational sites. Nonetheless, *Mt*UPRT is known to be active in the dormant *Mtb* and hence an attractive target to screen for potent inhibitors that would help in the treatment of latent TB infection.

The structure determination and mapping of spontaneous mutations on the PyrR revealed that most residues located in the PRPP or UMP binding site of the enzyme, suggesting that *Mtb* overcomes the drug action by mutating both the substrate binding sites thereby inhibiting the production of toxic metabolites. Interestingly, the frameshift and deletion mutations in both the enzymes suggest the redundancy and availability of functionally similar enzymes in *Mtb*.

In the light of pyrimidine analogs are considered to inhibit these enzymes in other bacterial models, the present structural insights into the enzymes and the mutational sites will aid in the screening of appropriate inhibitors and thus assist in TB drug design and development.

7

Reference List

(2010) Treatment of tuberculosis guidelines, fourth edition. *World Health Organisation*.

(2013) Global tuberculosis report. *World Health Organisation*.

Adams, P.D., P.V. Afonine, G. Bunkoczi, V.B. Chen, I.W. Davis, N. Echols, J.J. Headd, L.W. Hung, G.J. Kapral, R.W. Grosse-Kunstleve, A.J. McCoy, N.W. Moriarty, R. Oeffner, R.J. Read, D.C. Richardson, J.S. Richardson, T.C. Terwilliger & P.H. Zwart, (2010) PHENIX: a comprehensive Python-based system for macromolecular structure solution. *Acta Crystallogr D Biol Crystallogr* **66**: 213-221.

Alangaden, G.J., E.K. Manavathu, S.B. Vakulenko, N.M. Zvonok & S.A. Lerner, (1995) Characterization of fluoroquinolone-resistant mutant strains of Mycobacterium tuberculosis selected in the laboratory and isolated from patients. *Antimicrobial agents and chemotherapy* **39**: 1700-1703.

Altschul, S.F., W. Gish, W. Miller, E.W. Myers & D.J. Lipman, (1990) Basic local alignment search tool. *J Mol Biol* **215**: 403-410.

Aminov, R.I., (2010) A brief history of the antibiotic era: lessons learned and challenges for the future. *Frontiers in microbiology* **1**: 134.

Andersen, P., M.E. Munk, J.M. Pollock & T.M. Doherty, (2000) Specific immune-based diagnosis of tuberculosis. *Lancet* **356**: 1099-1104.

Antonova, O.V., D.A. Gryadunov, S.A. Lapa, A.V. Kuz'min, E.E. Larionova, T.G. Smirnova, E.Y. Nosova, O.I. Skotnikova, L.N. Chernousova, A.M. Moroz, A.S. Zasedatelev & V.M. Mikhailovich, (2008) Detection of mutations in Mycobacterium tuberculosis genome determining resistance to fluoroquinolones by hybridization on biological microchips. *Bull Exp Biol Med* **145**: 108-113.

Ashburn, T.T. & K.B. Thor, (2004) Drug repositioning: identifying and developing new uses for existing drugs. *Nat Rev Drug Discov* **3**: 673-683.

Attila, C., A. Ueda & T.K. Wood, (2009) 5-Fluorouracil reduces biofilm formation in Escherichia coli K-12 through global regulator AriR as an antivirulence compound. *Appl Microbiol Biotechnol* **82**: 525-533.

Baquero, F., (2001) Low-level antibacterial resistance: a gateway to clinical resistance. *Drug Resist Updat* **4**: 93-105.

Barnes, D.S., (2000) Historical perspectives on the etiology of tuberculosis. *Microbes and infection / Institut Pasteur* **2**: 431-440.

Barry, C.E., 3rd & M.S. Cheung, (2009) New tactics against tuberculosis. *Scientific American* **300**: 62-69.

Beena & D.S. Rawat, (2012) Antituberculosis Drug Research: A Critical Overview. *Medicinal research reviews*.

Betts, J.C., P. Dodson, S. Quan, A.P. Lewis, P.J. Thomas, K. Duncan & R.A. McAdam, (2000) Comparison of the proteome of Mycobacterium tuberculosis strain H37Rv with clinical isolate CDC 1551. *Microbiology* **146 Pt 12**: 3205-3216.

Blanchard, J.S., (1996) Molecular mechanisms of drug resistance in Mycobacterium tuberculosis. *Annual review of biochemistry* **65**: 215-239.

Brennan, P.J. & D.B. Young, (2008) Tuberculosis, Handbook of Anti-Tuberculosis Agents, Global Alliance for TB Drug Development.

Bressan, R.A., M.G. Murray, J.M. Gale & C.W. Ross, (1978) Properties of pea seedling uracil phosphoribosyltransferase and its distribution in other plants. *Plant Physiol* **61**: 442-446.

Bryskier, A. & J. Lowther, (2002) Fluoroquinolones and tuberculosis. *Expert opinion on investigational drugs* **11**: 233-258.

Cambier, C.J., S. Falkow & L. Ramakrishnan, (2014) Host evasion and exploitation schemes of Mycobacterium tuberculosis. *Cell* **159**: 1497-1509.

Caminero, J.A., (2006) Treatment of multidrug-resistant tuberculosis: evidence and controversies. *The international journal of tuberculosis and lung disease : the official journal of the International Union against Tuberculosis and Lung Disease* **10**: 829-837.

Chen, V.B., J.R. Wedell, R.K. Wenger, E.L. Ulrich & J.L. Markley, (2015) MolProbity for the masses-of data. *J Biomol NMR*.

Cheng, A.F., W.W. Yew, E.W. Chan, M.L. Chin, M.M. Hui & R.C. Chan, (2004) Multiplex PCR amplimer conformation analysis for rapid detection of gyrA mutations in fluoroquinolone-resistant Mycobacterium tuberculosis clinical isolates. *Antimicrobial agents and chemotherapy* **48**: 596-601.

Cole, S.T., R. Brosch, J. Parkhill, T. Garnier, C. Churcher, D. Harris, S.V. Gordon, K. Eiglmeier, S. Gas, C.E. Barry, 3rd, F. Tekaia, K. Badcock, D. Basham, D. Brown, T. Chillingworth, R. Connor, R. Davies, K. Devlin, T. Feltwell, S. Gentles, N. Hamlin, S. Holroyd, T. Hornsby, K. Jagels, A. Krogh, J. McLean, S. Moule, L. Murphy, K. Oliver, J. Osborne, M.A. Quail, M.A. Rajandream, J. Rogers, S. Rutter, K. Seeger, J. Skelton, R. Squares, S. Squares, J.E. Sulston, K. Taylor, S. Whitehead & B.G. Barrell, (1998) Deciphering the biology of Mycobacterium tuberculosis from the complete genome sequence. *Nature* **393**: 537-544.

Conde, M.B., A. Efron, C. Loredo, G.R. De Souza, N.P. Graca, M.C. Cezar, M. Ram, M.A. Chaudhary, W.R. Bishai, A.L. Kritski & R.E. Chaisson, (2009) Moxifloxacin versus ethambutol in the initial treatment of tuberculosis: a double-blind, randomised, controlled phase II trial. *Lancet* **373**: 1183-1189.

Cui, Z., J. Wang, J. Lu, X. Huang & Z. Hu, (2011) Association of mutation patterns in gyrA/B genes and ofloxacin resistance levels in Mycobacterium tuberculosis isolates from East China in 2009. *BMC Infect Dis* **11**: 78.

Dalhoff, A., (2012) Global fluoroquinolone resistance epidemiology and implictions for clinical use. *Interdiscip Perspect Infect Dis* **2012**: 976273.

Devasia, R., A. Blackman, S. Eden, H. Li, F. Maruri, A. Shintani, C. Alexander, A. Kaiga, C.W. Stratton, J. Warkentin, Y.W. Tang & T.R. Sterling, (2012) High proportion of fluoroquinolone-resistant Mycobacterium tuberculosis isolates with novel gyrase polymorphisms and a gyrA region associated with fluoroquinolone susceptibility. *Journal of clinical microbiology* **50**: 1390-1396.

Dong, H. & D. Zhang, (2014) Current development in genetic engineering strategies of Bacillus species. *Microb Cell Fact* **13**: 63.

Drlica, K., (1999) Mechanism of fluoroquinolone action. *Current opinion in microbiology* **2**: 504-508.

Drlica, K. & M. Malik, (2003) Fluoroquinolones: action and resistance. *Current topics in medicinal chemistry* **3**: 249-282.

Duncan, K., (2004) Identification and validation of novel drug targets in tuberculosis. *Curr Pharm Des* **10**: 3185-3194.

Emsley, P. & K. Cowtan, (2004) Coot: model-building tools for molecular graphics. *Acta Crystallogr D Biol Crystallogr* **60**: 2126-2132.

Ernst, J.D., (1998) Macrophage receptors for Mycobacterium tuberculosis. *Infection and immunity* **66**: 1277-1281.

Espinosa-Cueto, P., M. Escalera-Zamudio, A. Magallanes-Puebla, L.M. Lopez-Marin, E. Segura-Salinas & R. Mancilla, (2015) Mycobacterial glycolipids di-O-acylated trehalose and tri-O-acylated trehalose downregulate inducible nitric oxide synthase and nitric oxide production in macrophages. *BMC immunology* **16**: 38.

Field, S.K., D. Fisher, J.M. Jarand & R.L. Cowie, (2012) New treatment options for multidrug-resistant tuberculosis. *Therapeutic advances in respiratory disease*.

Florey, H.W., (1944) Penicillin: A Survey. *British medical journal* **2**: 169-171.

Fogel, N., (2015) Tuberculosis: A disease without boundaries. *Tuberculosis (Edinb)*.

Gengenbacher, M. & S.H. Kaufmann, (2012) Mycobacterium tuberculosis: success through dormancy. *FEMS Microbiol Rev* **36**: 514-532.

Ghode, P., C. Jobichen, S. Ramachandran, P. Bifani & J. Sivaraman, (2015) Structural basis of mapping the spontaneous mutations with 5-flurouracil in uracil phosphoribosyltransferase from Mycobacterium tuberculosis. *Biochem Biophys Res Commun* **467**: 577-582.

Ghode, P., S. Ramachandran, P. Bifani & J. Sivaraman, (2016) Structure and mapping of spontaneous mutational sites of PyrR from Mycobacterium tuberculosis. *Biochem Biophys Res Commun* **471**: 409-415.

Giannoni, F., E. Iona, F. Sementilli, L. Brunori, M. Pardini, G.B. Migliori, G. Orefici & L. Fattorini, (2005) Evaluation of a new line probe assay for rapid identification of gyrA mutations in Mycobacterium tuberculosis. *Antimicrobial agents and chemotherapy* **49**: 2928-2933.

Gillespie, S.H., A.M. Crook, T.D. McHugh, C.M. Mendel, S.K. Meredith, S.R. Murray, F. Pappas, P.P. Phillips, A.J. Nunn & R.E. Consortium, (2014) Four-month moxifloxacin-based regimens for drug-sensitive tuberculosis. *N Engl J Med* **371**: 1577-1587.

Ginsburg, A.S., J.H. Grosset & W.R. Bishai, (2003) Fluoroquinolones, tuberculosis, and resistance. *The Lancet infectious diseases* **3**: 432-442.

Glickman, M.S. & W.R. Jacobs, Jr., (2001) Microbial pathogenesis of Mycobacterium tuberculosis: dawn of a discipline. *Cell* **104**: 477-485.

Hawn, T.R., T.A. Day, T.J. Scriba, M. Hatherill, W.A. Hanekom, T.G. Evans, G.J. Churchyard, J.G. Kublin, L.G. Bekker & S.G. Self, (2014) Tuberculosis vaccines and prevention of infection. *Microbiology and molecular biology reviews : MMBR* **78**: 650-671.

Holm, L. & P. Rosenstrom, (2010) Dali server: conservation mapping in 3D. *Nucleic Acids Res* **38**: W545-549.

Huang, T.S., C.M. Kunin, S. Shin-Jung Lee, Y.S. Chen, H.Z. Tu & Y.C. Liu, (2005) Trends in fluoroquinolone resistance of Mycobacterium tuberculosis complex in a Taiwanese medical centre: 1995-2003. *The Journal of antimicrobial chemotherapy* **56**: 1058-1062.

Hughes, L.E., D.A. Beck & G.A. O'Donovan, (2005) Pathways of pyrimidine salvage in Streptomyces. *Curr Microbiol* **50**: 8-10.

Imperi, F., F. Massai, M. Facchini, E. Frangipani, D. Visaggio, L. Leoni, A. Bragonzi & P. Visca, (2013) Repurposing the antimycotic drug flucytosine for suppression of

Pseudomonas aeruginosa pathogenicity. *Proc Natl Acad Sci U S A* **110**: 7458-7463.

Jawahar, M.S., V.V. Banurekha, C.N. Paramasivan, F. Rahman, R. Ramachandran, P. Venkatesan, R. Balasubramanian, N. Selvakumar, C. Ponnuraja, A.S. Iliayas, N.P. Gangadevi, B. Raman, D. Baskaran, S.R. Kumar, M.M. Kumar, V. Mohan, S. Ganapathy, V. Kumar, G. Shanmugam, N. Charles, M.R. Sakthivel, K. Jagannath, C. Chandrasekar, R.T. Parthasarathy & P.R. Narayanan, (2013) Randomized clinical trial of thrice-weekly 4-month moxifloxacin or gatifloxacin containing regimens in the treatment of new sputum positive pulmonary tuberculosis patients. *PLoS One* **8**: e67030.

Jeon, D., (2015) Medical Management of Drug-Resistant Tuberculosis. *Tuberculosis and respiratory diseases* **78**: 168-174.

Kadziola, A., J. Neuhard & S. Larsen, (2002) Structure of product-bound Bacillus caldolyticus uracil phosphoribosyltransferase confirms ordered sequential substrate binding. *Acta Crystallogr D Biol Crystallogr* **58**: 936-945.

Kale, V.P., S.G. Amin & M.K. Pandey, (2015) Targeting ion channels for cancer therapy by repurposing the approved drugs. *Biochim Biophys Acta*.

Kantardjieff, K.A., C. Vasquez, P. Castro, N.M. Warfel, B.S. Rho, T. Lekin, C.Y. Kim, B.W. Segelke, T.C. Terwilliger & B. Rupp, (2005) Structure of pyrR (Rv1379) from Mycobacterium tuberculosis: a persistence gene and protein drug target. *Acta Crystallogr D Biol Crystallogr* **61**: 355-364.

Keeler, E., M.D. Perkins, P. Small, C. Hanson, S. Reed, J. Cunningham, J.E. Aledort, L. Hillborne, M.E. Rafael, F. Girosi & C. Dye, (2006) Reducing the global burden of tuberculosis: the contribution of improved diagnostics. *Nature* **444 Suppl 1**: 49-57.

Kocagoz, T., C.J. Hackbarth, I. Unsal, E.Y. Rosenberg, H. Nikaido & H.F. Chambers, (1996) Gyrase mutations in laboratory-selected, fluoroquinolone-resistant mutants of Mycobacterium tuberculosis H37Ra. *Antimicrob Agents Chemother* **40**: 1768-1774.

Ling, D.I., A.A. Zwerling & M. Pai, (2008) GenoType MTBDR assays for the diagnosis of multidrug-resistant tuberculosis: a meta-analysis. *The European respiratory journal* **32**: 1165-1174.

Lipsitch, M. & B.R. Levin, (1998) Population dynamics of tuberculosis treatment: mathematical models of the roles of non-compliance and bacterial heterogeneity in the evolution of drug resistance. *Int J Tuberc Lung Dis* **2**: 187-199.

Lonnroth, K., E. Jaramillo, B.G. Williams, C. Dye & M. Raviglione, (2009) Drivers of tuberculosis epidemics: the role of risk factors and social determinants. *Social science & medicine* **68**: 2240-2246.

Luria, S.E. & M. Delbruck, (1943) Mutations of Bacteria from Virus Sensitivity to Virus Resistance. *Genetics* **28**: 491-511.

Ma, Z., C. Lienhardt, H. McIlleron, A.J. Nunn & X. Wang, (2010) Global tuberculosis drug development pipeline: the need and the reality. *Lancet* **375**: 2100-2109.

Malik, S., M. Willby, D. Sikes, O.V. Tsodikov & J.E. Posey, (2012) New Insights into Fluoroquinolone Resistance in Mycobacterium tuberculosis: Functional Genetic Analysis of gyrA and gyrB Mutations. *PloS one* **7**: e39754.

Manabe, Y.C. & W.R. Bishai, (2000) Latent Mycobacterium tuberculosis-persistence, patience, and winning by waiting. *Nat Med* **6**: 1327-1329.

Manca, C., L. Tsenova, C.E. Barry, 3rd, A. Bergtold, S. Freeman, P.A. Haslett, J.M. Musser, V.H. Freedman & G. Kaplan, (1999) Mycobacterium tuberculosis CDC1551 induces a more vigorous host response in vivo and in vitro, but is not more virulent than other clinical isolates. *J Immunol* **162**: 6740-6746.

Martinussen, J. & K. Hammer, (1994) Cloning and characterization of upp, a gene encoding uracil phosphoribosyltransferase from Lactococcus lactis. *J Bacteriol* **176**: 6457-6463.

Maruri, F., T.R. Sterling, A.W. Kaiga, A. Blackman, Y.F. van der Heijden, C. Mayer, E. Cambau & A. Aubry, (2012) A systematic review of gyrase mutations associated with fluoroquinolone-resistant Mycobacterium tuberculosis and a proposed gyrase numbering system. *The Journal of antimicrobial chemotherapy* **67**: 819-831.

McCoy, A.J., Grosse-Kunstleve, A. R.W., P.D., M.D. Winn, L.C. Storoni & R.J. Read, (2007) *Phaser* crystallographic software. *Journal of Applied Crystallography* **40**: 658 - 674.

Merle, C.S., K. Fielding, O.B. Sow, M. Gninafon, M.B. Lo, T. Mthiyane, J. Odhiambo, E. Amukoye, B. Bah, F. Kassa, A. N'Diaye, R. Rustomjee, B.C. de Jong, J. Horton, C. Perronne, C. Sismanidis, O. Lapujade, P.L. Olliaro, C. Lienhardt & O.F.G.f.T. Project, (2014) A four-month gatifloxacin-containing regimen for treating tuberculosis. *N Engl J Med* **371**: 1588-1598.

Moadebi, S., C.K. Harder, M.J. Fitzgerald, K.R. Elwood & F. Marra, (2007) Fluoroquinolones for the treatment of pulmonary tuberculosis. *Drugs* **67**: 2077-2099.

Moellering, R.C., Jr., (2005) The management of infections due to drug-resistant gram-positive bacteria. *European journal of clinical microbiology & infectious diseases : official publication of the European Society of Clinical Microbiology* **24**: 777-779.

Mokrousov, I., T. Otten, O. Manicheva, Y. Potapova, B. Vishnevsky, O. Narvskaya & N. Rastogi, (2008) Molecular characterization of ofloxacin-resistant Mycobacterium tuberculosis strains from Russia. *Antimicrob Agents Chemother* **52**: 2937-2939.

Nuermberger, E. & J. Grosset, (2004) Pharmacokinetic and pharmacodynamic issues in the treatment of mycobacterial infections. *European journal of clinical microbiology & infectious diseases : official publication of the European Society of Clinical Microbiology* **23**: 243-255.

Nyendak, M.R., D.A. Lewinsohn & D.M. Lewinsohn, (2009) New diagnostic methods for tuberculosis. *Current opinion in infectious diseases* **22**: 174-182.

O'Brien, R.J. & P.P. Nunn, (2001) The need for new drugs against tuberculosis. Obstacles, opportunities, and next steps. *Am J Respir Crit Care Med* **163**: 1055-1058.

Otwinowski, Z. & W. Minor, (1997) Processing of X-ray Diffraction Data Collected in Oscillation Mode. *Methods in Enzymology* **276**: 307-326.

Pai, M., S. Kalantri & K. Dheda, (2006a) New tools and emerging technologies for the diagnosis of tuberculosis: part I. Latent tuberculosis. *Expert review of molecular diagnostics* **6**: 413-422.

Pai, M., S. Kalantri & K. Dheda, (2006b) New tools and emerging technologies for the diagnosis of tuberculosis: part II. Active tuberculosis and drug resistance. *Expert review of molecular diagnostics* **6**: 423-432.

Pai, M. & R. O'Brien, (2008) New diagnostics for latent and active tuberculosis: state of the art and future prospects. *Seminars in respiratory and critical care medicine* **29**: 560-568.

Pantel, A., S. Petrella, N. Veziris, F. Brossier, S. Bastian, V. Jarlier, C. Mayer & A. Aubry, (2012) Extending the definition of the GyrB quinolone resistance-determining region in Mycobacterium tuberculosis DNA gyrase for assessing fluoroquinolone resistance in M. tuberculosis. *Antimicrobial agents and chemotherapy* **56**: 1990-1996.

Perkins, M.D. & J. Cunningham, (2007) Facing the crisis: improving the diagnosis of tuberculosis in the HIV era. *The Journal of infectious diseases* **196 Suppl 1**: S15-27.

Pethe, K., P.C. Sequeira, S. Agarwalla, K. Rhee, K. Kuhen, W.Y. Phong, V. Patel, D. Beer, J.R. Walker, J. Duraiswamy, J. Jiricek, T.H. Keller, A. Chatterjee, M.P. Tan, M. Ujjini, S.P. Rao, L. Camacho, P. Bifani, P.A. Mak, I. Ma, S.W. Barnes, Z. Chen, D. Plouffe, P. Thayalan, S.H. Ng, M. Au, B.H. Lee, B.H. Tan, S. Ravindran, M. Nanjundappa, X. Lin, A. Goh, S.B. Lakshminarayana, C. Shoen, M. Cynamon, B. Kreiswirth, V. Dartois, E.C. Peters, R. Glynne, S. Brenner & T. Dick, (2010) A chemical genetic screen in Mycobacterium tuberculosis identifies carbon-source-dependent growth inhibitors devoid of in vivo efficacy. *Nat Commun* **1**: 57.

Pieters, J., (2001) Entry and survival of pathogenic mycobacteria in macrophages. *Microbes and infection / Institut Pasteur* **3**: 249-255.

Pitaksajjakul, P., W. Wongwit, W. Punprasit, B. Eampokalap, S. Peacock & P. Ramasoota, (2005) Mutations in the gyrA and gyrB genes of fluoroquinolone-resistant Mycobacterium tuberculosis from TB patients in Thailand. *The Southeast Asian journal of tropical medicine and public health* **36 Suppl 4**: 228-237.

Piton, J., S. Petrella, M. Delarue, G. Andre-Leroux, V. Jarlier, A. Aubry & C. Mayer, (2010) Structural insights into the quinolone resistance mechanism of Mycobacterium tuberculosis DNA gyrase. *PloS one* **5**: e12245.

Poissy, J., A. Aubry, C. Fernandez, M. Lott, A. Chauffour, V. Jarlier, R. Farinotti & N. Veziris, (2010) Should moxifloxacin be used for the treatment of extensively drug-resistant tuberculosis? An answer from a murine model. *Antimicrob Agents Chemother* **54**: 4765-4771.

Ramaswamy, S. & J.M. Musser, (1998) Molecular genetic basis of antimicrobial agent resistance in Mycobacterium tuberculosis: 1998 update. *Tuber Lung Dis* **79**: 3-29.

Rangel-Vega, A., L. Bernstein, E. Mandujano-Tinoco, S. García-Contreras & R. García-Contreras, (2015) Drug repurposing as an alternative for the treatment of recalcitrant bacterial infections. *Front Microbiol* **6**: 282.

Rowland, R. & H. McShane, (2011) Tuberculosis vaccines in clinical trials. *Expert review of vaccines* **10**: 645-658.

Schluger, N.W., N. El-Bassel, S. Hermosilla, A. Terlikbayeva, M. Darisheva, A. Aifah & S. Galea, (2013) Tuberculosis, drug use and HIV infection in Central Asia: an urgent need for attention. *Drug Alcohol Depend* **132 Suppl 1**: S32-36.

Schumacher, M.A., D. Carter, D.M. Scott, D.S. Roos, B. Ullman & R.G. Brennan, (1998) Crystal structures of Toxoplasma gondii uracil phosphoribosyltransferase reveal the atomic basis of pyrimidine discrimination and prodrug binding. *EMBO J* **17**: 3219-3232.

Sekiguchi, J., T. Miyoshi-Akiyama, E. Augustynowicz-Kopec, Z. Zwolska, F. Kirikae, E. Toyota, I. Kobayashi, K. Morita, K. Kudo, S. Kato, T. Kuratsuji, T. Mori & T. Kirikae, (2007) Detection of multidrug resistance in Mycobacterium tuberculosis. *J Clin Microbiol* **45**: 179-192.

Sherman, D.R., M. Voskuil, D. Schnappinger, R. Liao, M.I. Harrell & G.K. Schoolnik, (2001) Regulation of the Mycobacterium tuberculosis hypoxic response gene encoding alpha -crystallin. *Proc Natl Acad Sci U S A* **98**: 7534-7539.

Sindelar, G., X. Zhao, A. Liew, Y. Dong, T. Lu, J. Zhou, J. Domagala & K. Drlica, (2000) Mutant prevention concentration as a measure of fluoroquinolone potency against mycobacteria. *Antimicrobial agents and chemotherapy* **44**: 3337-3343.

Singh, K.P., M. Brown, M.E. Murphy & S.H. Gillespie, (2012) Moxifloxacin for tuberculosis. *The Lancet infectious diseases* **12**: 176; author reply 177-178.

Singh, V., M. Brecik, R. Mukherjee, J.C. Evans, Z. Svetlikova, J. Blasko, S. Surade, J. Blackburn, D.F. Warner, K. Mikusova & V. Mizrahi, (2015) The complex mechanism of antimycobacterial action of 5-fluorouracil. *Chem Biol* **22**: 63-75.

Sirgel, F.A., R.M. Warren, E.M. Streicher, T.C. Victor, P.D. van Helden & E.C. Bottger, (2012) gyrA mutations and phenotypic susceptibility levels to ofloxacin and moxifloxacin in clinical isolates of Mycobacterium tuberculosis. *The Journal of antimicrobial chemotherapy* **67**: 1088-1093.

Stefanova, T., (2014) Quality control and safety assessment of BCG vaccines in the post-genomic era. *Biotechnology, biotechnological equipment* **28**: 387-391.

Sun, Z., J. Zhang, X. Zhang, S. Wang, Y. Zhang & C. Li, (2008) Comparison of gyrA gene mutations between laboratory-selected ofloxacin-resistant Mycobacterium tuberculosis strains and clinical isolates. *International journal of antimicrobial agents* **31**: 115-121.

Sunamura, M., M. Oonuma, F. Motoi, H. Abe, Y. Saitoh, T. Hoshida, S. Ottomo, A. Horii & S. Matsuno, (2002) Gene therapy for pancreatic cancer targeting the genomic alterations of tumor suppressor genes using replication-selective oncolytic adenovirus. *Hum Cell* **15**: 138-150.

Switzer, R.L., R.J. Turner & Y. Lu, (1999) Regulation of the Bacillus subtilis pyrimidine biosynthetic operon by transcriptional attenuation: control of gene expression by an mRNA-binding protein. *Prog Nucleic Acid Res Mol Biol* **62**: 329-367.

Takiff, H.E., L. Salazar, C. Guerrero, W. Philipp, W.M. Huang, B. Kreiswirth, S.T. Cole, W.R. Jacobs, Jr. & A. Telenti, (1994) Cloning and nucleotide sequence of Mycobacterium tuberculosis gyrA and gyrB genes and detection of quinolone resistance mutations. *Antimicrob Agents Chemother* **38**: 773-780.

Tsukamura, M., (1979) In vitro susceptibility of mycobacteria, especially of Mycobacterium intracellulare, to 5-fluorouracil and pattern of development of resistance of Mycobacterium tuberculosis to the drug. *Microbiol Immunol* **23**: 427-429.

Valway, S.E., M.P. Sanchez, T.F. Shinnick, I. Orme, T. Agerton, D. Hoy, J.S. Jones, H. Westmoreland & I.M. Onorato, (1998) An outbreak involving extensive transmission of a virulent strain of Mycobacterium tuberculosis. *N Engl J Med* **338**: 633-639.

Villela, A.D., R.G. Ducati, L.A. Rosado, C.J. Bloch, M.V. Prates, D.C. Goncalves, C.H. Ramos, L.A. Basso & D.S. Santos, (2013) Biochemical characterization of uracil phosphoribosyltransferase from Mycobacterium tuberculosis. *PLoS One* **8**: e56445.

Villela, A.D., Z.A. Sanchez-Quitian, R.G. Ducati, D.S. Santos & L.A. Basso, (2011) Pyrimidine salvage pathway in Mycobacterium tuberculosis. *Curr Med Chem* **18**: 1286-1298.

Von Groll, A., A. Martin, P. Jureen, S. Hoffner, P. Vandamme, F. Portaels, J.C. Palomino & P.A. da Silva, (2009) Fluoroquinolone resistance in Mycobacterium tuberculosis and mutations in gyrA and gyrB. *Antimicrob Agents Chemother* **53**: 4498-4500.

Wallis, R.S., M. Pai, D. Menzies, T.M. Doherty, G. Walzl, M.D. Perkins & A. Zumla, (2010) Biomarkers and diagnostics for tuberculosis: progress, needs, and translation into practice. *Lancet* **375**: 1920-1937.

Walsh, C., (2003a) Where will new antibiotics come from? *Nat Rev Microbiol* **1**: 65-70.

Walsh, C., (2003b) Where will new antibiotics come from? *Nat Rev Microbiol* **1**: 65-70.

Warner, D.F. & V. Mizrahi, (2013) Complex genetics of drug resistance in Mycobacterium tuberculosis. *Nature genetics* **45**: 1107-1108.

Wayne, L.G. & K.Y. Lin, (1982) Glyoxylate metabolism and adaptation of Mycobacterium tuberculosis to survival under anaerobic conditions. *Infect Immun* **37**: 1042-1049.

WHO, (2014) Global tuberculosis report. *World Health Organisation*.

Xu, C., B.N. Kreiswirth, S. Sreevatsan, J.M. Musser & K. Drlica, (1996) Fluoroquinolone resistance associated with specific gyrase mutations in clinical isolates of multidrug-resistant Mycobacterium tuberculosis. *The Journal of infectious diseases* **174**: 1127-1130.

Yew, W.W., C.K. Chan, C.H. Chau, C.M. Tam, C.C. Leung, P.C. Wong & J. Lee, (2000) Outcomes of patients with multidrug-resistant pulmonary tuberculosis treated with ofloxacin/levofloxacin-containing regimens. *Chest* **117**: 744-751.

Zhou, J., Y. Dong, X. Zhao, S. Lee, A. Amin, S. Ramaswamy, J. Domagala, J.M. Musser & K. Drlica, (2000) Selection of antibiotic-resistant bacterial mutants: allelic diversity among fluoroquinolone-resistant mutations. *The Journal of infectious diseases* **182**: 517-525.

Zumla, A. & J.M. Grange, (2001) Multidrug-resistant tuberculosis--can the tide be turned? *The Lancet infectious diseases* **1**: 199-202.

Zumla, A., P. Nahid & S.T. Cole, (2013) Advances in the development of new tuberculosis drugs and treatment regimens. *Nat Rev Drug Discov* **12**: 388-404.

Biochemical and Biophysical Research Communications 467 (2015) 577–582

Contents lists available at ScienceDirect

Biochemical and Biophysical Research Communications

journal homepage: www.elsevier.com/locate/ybbrc

Structural basis of mapping the spontaneous mutations with 5-flurouracil in uracil phosphoribosyltransferase from *Mycobacterium tuberculosis*

Pramila Ghode [a, b], Chacko Jobichen [a], Sarath Ramachandran [a], Pablo Bifani [b], J. Sivaraman [a, *]

[a] Department of Biological Sciences, National University of Singapore, 14 Science Drive 4, Singapore, 117543, Singapore
[b] Novartis Institute for Tropical Diseases, 10 Biopolis Road, Singapore, 138670, Singapore

ARTICLE INFO

Article history:
Received 18 September 2015
Accepted 23 September 2015
Available online 8 October 2015

Keywords:
Uracil phosphoribosyltransferase (UPRT)
Mycobacterium tuberculosis (*Mtb*)
upp (Rv3309c)
5-fluorouracil (5-FU)
Spontaneous mutants

ABSTRACT

Tuberculosis (TB) remains the second leading cause of death from an infectious disease globally, despite the incessant efforts to control it. Research and development into new TB medicines is imperative for effective TB control; however, new strategies for the rational use of existing drugs, such as through the identification of new drug targets, could also significantly enhance this process. Key enzymes involved in the essential metabolic and regulatory pathways are usually sought in the pursuit of potential drug targets. Uracil phosphoribosyltransferase (UPRT) is a key salvage pathway enzyme in the synthesis of uridine 5′-monophosphate (UMP) and a probable target of 5-fluorouracil (5-FU) in *Mycobacterium tuberculosis* (*Mtb*). To date, there is no structure available for UPRT from *Mtb* (*Mt*UPRT) that would assist in the identification of appropriate inhibitors for the enzyme. Here we report the structure of *Mt*UPRT along with its spontaneous mutational studies in the presence of 5-FU. We further mapped these four single nucleotide polymorphisms (SNPs) onto the *Mt*UPRT structure, with two residues found to be conserved among the *Mt*UPRT homologs. Notably, none of these SNPs are located in the 5-FU binding pocket. However, the mutants harboring these mutations showed increased MICs (minimum inhibitory concentration) as compared to wild type strains. The present study will aid in the screening of inhibitors of *Mt*UPRT and thus assist in TB drug design and development.

© 2015 Elsevier Inc. All rights reserved.

1. Introduction

Tuberculosis (TB) is an infectious disease caused by *Mycobacterium tuberculosis* (*Mtb*). In 2013, TB claimed 1.5 million lives along with an estimated 9 million new cases (WHO). The emergence and alarming rate at which multidrug-resistant TB (MDR TB) and extensively drug-resistant TB (XDR TB) has spread has rendered the existing TB drugs inefficient [1]. This rise in the prevalence of MDR and XDR cases is predominantly the result of poor patient compliance (owing to the long treatment duration and side effects) and the characteristic ability of *Mtb* to go into non-replicating latent (LTBI) or dormant states. Approximately one-third of the world's population harbors LTBI, with 5%–20% of the cases developing into active TB infection if left untreated. The situation is further exacerbated by the increasing rates of co-infection with HIV [2]. Together, these factors present a major challenge for controlling TB and illustrate the need for either new anti-TB drugs that could shorten treatment duration, or the identification of novel drug targets with unique mechanism(s) of action [3]. Interestingly, the diagnosis and treatment of LTBI is predicted to have an impact on the eradication of active TB. Nonetheless, there is no specific diagnostics or treatment for LTBI so far, and this is attributed to the inadequate scientific research on the fundamentals of LTBI. The global TB control program puts emphasis on accelerating research on the pathogenesis of *Mtb*, and this would, in turn, help in the identification of biomarkers and drug targets for the effective diagnosis and treatment of LTBI [4].

A previous study has indicated *Mtb* UPRT (*Mt*UPRT) as an anti-TB target with probable activity in LTBI. Essential biological pathways associated with DNA/RNA synthesis are often interrogated for favorable drug targets [5]. This is the case for uracil phosphoribosyltransferase (UPRT; EC 2.4.2.9), an enzyme involved in the low

* Corresponding author.
E-mail address: dbsjayar@nus.edu.sg (J. Sivaraman).

http://dx.doi.org/10.1016/j.bbrc.2015.09.133
0006-291X/© 2015 Elsevier Inc. All rights reserved.

Biochemical and Biophysical Research Communications 471 (2016) 409–415

Contents lists available at ScienceDirect

Biochemical and Biophysical Research Communications

journal homepage: www.elsevier.com/locate/ybbrc

Structure and mapping of spontaneous mutational sites of PyrR from *Mycobacterium tuberculosis*

Pramila Ghode [a, b], Sarath Ramachandran [a], Pablo Bifani [b], J. Sivaraman [a, *]

[a] Department of Biological Sciences, National University of Singapore, 14 Science Drive 4, Singapore, 117543, Singapore
[b] Novartis Institute for Tropical Diseases, 10 Biopolis Road, Singapore, 138670, Singapore

ARTICLE INFO

Article history:
Received 5 February 2016
Accepted 17 February 2016
Available online 18 February 2016

Keywords:
PyrR
Mycobacterium tuberculosis (*Mtb*)
pyrR (*Rv1379*)
5-Fluorouracil (5-FU)
Spontaneous mutants

ABSTRACT

The emergence of resistant *Mycobacterium tuberculosis* (*Mtb*) infection and the dearth of drugs against tuberculosis have made it imperative to identify and validate novel targets and classes of drugs for treatment. The pyrimidine operon regulatory protein (PyrR), a regulator of *de novo* pyrimidine synthesis, is an essential enzyme and a probable 5-fluorouracil (5-FU) target in *Mtb*, with mutations in PyrR attributable to 5-FU resistance. Here we report, for the first time, the co–crystal structure of the PyrR–5-FU complex along with mapping of spontaneous mutational sites of PyrR. A cluster of mutations in the presence of the drug usually indicates a plausible region of drug–target interaction. Notably, we observed that three of the mutated PyrR residues lie in close proximity to the 5-FU binding site, including the amino acid Val178, which is involved in water mediated hydrogen bonding contact with 5-FU. Computational modeling of the PyrR–5'-phosphoribosyl-α-1'-pyrophosphate (PRPP) complex revealed the location of several other mutations at the PRPP binding site of PyrR, indicating their probable role in resistance. Indeed, 5-FU-resistant strains harboring these mutations exhibited decreased susceptibility to 5-FU. Considering that pyrimidine analogs are predominantly regarded to inhibit PyrR, the present studies will be beneficial for the screening of appropriate inhibitors of PyrR and help provide insight into future TB drug design and development.

© 2016 Elsevier Inc. All rights reserved.

1. Introduction

Tuberculosis (TB), caused by the pathogen *Mycobacterium tuberculosis* (*Mtb*), remains the leading cause of death from an infectious disease (alongside HIV) globally despite persistent efforts to control it. Each year, TB claims approximately 1.5 million lives and, in the last decade, there have been a reported 8 to 9 million new cases annually [1]. Since the 1950s, chemotherapy drugs have proven to be an effective treatment strategy against TB, but this ceases to be the case once patients demonstrate TB recurrence. Indeed, there was a resurgence in the prevalence of drug-resistant bacilli in the 1970s [2,3]. In the 1980s, TB control programs were further hampered by the HIV outbreak, with many patients developing TB co-infection, in part due to the incompatibility between antitubercular and antiviral drugs [1,4]. Efforts to curb TB tend to be compromised by poor patient compliance, stemming from the long treatment duration required as well as the onset of side effects, which are particularly seen during the treatment of multidrug-resistant (MDR) and extensively drug-resistant (XDR) TB [5]. In addition, the ability of *Mtb* to enter into a persistent stage in the host without causing any disease symptoms is fundamental to the pathogenic success of *Mtb* [6].

The TB drug pipeline has been stagnant until recently [3]. No new class of chemical compounds had been developed in the past four decades since the introduction of quinolones in the 1960s [7]. However, a few drugs from the chemical classes diarylquinolones, rifamycins, fluoroquinolones, oxazolidinones and nitroimidazoles have progressed to the clinical development stage over the past decade. Despite this, there is still an urgent need for the development of new drugs, with novel mechanisms of actions that can circumvent the aforementioned issues [8].

The development of an entirely new drug, however, will require a detailed clinical analysis of the pharmacokinetics, toxicity, and formulation of the compound—time consuming and expensive pursuits [9]. Repurposing an already approved drug, on the other hand, could provide a faster and possibly safer turnaround because these clinical tests have already been carried out [10]. For example,

* Corresponding author.
E-mail address: dbsjayar@nus.edu.sg (J. Sivaraman).

http://dx.doi.org/10.1016/j.bbrc.2016.02.071
0006-291X/© 2016 Elsevier Inc. All rights reserved.